APPLICATION POSSIBILITIES AND PERFORMANCE OF FORWARD OSMOSIS IN INDUSTRIAL WATER MANAGEMENT

ANITA HAUPT

Dissertation zur Erlangung des akademischen Grades Doktoringenieur (Dr.-Ing.) an der Fakultät Umweltwissenschaften der Technischen Universität Dresden

vorgelegt von Dipl.-Ing. Anita Haupt

geboren am 31. Dezember 1982 in Dresden

Datum der Verteidigung: 23.06.2020

Die Übereinstimmung dieses Exemplars mit dem Original der Dissertation zum Thema: "Application possibilities and performance of forward osmosis in industrial water management" wird hiermit bestätigt.

Gutachter:

Prof. Dr.-Ing. André Lerch

Technische Universität Dresden

Institut für Siedlungs- und Industriewasserwirtschaft,
Professur für Verfahrenstechnik in Hydrosystemen

Dresden, Germany

Prof. Dr.-Ing. Sven-Uwe Geißen

Technische Universität Berlin

Institut für Technischen Umweltschutz,
Fachgebiet Umweltverfahrenstechnik

Berlin, Germany

Prof. E.R. (Emile) Cornelissen, PhD MSc

KWR Watercycle Research Institute

Nieuwegein, the Netherlands

Preface

Conventional pressure driven membrane processes such as micro-, ultra- and nanofiltration as well as reverse osmosis are of essential importance in municipal and industrial water management and frequently used to achieve the sustainable development goals (SGD) of the United Nations. In this respect, these membrane processes are often operated in water recycling schemes in industrial water and waste water treatment, which gain more and more importance due to different reasons. In addition to the economic reasons, limited access to sufficient water resources and restrictions on wastewater disposal are of concern. In order to obtain more economic and maybe even ecologic water recycling, it is necessary to develop and apply new, innovative water treatment processes in the industry. One of these processes is forward osmosis (FO), which uses the naturally occurring osmotic pressure gradient between two liquids to generate the water flow through a semi-permeable membrane. Dr.-Ing. Anita Haupt focused on the applicability of this innovative membrane process in three different industrial branches and investigated the potential of FO in these industrial water sectors.

The relevance of her work can be rated as high. Especially her high-quality review on FO in manufacturing industries, which started to get cited frequently in 2020, was a contribution to the scientific community with impact. Additionally, the outcome of her work showed that those scenarios in which both the feed and the draw solution (FS and DS) are industrial waters and two liquids are treated simultaneously in one-step are of particular interest. It becomes clear that also beyond the borders of one's own industrial sectors, suitable waters should be sought and used, be it as DS, which has to be diluted or FS, which has to be concentrated. For this, she proposed a way of how to proceed and therefore contributed to the progress of engineering sciences.

The presented work and thesis of Dr.-Ing Anita Haupt was conducted within the framework of a Saxony state doctoral scholarship, supported by the European Social Fund (SAB-ESF). We greatly acknowledge the funding.

Personally, I am very pleased to have successfully accompanied "my" first doctoral student to graduate as a "Doktor der Ingenieurwissenschaften (Dr.-Ing.)". She did a very good job and finished her doctoral thesis with great commitment, taking into account good scientific practice always. Anita, it has always given me a lot of pleasure and I learnt a lot on FO.

Prof. Dr.-Ing. André Lerch

Abstract

Membrane filtration processes such as micro-, ultra- and nanofiltration as well as reverse osmosis are frequently used in industrial water treatment and waste water treatment. They use a high physical pressure difference as a driving force to press water through a semi-permeable membrane and produce purified water. For this reason, large amounts of energy are required. In contrast, forward osmosis is an innovative membrane filtration process that uses the naturally occurring osmotic pressure gradient between two liquids to generate the water flow through the semi-permeable membrane. In forward osmosis, one liquid with low osmotic pressure is concentrated (so-called Feed Solution) and a second liquid is diluted (so-called Draw Solution). If "pure" water is to be obtained, a second treatment stage is necessary to regenerate the draw solution. Due to its natural driving force, forward osmosis offers the potential for energy-efficient treatment of water from various sources. This makes it a promising process for further concentration of aqueous product and waste water streams. For this reason, the application possibilities and the potential of forward osmosis in the industrial water sector were examined in more detail within the scope of this thesis.

Within laboratory tests, forward osmosis treatment of different liquid streams of a dairy, an automobile production as well as a semiconductor production was examined. The core of the laboratory test set-up was a membrane test cell for flat sheet membranes with an effective membrane area of 48 cm². Special forward osmosis membranes from various manufacturers were used. The feed and draw solutions were circulated and increasingly concentrated or diluted during the course of the experiment. The permeate flow was determined by recording the change in mass. Conductivity measurements as well as analyses of the examined waters before and after the experiments allowed conclusions to be drawn about possible solute diffusion through the membrane. In addition to the laboratory tests, a model was developed and validated to simulate the experiments. Three partially adapted models from literature were used.

The average permeate fluxes achieved in the laboratory experiments with real industrial water depended mainly on the osmotic pressure difference between feed and draw solution. The permeate fluxes were between 0.1 and 19.4 L/(m²·h) for the automotive industry, between 7.9 and 21.0 L/(m²·h) for the dairy industry and between 10.5 and 33.4 L/(m²·h) for the semiconductor industry. The reverse solute fluxes determined were between 37.7 and 21.3 g/(m²·h), between 4.1 and 12.2 g/(m²·h) and between 8.0 and 40.9 g/(m²·h). Within modelling, the tests with waters from automobile production were simulated. For the most part, the permeate fluxes could be well represented. The calculation of the reverse solute fluxes sometimes showed large deviations from the actual measurements. Standardized membrane performance tests were used to evaluate

the development of permeate flux and to indicate fouling. Depending on the substances contained in the water, fouling occurred in the test series. In addition, deposits on the membrane surface were visible in some tests. However, the visible deposits did not always lead to a decrease in permeate flow. In an exemplary cleaning test, the membrane performance could be restored by rinsing with sodium hydroxide solution and hydrochloric acid.

As a result of this thesis, different forward osmosis application scenarios in the examined industrial enterprises could be developed. For economic reasons, those scenarios in which both the feed and the draw solution are industrial waters and two liquids are treated simultaneously in one step are of particular interest. The use of an artificial Draw Solution and its treatment is unnecessary in this case. Such application scenarios could be derived for dairy and semiconductor production. No suitable Draw Solution could be identified in the investigated automobile production, which is why only applications with an artificial Draw Solution are conceivable here. In general, the critical points when using forward osmosis are the reverse solute flux through the membrane, the deterioration of the membrane performance due to fouling and the economic efficiency of the process. More in-depth investigations are required here.

Kurzfassung

Membranfiltrationsverfahren wie die Mikro-, Ultra- und Nanofiltration sowie die Umkehrosmose werden häufig in der industriellen Wasseraufbereitung sowie Abwasserbehandlung eingesetzt. Sie nutzen einen hohen physikalischen Druckunterschied als Triebkraft, um Wasser durch eine semipermeable Membran zu pressen und gereinigtes Wasser zu erzeugen. Dafür sind große Energiemengen nötig. Im Gegensatz dazu ist die Vorwärtsosmose ein innovatives Membranfiltrationsverfahren, welches den natürlich vorkommenden osmotischen Druckgradienten zwischen zwei Flüssigkeiten nutzt, um einen Wasserfluss durch die semipermeable Membran zu erzeugen. Dabei wird eine Flüssigkeit mit niedrigem osmotischen Druck aufkonzentriert (sog. Feed Solution) und eine zweite Flüssigkeit verdünnt (sog. Draw Solution). Soll „reines" Wasser gewonnen werden, ist eine zweite Aufbereitungsstufe zur Regeneration der Draw Solution notwendig. Durch die natürliche Triebkraft bietet die Vorwärtsosmose das Potenzial zur energieeffizienten Behandlung von Wässern verschiedener Herkunft. Damit ist sie ein vielversprechendes Verfahren zur weitergehenden Aufkonzentrierung von wässrigen Produkt- und Abwasserströmen. Aus diesem Grund wurden die Einsatzmöglichkeiten und das Potenzial der Vorwärtsosmose im industriewasserwirtschaftlichen Bereich im Rahmen dieser Arbeit näher untersucht.

Im Rahmen von Laborversuchen wurde die Aufbereitung von verschiedenen Flüssigkeitsströmen einer Molkerei, einer Automobilproduktion sowie einer Halbleiterfertigung mittels Vorwärtsosmose untersucht. Kernstück der Laborversuchsanlage war eine Membrantestzelle für Flachmembranen mit einer wirksamen Membranfläche von 48 cm². Zum Einsatz kamen spezielle Vorwärtsosmosemembranen verschiedener Hersteller. Die genutzten Feed und Draw Solutions wurden im Kreislauf geführt und im Versuchsverlauf zunehmend aufkonzentriert bzw. verdünnt. Über die Erfassung der Masseänderung wurde der Permeatfluss bestimmt. Leitfähigkeitsmessungen sowie Analysen der untersuchten Wässer vor und nach den Versuchen ließen Schlussfolgerungen über eventuell auftretende Stoffdiffusion durch die Membran zu. Zusätzlich zu den Laborversuchen wurde ein Modell zur Simulation der Experimente erstellt und validiert. Dabei wurden drei, teilweise adaptierte, Modellansätze aus der Literatur verwendet.

Die durchschnittlichen Permeatflüsse, welche bei den Laborversuchen mit reellen industriellen Wässern erreicht wurden, hingen vorrangig von der osmotischen Druckdifferenz zwischen Feed und Draw Solution ab. Die Permeatflüsse lagen für die Automobilindustrie zwischen 0,1 und 19,4 L/(m²·h), für die Molkerei zwischen 7,9 und 21,0 L/(m²·h) und für die Halbleiterindustrie zwischen 10,5 und 33,4 L/(m²·h). Die ermittelten Salzrückflüsse betrugen zwischen 37,7 und 21,3 g/(m²·h), zwischen 4,1 und

12,2 g/(m²·h) sowie zwischen 8,0 und 40,9 g/(m²·h). Im Rahmen der Modellierung wurden die Versuche mit Wässern der Automobilproduktion nachgebildet. Dabei konnten die Permeatflüsse größtenteils gut dargestellt werden. Die Berechnung der Salzrückflüsse wies gegenüber den tatsächlichen Messungen mitunter große Abweichungen auf. Durch standardisierte Membranleistungstests konnte die Entwicklung des Permeatflusses evaluiert und Fouling nachgewiesen werden. In Abhängigkeit der Wasserinhaltsstoffe trat Fouling in den Versuchsreihen auf. Zusätzlich waren bei einigen Versuchen Ablagerungen auf der Membranoberfläche sichtbar. Jedoch führten die sichtbaren Ablagerungen nicht in allen Fällen zu einem Rückgang des Permeatflusses. In einem exemplarisch durchgeführten Reinigungsversuch konnte die Membranleistung durch Spülprozesse mit Natronlauge und Salzsäure wiederhergestellt werden.

Als Ergebnis der Arbeit konnten verschiedene Anwendungsszenarien für den Einsatz der Vorwärtsosmose in den untersuchten Industriebetrieben entwickelt werden. Hierbei sind aus wirtschaftlichen Gründen vor allem jene Szenarien interessant, bei denen sowohl die Feed als auch die Draw Solution industrielle Wässer sind und zwei Flüssigkeiten simultan in einem Schritt aufbereitet werden. Der Einsatz einer künstlichen Draw Solution und deren Aufbereitung ist in diesem Fall unnötig. Solche Anwendungsszenarien konnten für die Molkerei sowie die Halbleiterherstellung abgeleitet werden. In der untersuchten Automobilproduktion konnte keine geeignete Draw Solution identifiziert werden, weshalb hier lediglich Anwendungen mit einer künstlichen Draw Solution denkbar sind. Als kritische Punkte beim Einsatz der Vorwärtsosmose stellten sich der auftretende Salzrückfluss durch die Membran, die Verschlechterung der Membranleistung durch Fouling sowie die Wirtschaftlichkeit des Verfahrens heraus. Hier besteht weitergehender Forschungsbedarf.

Schlagwörter

Abwasserbehandlung, Automobilindustrie, Halbleiterindustrie, Industriewasserwirtschaft, Membranfiltration, Modellierung, Molkerei, Vorwärtsosmose

Acknowledgement

Danksagung

Content

1 Introduction

1.1 Background & Motivation

The availability of the resource water in sufficient quantity and quality is important for a sustainable development of ecologically progressive industries. Especially, the manufacturing industry depends on considerable quantities of water. After being used, this wastewater (so-called process water) must be treated to be either recycled or discharged. In the industrial context, resource efficiency plays an important role, e.g. through the use of sustainable ecological processes such as recycling processes, as well as economic efficiency, e.g. through energy savings, raw material recovery and low infrastructure costs.

Water recycling in industries has gained more and more importance due to different reasons. Among them are economic reasons, legal requirements, company's philosophy as well as water scarcity or insufficient wastewater disposal options. In some cases, water cycles are narrowed or even completely closed to achieve the state of zero liquid discharge (ZLD): a production without any liquid waste streams [1, 2].

Biological, chemical and physical water treatment processes are used in industrial water treatment processes [3]. Physical water treatment processes include membrane-based filtration processes. The conventional membrane processes are microfiltration (MF), ultrafiltration (UF), nanofiltration (NF) and reverse osmosis (RO). They use mechanical energy to generate high pressures in order to press water through the membrane and thus produce purified water [4]. Therefore, they require large amounts of energy. In addition, the maintenance and cleaning effort is enormous due to the high pressures and their consequences (e.g. fouling). This leads to high operating costs for water circulation in industrial plants.

In order to obtain more economic water recycling, it is necessary to develop new, innovative water treatment processes and to make them applicable for industry. Recently, membrane-based technologies were developed that use thermal, electrical and chemical energy sources instead of mechanical energy. These emerging technologies are membrane distillation (MD), membrane-capacitive deionization (MCDI), electrodialysis (ED), membrane contactors and forward osmosis (FO) [5]. An overview of membrane-based technologies for water treatment is given in Figure 1.

Instead of high pressures, forward osmosis (FO) uses the natural process of osmosis, which also takes place in plant and body cells, for the purification of water. In osmosis, two liquids are separated by a semi-permeable membrane, which is only permeable to water. If the two liquids have different salt concentrations and thus different osmotic pressures, water begins to diffuse through the membrane quasi automatically due to the

difference in osmotic pressure (Δπ) until an equilibrium is reached and both liquids have the identical salt concentration (Figure 2a).
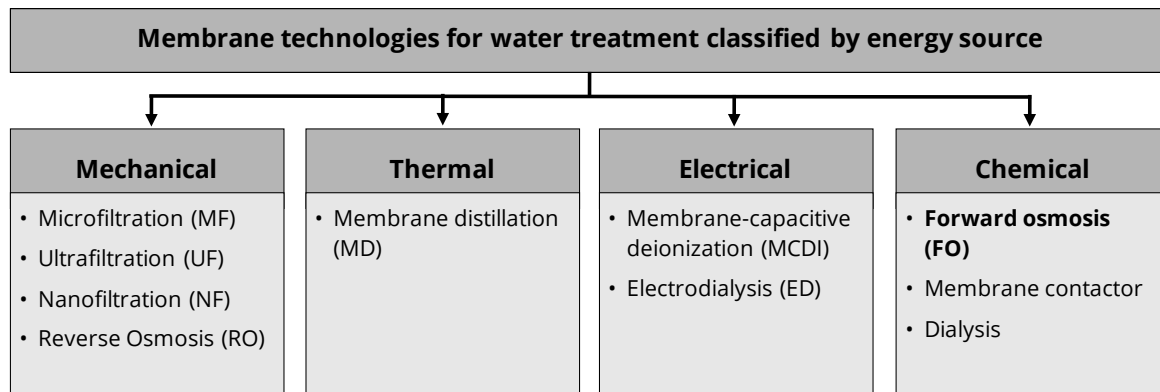
Figure 1. Membrane technologies for water treatment classified by energy source.

In forward osmosis, the osmotic pressure difference is used technically. Water diffuses from a feed solution (FS) with low osmotic pressure, e.g. industrial process water, into the draw solution (DS), which has a high osmotic pressure (Figure 2b). During FO process, the feed solution is concentrated and the draw solution is diluted. If desired, the draw solution can be regenerated after forward osmosis. In this case, the final product is clean water suitable for reuse and the draw solution can be recycled. The concentrated feed solution can be effectively further treated or recycled.
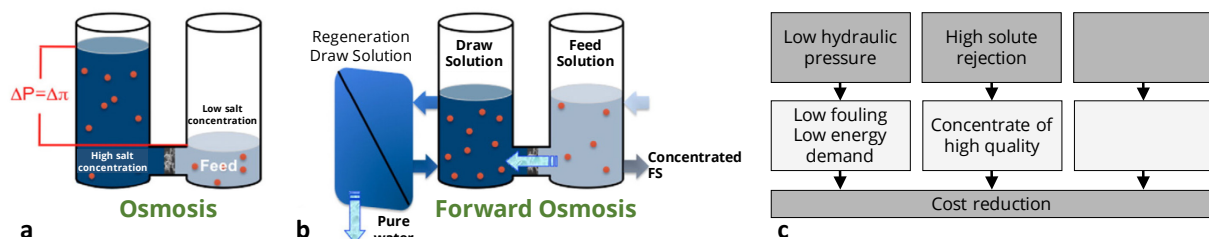
Figure 2. Working principle of osmosis (a) and forward osmosis (b) [3]; forward osmosis advantages (c) [6]

In contrast to conventional pressure-driven membrane processes, forward osmosis is only driven by the difference in concentration between the feed and draw solution. In addition to the lower energy requirement, this results in a significantly lower "risk of clogging" due to the formation of deposition layers or fouling and thus significantly lower maintenance costs. This, together with the advantages mentioned in Figure 2c, results in reduced operating costs and thus improved economic efficiency for the company.

With the increasing interest of the media, politics and society in researching and reducing anthropogenic environmental influences in recent years, the topic of forward osmosis has also attracted increasing attention as a field of research [6, 7]. The results are commercial forward-osmosis technologies, e.g. in drinking water treatment, the treatment of waste water from oil and gas production, landfill leachate treatment and the

treatment of concentrates from biogas plants [6–8]. So far, however, forward osmosis has not been used to treat industrial wastewater, which is why there is a great need for research.

For this reason, possible FO application scenarios and FO performance in industrial water management were investigated for different industrial branches. The results of which are presented in this thesis.

1.2   Objective & Approach

The objective of this thesis was to investigate the applicability of forward osmosis process in industrial water management in order to establish a sustainable and economically advantageous process for industrial process water treatment. The following questions were addressed:

- Which wastewaters, process waters or effluents are suitable for FO treatment?
- In which industrial branches can FO be reasonably applied?
- Which permeate flux is feasible?
- Which solute flux occurs through the membrane either from DS to FS but also from FS to DS?
- To what extent does membrane fouling and blocking influence the process?
- Which operating parameters have to be set?

Finding adequate answers to this research questions was accomplished through:

- in-depth literature research and evaluation,
- proof-of-principle studies for exemplary industries,
- modelling of FO process.

The literature research focused on the state of art regarding FO application in manufacturing industries to see for which industrial branches FO application had already been investigated to which extent. Moreover, it focused on FO technology itself including advantages and disadvantages and the state of commercial implementation.

Since, industrial wastewater differs strongly depending on the type of industrial branch, it was decided to investigate the FO application for exemplary branches. Thus, proof-of-principle studies were conducted for three exemplary industrial branches, which were dairy industry, automobile industry and semiconductor industry. The studies based on the corporation with one company of each branch. In a first step, the wastewater situation of the companies was evaluated to find suitable effluents to be treated by FO either as FS

or DS. Here, analytical data was used to characterize the different effluents and determine the osmotic pressure. Furthermore, the companies gave information about effluents that were rather difficult to treat with conventional treatment methods and effluents where a concentration or dilution would be favorable. After identifying potential FS and DS, experiments were conducted with a lab-scale FO set-up using samples of the effluents. Different combinations of FS and DS were tested and evaluated. However, only FS and DS from one company were combined to make sure that the combined treatment would also be feasible in practice.

In addition to the experiments, different FO models were taken from literature and partly adapted, to describe the FO process. These models were evaluated with the data from the FO experiments with effluents from the automobile industry.

1.3   Structure

According to the research approach outlined above, the thesis is split into four main parts. First, the state of the art of FO application in wastewater treatment of manufacturing industries is described (chapter 2). Here, information is also given about the working principle of FO, advantages and disadvantages of the technology, companies working in FO, and the state of FO implementation. Second, the results of lab-scale FO experiments with wastewaters from semiconductor industry, dairy and automobile industry are presented (chapters 3 and 4). In these chapters, the lab-scale FO setup and the experimental procedure are described in detail and the results are evaluated. Third, developed FO models and their evaluation with experimental results are described (chapter 5). Finally, all results are compared and evaluated before final conclusions are drawn about potential FO application for industrial wastewater treatment (chapter 6). The structure of this thesis is illustrated in Figure 3. The corresponding chapters are indicated with { }.
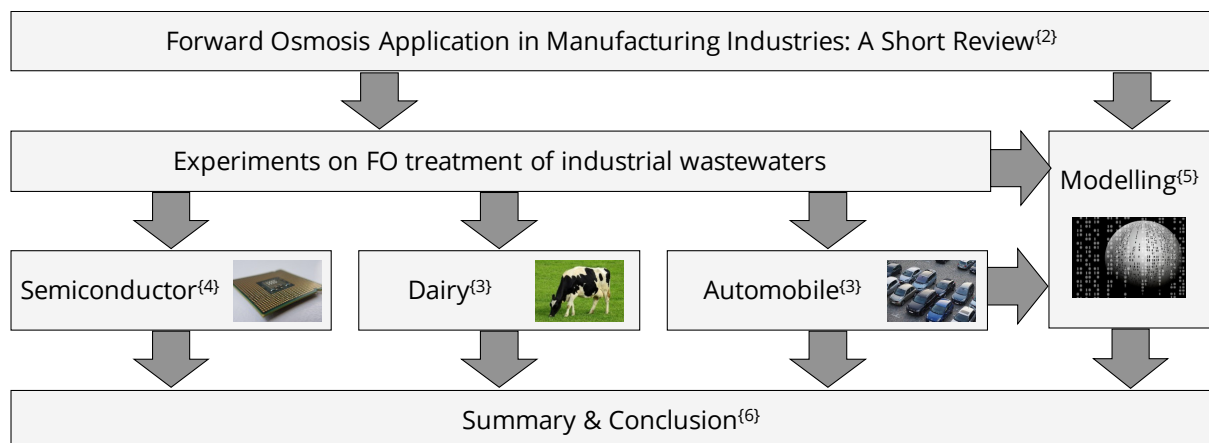
Figure 3. Schematic outline of thesis structure. Corresponding chapters are indicated in { }.

The chapters 2, 3, 4, and 5 of this thesis are based on four peer-reviewed journal publications which are listed below:

- Haupt, Anita and André Lerch. Forward osmosis application in manufacturing industries: A Short Review. *Membranes* 8, 3 (2018): 47. https://doi.org/10.3390/membranes8030047.

- Haupt, Anita and André Lerch. Forward osmosis treatment of effluents from dairy and automobile industry – Results from short-term experiments to show general applicability. *Water Science and Technology* 78, 3 (2018): 467–75. https://doi.org/10.2166/wst.2018.278.

- Haupt, Anita and André Lerch. Forward osmosis application for semiconductor wastewater. *Manuscript*.

- Haupt, Anita, Christian Marx and André Lerch. Modelling forward osmosis treatment of automobile wastewaters. *Membranes* 9, 9 (2018): 106. https://doi.org/10.3390/membranes9090106.

References of Chapter 1

1. Götz, G.; Teschke, P.; Netzel, L.; Geißen, S.-U. Zero Liquid Discharge für eine abwasserfreie Industrieproduktion. *Chem. Ing. Tech. 0.*

2. Muhammad Yaqub; Lee, W. Zero-liquid discharge (ZLD) technology for resource recovery from wastewater: A review. *Sci. Total Environ.* **2019**, *681*, 551–563.

3. Bhandari, V.M.; R. *Industrial wastewater treatment, recycling, and Reuse /*; IChemE; Butterworth-Heinemann: Oxford [u.a.], 2014; ISBN 978-0-08-099968-5.

4. Pinnekamp, J. *Membrane Technology for Waste Water Treatment*; FiW-Verlag, 2006; ISBN 978-3-939377-01-6.

5. Basile, A.; Cassano, A.; Rastogi, N.K. *Advances in Membrane Technologies for Water Treatment: Materials, Processes and Applications*; Elsevier, 2015; ISBN 978-1-78242-126-9.

6. Cath, T.Y.; Childress, A.E.; Elimelech, M. Forward osmosis: Principles, applications, and recent developments. *J. Membr. Sci.* **2006**, *281*, 70–87.

7. Lutchmiah, K.; Verliefde, A.R.D.; Roest, K.; Rietveld, L.C.; Cornelissen, E.R. Forward osmosis for application in wastewater treatment: A review. *Water Res.* **2014**, *58*, 179–197.

8. Coday, B.D.; Xu, P.; Beaudry, E.G.; Herron, J.; Lampi, K.; Hancock, N.T.; Cath, T.Y. The sweet spot of forward osmosis: Treatment of produced water, drilling wastewater, and other complex and difficult liquid streams. *Desalination* **2014**, *333*, 23–35.

2 Forward Osmosis Application in Manufacturing Industries: A Short Review

Anita Haupt and André Lerch, *Membranes* **2018**, *8*, 47.

Abstract

Forward osmosis (FO) is a membrane technology that uses the osmotic pressure difference to treat two fluids at a time giving the opportunity for an energy-efficient water and wastewater treatment. Various applications are possible; one of them is the application in industrial water management. In this review paper, the basic principle of FO is explained and the state-of-the-art regarding FO application in manufacturing industries is described. Examples of FO application were found for food and beverage industry, chemical industry, pharmaceutical industry, coal processing, micro algae cultivation, textile industry, pulp and paper industry, electronic industry, and car manufacturing. FO publications were also found about heavy metal elimination and cooling water treatment. However, so far FO was applied in lab-scale experiments only. The up-scaling on pilot- or full-scale will be the essential next step. Long-term fouling behavior, membrane cleaning methods, and operation procedures are essential points that need to be further investigated. Moreover, energetic and economic evaluations need to be performed before full-scale FO can be implemented in industries.

2.1   Introduction

2.1.1   Demand for Innovative, Energy-Efficient Water and Wastewater Treatment

Many of the sustainable development goals (SDG), provided by the United Nations in 2015, are related to a sufficient water supply [1, 2]. Agriculture consumes 70% of the world's freshwater, followed by industry that consumes 19% [3]. For this reason, efficient water usage in agriculture but also in industrial production processes is necessary to achieve all SDG. Industries nowadays apply treatment technologies to treat water and wastewater. Often, recycling of water is accomplished and freshwater demand as well as wastewater amounts are reduced. However, most treatment technologies consume large amounts of energy [4]. Aiming for sustainability, the energy efficiency of water and wastewater treatment needs to be improved.

Membrane filtration processes are often used in water recycling processes. Conventional membrane technologies are micro-, ultra-, and nano-filtration as well as reverse osmosis (MF, UF, NF, RO). They use a transmembrane pressure difference which is generated by pumping. Thus, water molecules pass through the membrane and impurities are rejected. The energy demand of these pressure-driven membrane processes is very high. In contrast to that, forward osmosis (FO) is a membrane technology that uses the osmotic pressure difference between two solutions to generate a water flow through the membrane [4]. Therefore, only little external energy is required and energy-efficient water treatment is achieved [5]. Membrane filtration processes are often applied off-line or off-site in relation to the regular production processes. More beneficial, however, is the application in-situ or in-line enabling direct recovery and recycle of resources or water. Several examples in various fields, including forward osmosis, have been published [6–9].

For these reasons, forward osmosis is potentially applicable in industrial water treatment to enhance energy efficiency. It might even be applied for wastewaters that so far cannot be treated by pressure-driven membrane technologies [10]. Since there is a large variety of industrial wastewaters, FO might also be suitable to treat two wastewaters in only one treatment step providing one concentrated wastewater and one diluted wastewater. This energy-efficient combination could lead to an optimized, more economic water and resources management in industries.

In order to show the current state of the art, a literature review was performed about forward osmosis application in manufacturing industries. The results of which are presented in this paper. There are numerous other literature reviews about forward osmosis in general [4, 10–17] or special aspects, e.g., membrane fouling [18–20], membrane characteristics [21], draw solutions [22–24], hybrid processes [25, 26], application in seawater desalination [27–31], application in wastewater treatment [32], application in produced water treatment [33, 34], application in food processing [35],

application for resource recovery from municipal wastewater [36], and osmotic membrane bioreactors [37].

2.1.2   Forward Osmosis Technology

Forward osmosis is a technology that uses a membrane to treat two liquid streams. Figure 1 illustrates the operating principle. On one side of the membrane is the so-called feed solution (FS). The FS has a low osmotic pressure. On the other side of the membrane is the so-called draw solution (DS) that has a higher osmotic pressure. A semi-permeable membrane separates FS and DS. Due to the difference in osmotic pressure, water passes through the membrane from the FS to the DS side. This diffusing water dilutes the DS; simultaneously, the FS is concentrated. Usually, no physical pressure is needed. Therefore, the only energy demand results from the pumping of FS and DS through the flow channels next to the membrane. Compared to other treatment technologies, FO offers the following advantages:

- low energy consumption,

- simultaneous treatment of two streams in one treatment step,

- easy removability of fouling layers due to absence of compression,

- treatment of liquids that are not suitable for other membrane processes.
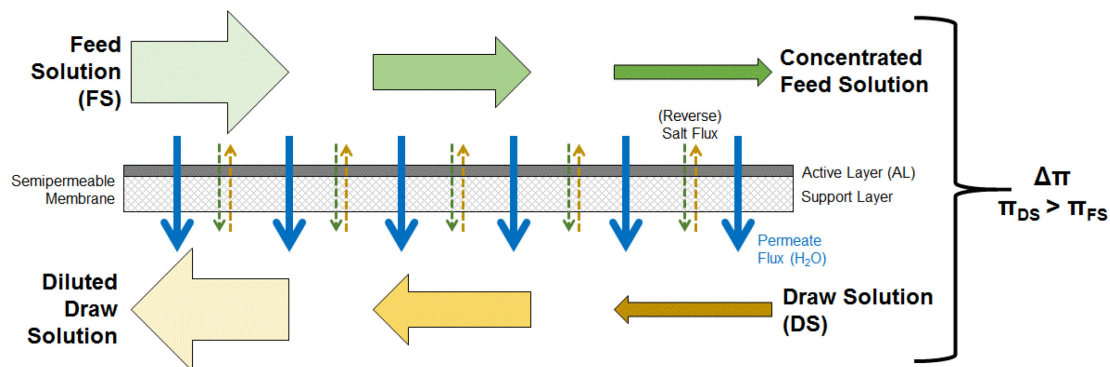
Figure 1. Schematic illustration of the forward osmosis process with membrane active layer facing towards the feed solution (ALFS or FO-mode).

An important aspect in FO operation is the concentration polarization (CP) and its influence on the water passing through the membrane (permeate flux) [38]. Concentration polarization describes the fact that due to the water flux through the membrane FS is concentrated on the membrane surface. This phenomenon also occurs in conventional membrane filtration processes such as RO. In FO it is called concentrative CP. The difference in FO is that on the other side of the membrane, DS is diluted and so-called dilutive CP takes place. Due to CP, the real effective osmotic pressure gradient is lower than the osmotic pressure difference between inlet FS and DS. Thus, permeate

fluxes are lower than expected. Concentration polarization occurs on the membrane surface (external concentration polarization ECP) and within the porous support layer of the membrane (internal concentration polarization ICP).

FO membranes usually consist of an active layer (AL) and a porous support layer (SL). The membrane can either be used with active layer facing the FS (ALFS or FO mode) or with active layer facing the DS (ALDS or PRO mode). In ALDS mode, concentration polarization is less severe and permeate fluxes are higher [38]. However, in many cases the ALFS mode is used because fouling can be removed easier from the dense active layer than from the porous support layer [38].

An effect occurring during FO treatment is the so-called reverse salt flux. This term describes that substances from the DS diffuse into the FS through the membrane due to concentration differences, possibly changing FS composition [9].

In FO process, the FS is concentrated and the DS is diluted. In some cases, two liquid streams might be combined where these effects are desired. Then, no additional technology is needed. In many cases however, an artificial DS is used and recycled. For this, the DS has to be concentrated after FO and a regeneration step is required (Figure 2) [7, 8]. Pure water is obtained as a valuable product. Those combined technologies are often referred to as "FO hybrid technologies". In contrast, the term "direct FO application" is used in this review paper to describe cases where no DS regeneration is necessary.
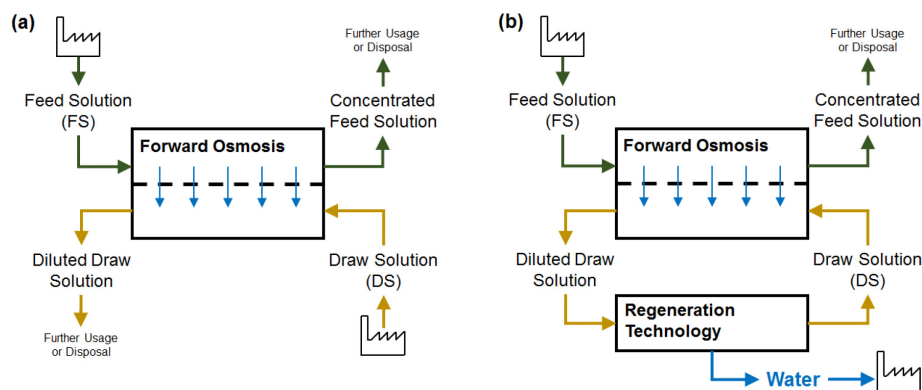
Figure 2. FO process with direct usage of FS and DS (**a**); FO process with DS regeneration step (**b**).

Potential regeneration steps are all technologies that somehow recover water from a solution. They are evaporation, heating, membrane distillation, and pressurized membrane technologies (e.g., RO) [26]. Furthermore, there are studies where the DS substance is extracted from the diluted DS, e.g., by magnetic field or electric current application [22]. The DS regeneration strongly depends on the used DS. Since additional treatment technologies require energy, the overall energy demand of hybrid FO processes has to be taken into consideration. In one example for seawater desalination, the specific energy demand is 2.5–4.0 and 1.3–1.5 with conventional RO and FO with low

pressure RO, respectively [39]. Mazlan et al. stated that for seawater desalination with 75% water recovery the energy demand is 2.3 kWh/m3 using two-stage RO; applying FO with different DS types and regeneration technologies it is between 1.2 and 3.3 kWh/m³ [5]. FO alone requires less than 0.25 kWh/m³ energy [40]. For this reason, an energy-efficient regeneration of a suitable DS is crucial for FO hybrid processes.

The high osmotic pressure of the DS is usually achieved through high concentrations of solutes. In some applications, combined treatment of two (waste) water streams might be possible. Here, no synthetic DS would be necessary. However, in other applications, only one water stream is treated by FO and an artificial DS is necessary.

Johnson et al. summarize the current state of knowledge about synthetic DS [22]. A suitable DS has to be chosen considering osmotic pressure, viscosity, reverse salt flux, internal concentrative polarization, availability, costs, regeneration, and toxicity. Potential synthetic DS are:

- gases and volatile compounds,

- inorganic draw solutes (e.g., salts),

- organic draw solutes (e.g., sugar, organic ionic liquids, switchable polarity solvents (SPS), organic ionic salts, polyelectrolytes, polymers, hydrogels),

- functionalized nanoparticles.

Besides the "normal" forward osmosis process, there are similar FO-related processes that somehow utilize physical pressure. They are pressure-assisted or pressure-enhanced osmosis (PAO or PEO), and pressure-retarded osmosis (PRO) (Figure 3).
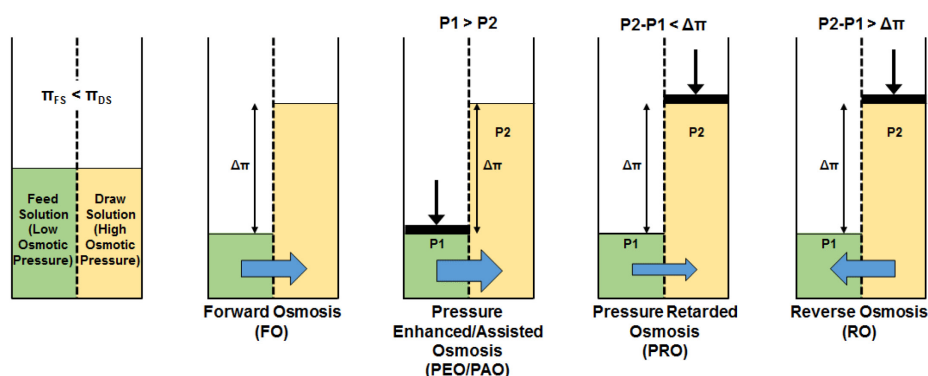
Figure 3. Osmotic membrane technologies (reprinted from [41] with permission from author).

In the 1970s, first FO experiments used RO membranes [42, 43]. However, FO permeate fluxes were very low because of the high concentration polarization and no more efforts were made to establish forward osmosis as water treatment technology. This is because RO membranes usually have two layers: a dense active layer and a porous support layer [44]. The support layer requires a certain thickness due to the necessity to withstand high

physical pressures. Due to the thick support layer, internal CP is very high in FO application producing only low permeate fluxes.

In the course of ongoing membrane development, special FO membranes were developed with a thinner support layer [21, 45, 46]. As no high hydraulic pressure occurs in FO, the support layer does not need to be as thick as in RO. With a thinner support layer, concentration polarization decreases allowing higher permeate fluxes. Since 2004, the number of scientific publications on forward osmosis has increased rapidly (Figure 4). This shows that FO is of high interest having the potential to treat water and wastewater efficiently. Still, the wastewater that originates from membrane manufacturing itself has to be taken into account when considering overall process sustainability [47].
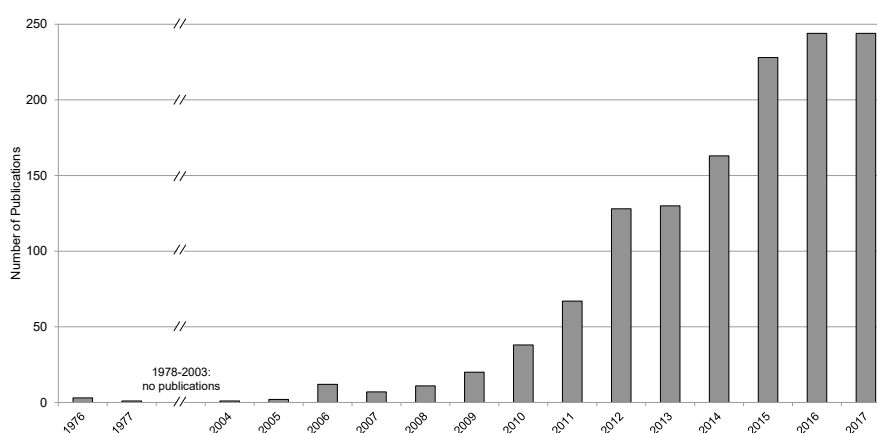
Figure 4. Number of annual publications on forward osmosis (Database: Google Scholar; searching exact phrase "forward osmosis" in the title of the article; patents and citations excluded).

2.2   Forward Osmosis Application—State of Implementation

2.2.1   Bench- and Lab-Scale

Reported bench- or lab-scale FO set-ups are usually very similar (Figure 5). They include a membrane test cell with a FS and DS circulation loop driven by pumps. The membrane test cells mostly include a flat sheet membrane sample and a flow channel on both sides of the membrane. Spacers are sometimes used in the flow channels. The membrane active layer can be placed either towards the FS (ALFS or FO mode) or towards the DS (ALDS or PRO mode). FS and DS flow velocity is usually adjusted via the circulation pumps and flow rate measurement. FS and DS can flow concurrently or counter-currently in the flow channels, resulting in different development of osmotic pressure difference along the membrane. Theoretically, membrane test cells could also be constructed to enable cross-current flow. However, to the authors' knowledge no such test cell has been used in lab-scale experiments for industrial wastewater application so far.

FS and DS are stored in containers of varying sizes and pumped through the test cell back into the containers, the contents of which are usually stirred. In the course of FO experiment, water permeates from the FS into the DS. Thus, using this type of batch experiment, FS is concentrated and DS is diluted and the osmotic pressure difference across the membrane decreases. In some cases, DS concentration is kept constant by dosing DS concentrate into the DS container, either continuously or periodically. Often DS conductivity measurements control this dosage. This way, only the FS osmotic pressure increases and the osmotic pressure difference between FS and DS declines more slowly. Occasionally, water baths or other devices are used to control the FS and DS temperature.
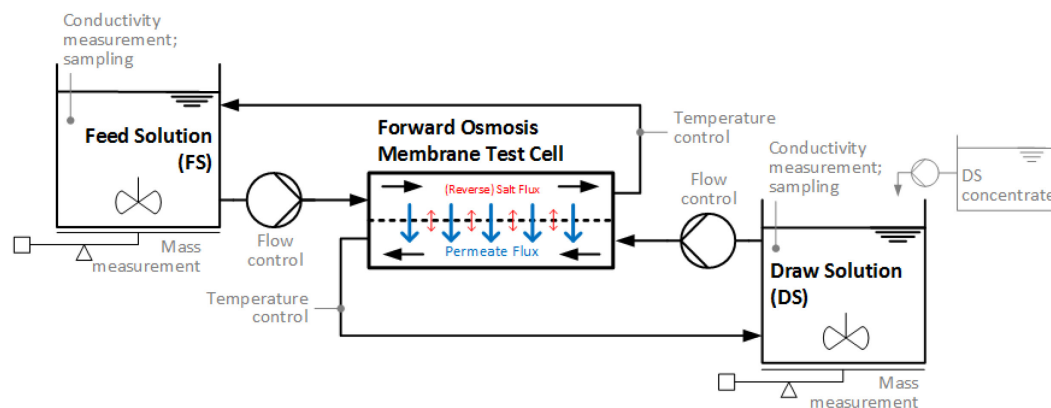
Figure 5. Typical lab-scale forward osmosis set-up (optional parts in grey).

FS or DS mass measurements deliver data for permeate flux calculation. Conductivity measurements or sample analyzes provide information about FS and DS composition and substance fluxes through the membrane (e.g., reverse salt flux). Since membrane test cells often consist of acrylic glass, the membrane surface can be monitored during the experiments.

Two different FO lab-scale set-ups are illustrated in Figure 6. Here, either the FS or both FS and DS are not circulated but stored directly above or beside the membrane. In the first published research paper dealing with FO application in manufacturing industry, a lab-scale set-up is described which is similar to the one illustrated in Figure 5. Only the DS and FS were not circulated but passed through the membrane test cell only once [42, 43].
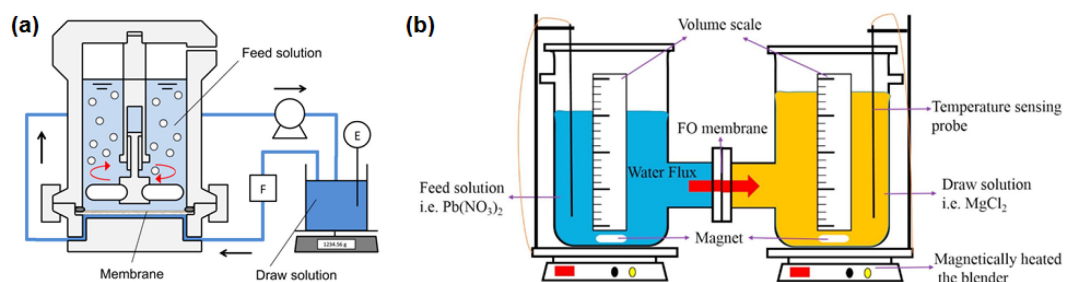
Figure 6. FO laboratory set-up (**a**) without FS circulation [48] and (**b**) without FS and DS circulation [49] (reprinted with permission from Elsevier).

Within this review paper, 51 original research papers were found and evaluated that dealt with FO application in manufacturing industry. All of these research results are based on lab-scale experiments. Figure 7 shows a summary of the different lab-scale set-ups comparing initial FS and DS volume, flow features through the membrane test cell, membrane characteristics, and duration of experiments.
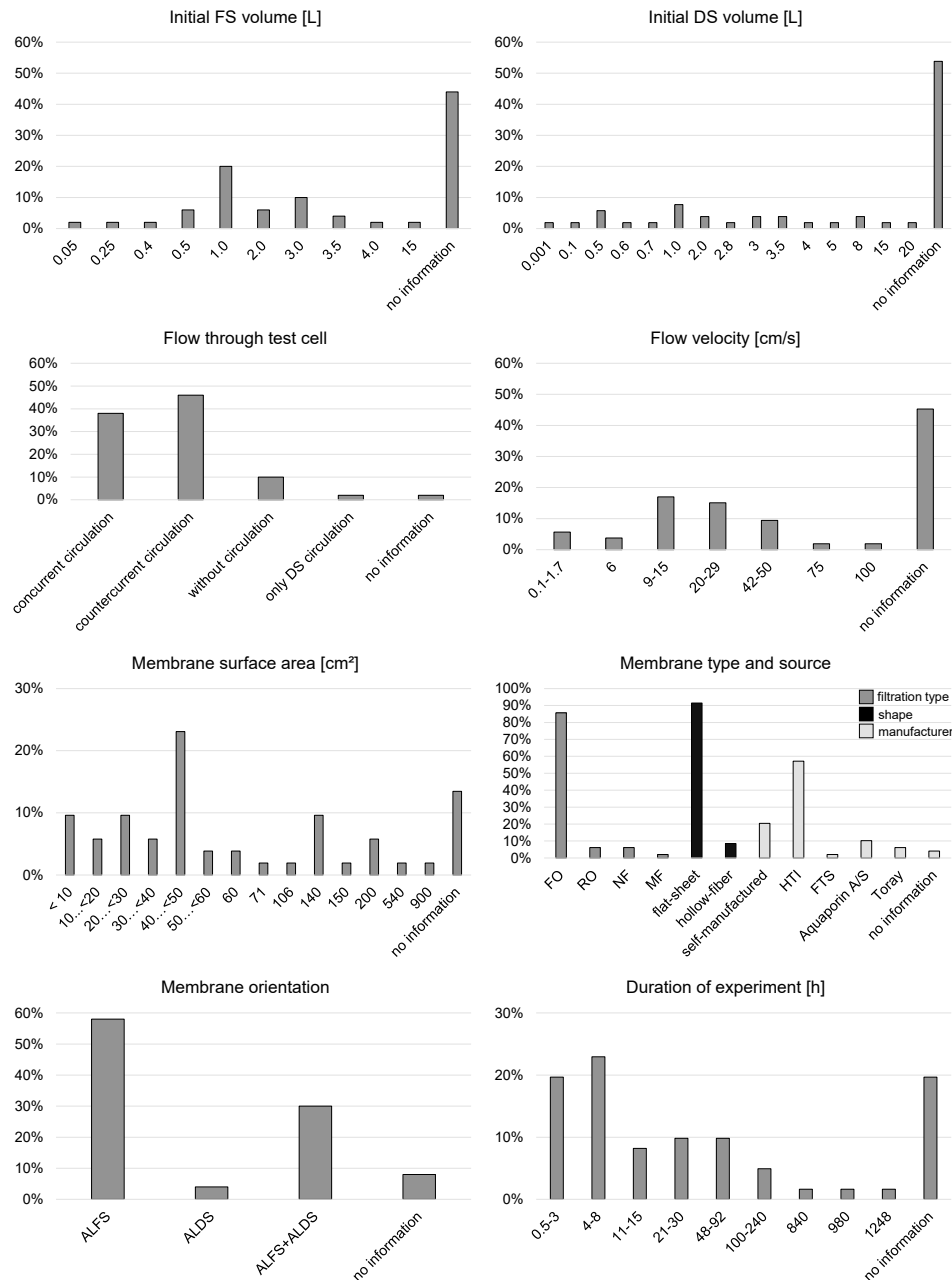
Figure 7. Evaluation of different FO lab-scale set-ups based on 51 original research papers.

Initial FS and DS volume was 0.05–15 and 0.001–20 L, respectively. The smallest initial DS volume of 0.001 L results from an experiment where coal powder was directly applied on the membrane surface [50]. The smallest initial liquid DS volume is 0.1 L. However, in 44% and 54% of the papers no information was given about the initial FS and DS volume, respectively.

As mentioned above, FO lab-scale set-ups usually have FS and DS circulation. Only 10% of the experiments were conducted without circulation. FS and DS were circulated concurrently in 38% and countercurrently in 46% of the included experiments. Flow velocity across the membrane was set to be between 0.1 and 100 cm/s. Mostly, flow velocities between 9 and 50 cm/s were chosen though. 45% of the papers did not give information about the flow velocity although it is an important parameter. Only the flow rate of FS and DS was given in many papers. However, without information about the flow channel dimensions, this parameter cannot be compared to other experiments.

The active membrane surface area ranged from 1.33 up to 900 cm². Still, in 13% of the papers this information is missing. The majority of experiments were conducted with a membrane surface area between 40 and 50 cm². Nearly all FO experiments used flat-sheet FO membranes. 20% of the membranes were self-manufactured and 76% were commercial membranes. HTI (Hydration Technology Innovations, LLC, Albany, OR, USA), a company, which to the authors' knowledge has gone out of business, delivered most of the commercial membranes (57%). Other commercial suppliers were Aquaporin A/S (Kongens Lyngby, Denmark), Toray Korea Chemicals Inc. (Seoul, Korea), and FTS (Fluid Technology Solutions, Inc., Albany, OR, USA). The membranes were applied in ALFS mode in 58% or both in ALFS and ALDS mode in 30% of the experiments. Just 4% of the experiments were conducted with ALDS membrane orientation only.

Duration of experiments was reported to be between 0.5 and 1248 h. The majority of experiments lasted 0.5 to 8 h. The longest FO experiments lasting one month or longer were all related to biological processes like microalgae cultivation or biological wastewater treatment. The experiment duration is not exactly mentioned in 20% of the papers.

Due to the different lab-scale set-ups, the results of the papers cannot be compared easily. Especially, permeate fluxes are presented in different ways ranging from average permeate fluxes to start and end permeate fluxes. For this reason, permeate fluxes are not included in this summarizing evaluation but are given in the more detailed description in chapter 2.3 as well as in the Supplementary Material. The partial incomplete description of experimental parameters complicates repetition of experiments with comparable parameters, too. The parameters that should always be indicated are listed in Table 1.

Table 1. Parameters to be indicated with lab-scale forward osmosis experiments.

Feed Solution	Draw Solution	Membrane	Operation
• type • initial volume	• type • initial volume	• type • supplier • active surface area • orientation (ALFS/ALDS)	• type of circulation (concurrent, countercurrent etc.) • Flow velocity across membrane (or flow rate and flow channel dimensions) • duration of experiment • cleaning procedures

2.2.2   Pilot-Scale

Pilot-scale investigations are necessary to prove the technical practicability of forward osmosis. One pilot-scale plant, which is shown in Figure 8, is operated by the working group of Prof. Shon in Sydney [51, 52]. The overall layout is similar to the one for the lab-scale experiments. It contains two spiral wound FO membrane modules with one 8" FO element each. The FO modules are operated in parallel. Different FO membrane modules have been used:

- two CTA FO modules from HTI (20.2 m²) [51],
- CTA FO module from HTI (9 m²) [52, 53],
- TFC FO module from Toray Chemical Korea Inc. (15 m²) [52].

A nanofiltration module is intended for DS regeneration [51]. Although the system is designed for continuous operation, FO and NF have so far been operated batch-wise. During FO treatment, the volume of DS increases due to permeate flux. The volume of FS decreases but is kept constant by adding fresh FS continuously. Thus, the FS concentration increases slightly during FO operation. The volumes of the FS and DS tank are 5000 L.

The pilot-scale plant was used for experiments on FO application in fertigation, brackish water desalination and coal mining wastewater treatment [51, 53]. It has not been used in manufacturing industries yet.
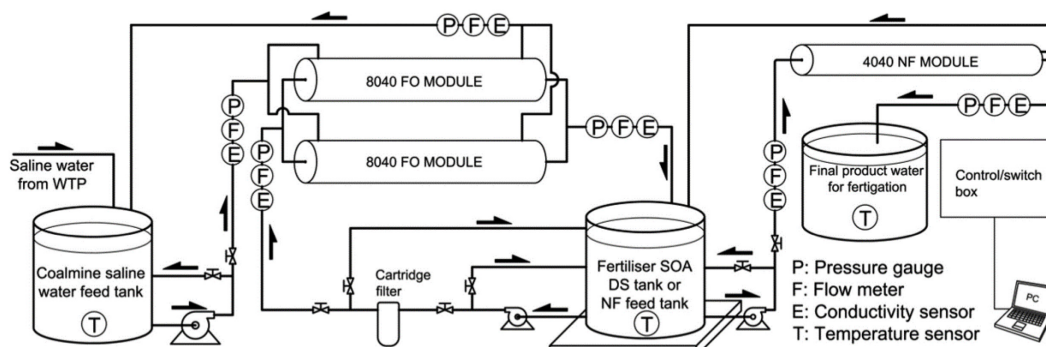
Figure 8. FO pilot-scale plant (reprinted from [51] with permission from Elsevier).

In 2018 two studies have been published about pilot-scale investigations on plate-and-frame FO elements from Porifera, Inc. (Hayward, CA, USA) [54,55]. Proprietary flat-sheet membranes are arranged in membrane plates to enable a cross-current flow of FS and DS. Up to six elements can be combined in one module. A spacer in the FS channel is optional. The active layer of the membrane is facing the FS. These plate-and-frame elements have a lower packing density compared to spiral wound FO elements. Due to their simple flow channel configuration, wastewater with foulants or high viscosity is supposedly treated more easily. Figure 9 illustrates the flow channel configuration in a spiral wound FO element and a plate-and-frame FO element.
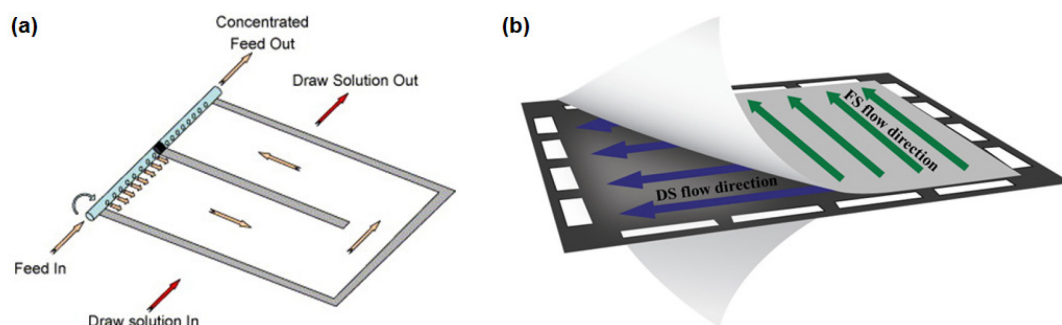
Figure 9. Flow channel configuration in (**a**) spiral wound FO element [4] and (**b**) plate-and-frame FO element (reprinted from [54] with permission from Elsevier).

Song et al. used one single plate-and-frame FO element with a membrane area of 7 m² consisting of 14 membrane sheets and performed regular FO experiments as well as pressure assisted FO experiments [54]. The experiments focused mainly on operating parameters, not on a special FO application case. Thus, mainly tap water was used as feed and draw solution, sometimes with an increased osmotic pressure. However, it is not mentioned which substance was used to increase the osmotic pressure of the tap water.

Lee et al. used three FO modules with one, three, and six plate-and-frame elements, respectively [55]. The membrane area of one element was 7 m². Since the three and six element modules could be run in series, a maximum membrane area of 63 m² was achieved. Tap water and sodium chloride solution with varying concentrations were the FS and DS to investigate different operating parameters. Real FO application was not investigated.

Within the research project "INSPIREWATER" funded by the European Union, lab-scale as well as pilot-scale studies on FO application in the chemical industry are conducted [56–58]. Chemical wastewater is first treated in an activated sludge plant. The effluent is then filtered by ultrafiltration and filtrate is lead to a reverse osmosis step. RO concentrate is further concentrated by FO using a synthetic DS (1 M NaCl, $MgCl_2$, Na_2SO_4) which is regenerated by another RO step or membrane distillation. Furthermore, a second FO will be investigated for further concentration of concentrated FS from the first FO. So far, only results from lab-scale experiments have been published and are discussed in chapter 2.4.3 [57].

Information on pilot-scale FO application can also be found on websites from FO companies. Forward osmosis application in the semiconductor industry will be investigated on pilot-scale in a project run by the companies Darco Water Technologies Ltd. (Singapore) and Aquaporin (A/S) [59]. Based on a successful proof-of-principle study, semiconductor wastewater streams will be treated by FO in a pilot project.

An application of forward osmosis in dairy industry is the dewatering of raw milk. If raw milk was dewatered right after the milking process before transportation to the dairy

plant, transportation costs and emissions could be reduced. The U.S. company Porifera Inc. (USA) report that they operated a pilot plant to treat 45,000 kg/h milk with their patented FO system [60]. The milk was concentrated 4 times producing 11,250 kg/h milk concentrate. Compared to a thermal evaporation process, FO could save 44% energy, 24% steam, 80% investments costs (CAPEX), and 50% operating costs (OPEX). Forward osmosis application in a dairy from ARLA Food in Denmark is currently investigated on pilot-scale, as reported by the Danish company Aquaporin A/S [61]. Unfortunately, no detailed information is given.

2.2.3   Industrial Scale

So far, FO application for industrial scale has rarely been reported. The British company Modern Water plc reports on its website about building a commercial FO plant in Al Khaluf (Oman) where seawater is desalinated for drinking water purposes. Another Modern Water seawater desalination plant (500 m³/d) is being constructed and will start operation in the beginning of 2018 [62–64]. Oasys Water Inc. (Cambridge, MA, USA) states on its website the construction of a commercial FO plant to treat 630 m³/d wastewater from a power plant [65]. In combination with other treatment technologies, a zero liquid discharge (ZLD) concept shall be realized.

There are a few companies worldwide offering commercial FO systems. They are (in alphabetical order):

- Aquaporin A/S (Kongens Lyngby, Denmark) [66, 67],
- Aquaporin Asia Pte. Ltd. (Singapore) [68, 69],
- BLUE-tec BV (Renkum, The Netherlands) [56, 70],
- Darco Water Technologies Ltd. (Singapore) [71, 72],
- De.mem Ltd. (Singapore) [73],
- Fluid Technology Solutions, Inc. (FTS, Albany, OR, USA) [74],
- Hydration Technology Innovations, LLC (HTI, Albany, OR , USA)—meanwhile out of business [52],
- Modern Water plc. (London, UK) [62–64],
- Oasys Water, Inc. (Cambridge, MA, USA) [75, 76],
- Porifera, Inc. (Hayward, CA, USA) [55],
- Toray Chemical Korea, Inc. (Seoul, Korea) [52],
- Trevi Systems, Inc. (Petaluma, CA, USA) [77],
- W.O.G. Technologies Pte Ltd. (Singapore) [69].

2.2.4   Fields of Forward Osmosis Application

Investigation of forward osmosis application ranges from lab-scale experiments (with either synthetic or real water) to full-scale implementation (with real water) and covers many fields, including:

- seawater desalination to produce drinking water [62–64],

- emergency water supply with so-called hydration bags [78],

- treatment of wastewater from oil and gas production as well as from mining [34, 79–82],

- agricultural use for fertigation [83–85],

- biological wastewater treatment with osmotic membrane bioreactors [37, 86–89],

- treatment of anaerobic digester centrate [90, 91],

- microbial fuel cells [92–98],

- removal of trace organic compounds [99–104].

As can be seen, different types of water are subject for FO application. Another field of FO application might be the treatment of industrial effluents and wastewaters as they occur in manufacturing industries. Here as well as in other applications, energy efficient and economic treatment technologies are of great interest.

2.3   Application of Forward Osmosis Technology in Manufacturing Industries

2.3.1   Overview

The first research about FO application related to industries was published in the 1970s [42, 43]. Here two lab-scale plants (13 and 58 cm² membrane surface area) and a pilot-scale plant were constructed. Deionized water, copper solution, chromium solution, and wastewater from a fish and shell fish processing plant were used as FS. DS were synthetic seawater and concentrated sugar solution. 10 commercial RO membranes and one self-manufactured CTA membrane were tested. FO experiments were run without FS and DS circulation. Since the highest permeate flux in the lab-scale experiments was only 4.5 L/(m²·h), no pilot-scale experiments were conducted. Substance diffusion through the membrane, either from DS into FS or from FS into DS, was very high. The research project was stopped because no suitable FO membranes were available.

From 1977 until 2004, no articles were published about forward osmosis. Since 2004, FO research and publications have increased rapidly. FO technology was further developed and first industrial scale applications were realized, e.g., in seawater desalination.

Because of its benefits, FO technology might also be beneficial for industrial wastewater treatment. This paper gives an overview about the current FO application in industries, focusing on manufacturing industries. The following branches are included:

- food and beverage industry,
- chemical industry,
- pharmaceutical industry,
- coal processing industry,
- micro-algae cultivation,
- textile industry,
- pulp and paper industry,
- electronic industry,
- car manufacturing industry,
- industries with heavy metal usage.

All in all, 51 original research papers were identified and evaluated. FO desalination for the production of drinking water was not included because there is only little relation to manufacturing industry. Other review papers have already described the concentration of fruit and vegetable juices by FO. Therefore, this topic is only briefly mentioned here. Figure 10 illustrates the percentage distribution of the 51 papers on the different branches.
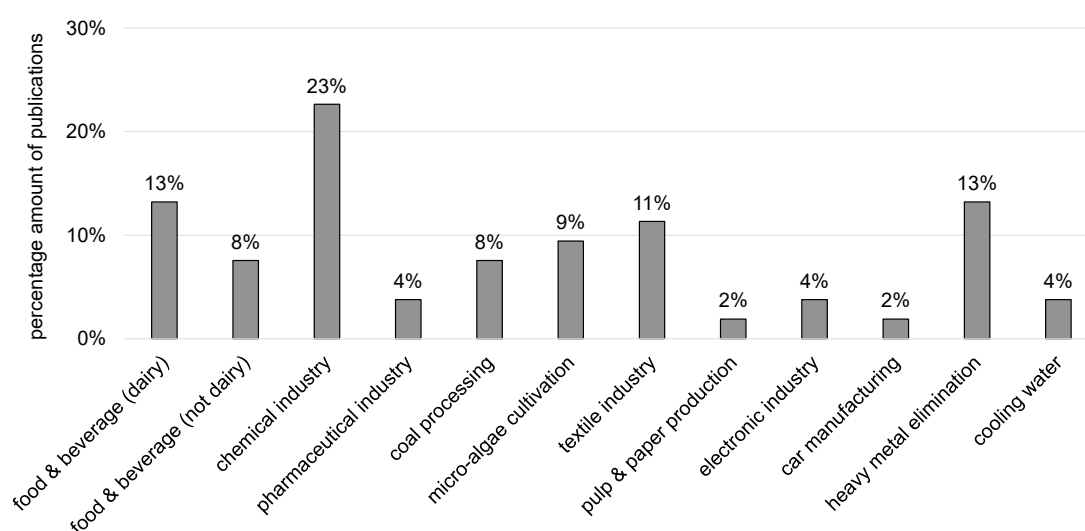
Figure 10. Industrial branches of evaluated research papers and percentage distribution.

Most articles were published about FO application in chemical industry. Heavy metal elimination by FO was also often addressed and included in this review because heavy metals are often present in industrial wastewaters. Many articles were found about FO application in the food and beverage industry including dairy industry. Here, FO was mainly used to treat the products (milk, juice, whey) but also wastewaters.

More information on the individual applications are given in the following chapters of this review focusing on implemented feed and draw solutions, resulting permeate fluxes, and applied hybrid technologies. A summary with more details can be found in the Supplementary Material of this article.

2.3.2 Food & Beverage Industry

2.3.2.1 Dairy Industry

Dairy industry uses raw milk to produce several food items like long-life milk, cheese, and yogurt. Large amounts of wastewater result from the manufacturing from either cleaning procedures or dewatering processes [105]. Usually, this wastewater is treated before disposal. Wastewater recycling or reuse is also an issue in dairy industry.

Several research results were published about FO treatment for whey dewatering. During cheese manufacturing, whey is a waste product that is nowadays further processed into valuable products e.g., whey powder. Pressure-driven membrane processes and evaporation processes are used to dehydrate raw whey. However, those conventional processes consume a lot of energy. Forward osmosis might be applicable for energy-efficient whey dewatering.

The concentration of dairy whey with forward osmosis was investigated in several studies in Turkey [106–111]. Raw whey from a cheese manufacturing was used as FS. The DS were either NaCl (2 M or 3 M) or NH_4HCO_3 (2 M). In lab-scale experiments, the performance of different whey processing technologies was measured and compared. Economic evaluation was also included in the studies. The technologies for whey dewatering and—in case of applied FO—corresponding DS regeneration were:

- ultrafiltration and reverse osmosis (UF-RO) [106, 108],
- forward osmosis with reverse osmosis (FO-RO, NaCl as DS) [106, 108, 109],
- forward osmosis with reverse osmosis (FO-RO, 2 M NH_4HCO_3 as DS with thermal enhanced DS regeneration) [106],
- forward osmosis with membrane distillation (FO-MD, 2 M NaCl as DS) [106, 107],
- membrane distillation and reverse osmosis (MD-RO) [106, 107].

They found that, if waste heat was available, FO-MD and MD-RO were the most economic treatment technologies for whey dewatering. Without waste heat usage, FO-RO and MD-RO were the recommended treatment option. Figure 11 illustrates the proposed FO-MD application for whey dewatering.

Wang et al. reported about FO lab-scale experiments with artificial whey solution obtained by mixing whey powder with deionized water [112]. The 6% whey solution was the FS; NaCl the DS (mostly 0.5 M, but also 0.3 and 1.0 M). A self-manufactured hollow-fiber membrane was used. Permeate fluxes were between 9.5 and 14 L/(m²·h) in the beginning of the experiments and decreased by 11% during the experiments.

Figure 11. FO-MD application scenario for dairy whey dewatering (I water recovery line, II centralized wastewater treatment line, III packaged whey powder product line) (reprinted from [107] with permission from Elsevier).

Pal et al. reported about sweet cheese whey which was separated into whey lactose for acetic acid manufacturing by fermentation and whey protein solution for the production of whey protein powder [113]. FO was investigated to be implemented in two ways. First, FO was used as pretreatment step before fermentation. Sweet cheese whey was either treated by MF and the permeate was then used as FS in FO treatment, or sweet cheese whey was filtered by MF und concentrated by UF and then used as FS in FO treatment. Thereby, whey protein solution could be concentrated before drying. Second, FO was used as fermentation follow-up treatment for concentrating the acetic acid that was separated from the fermentation broth by NF. In both cases, the DS was 1 M MgSO₄ and NF was the DS regeneration technology. Without pressure, FO permeate fluxes were 19 and 25 L/(m²·h) for whey dewatering and acetic acid dewatering, respectively. If external pressure was applied (up to 2 bar), this pressure-enhanced osmosis enabled higher permeate fluxes up to 42 and 44 L/(m²·h). Protein and acetic acid rejection was between

71 and 84%. Pal et al., (2016) also evaluated the economic factors comparing the suggested FO including technology with a conventional system. They found that FO requires less energy and less space resulting in lower costs.

The hybrid system of FO and MD was investigated from Song et al. [114]. They used real dairy wastewater as FS and NaCl as DS as well as two different FO membranes. As a result, FO could concentrate real dairy wastewater and MD could obtain desalted water. FO permeate fluxes were between 10.7 and 3.5 L/(m²·h) in the FO experiments without DS regeneration and between 18 and 6 L/(m²·h) in FO-MD hybrid experiments. Fouling of the FO membrane occurred, but membrane cleaning (rinsing with deionized water and osmotic backwash) could restore the membrane performance up to 90%.

Another study investigated if RO concentrate from a dairy wastewater treatment plant was suitable as FS and if cheese brine could be used as DS in forward osmosis [115]. Dairy cheese brine proved to be a good DS: average permeate flux was 21.0 L/(m²·h) with deionized water as FS. RO concentrate was further concentrated by FO with an average permeate flux of 7.9 L/(m²·h) when 1 M NaCl was used as DS. When FS was RO concentrate and DS was cheese whey, the average permeate flux was 15.1 L/(m²·h). This shows that—with FO—a combined treatment of both wastewaters is possible and thus no separate DS regeneration is necessary.

2.3.2.2 Juice Processing

Fruit and vegetable juices are often concentrated to reduce its volume and safe transportation and storage costs. Moreover, natural colorants are obtained from fruit juices by concentration. This concentration is conventionally done by pressure-driven membrane filtration processes like reverse osmosis or thermally driven evaporation [35]. In both cases, the composition and characteristics of the juice (color, flavor, and nutritional compounds) might be negatively influenced. Forward osmosis possibly concentrates juice without high pressures and without heating. Thus, the characteristics of the juice remains unchanged.

There are numerous publications on juice concentration by FO. Rastogi et al. [35] summarize the state of knowledge up to January 2016. They report about the FO concentration of grape juice, tomato juice, pineapple juice, and raspberry juice. Furthermore, they describe that FO concentrates plant-based colorants (anthocyanin extract from red radish or kokum, betalain extract from beetroot), orange peel press liquor, and artificial sugar solutions. All results are based on lab-scale FO experiments though. Juices were concentrated up to a sugar content of 30 to 60° Brix. Reported FO permeate fluxes were between 2.5 and 9.1 L/(m²·h). Draw solutions were NaCl, $CaCl_2$, $Ca(NO_3)_2$, sucrose solution, fructose solution, high fructose corn syrup, and polyethylene glycol.

2.3.2.3 Other Food & Beverage Application

Marques et al. investigated FO to produce tea extracts [116]. Although the process is called osmotic evaporation and a hollow-fiber membrane contactor is used for experiments, the operating principle is the same as forward osmosis. Tea is used as FS and 5 M $CaCl_2$ as DS. Within 5 h, a tea concentration of 40% was obtained. Permeate flux could be kept constant apart from the decrease due to declining osmotic pressure difference.

FO treatment of olive mill wastewater was studied by Gebreyohannes et al. [117]. They used real wastewater which is rich in biophenolic compounds as FS and $MgCl_2$ as DS. Long-term experiments were conducted for 8 days, in which FS and DS were refreshed daily. FO permeate flux was between 9.8 and 7.1 L/(m²·h). Fouling was observed but pure water permeability could be restored to 95% by rinsing and osmotic backwashing. All in all, volume reduction was 71%. Different pre-treatment methods were tested for the wastewater. Particle retention by microfiltration increased FO permeate flux. Biological treatment in a membrane bioreactor combined with microfiltration even further enhanced FO permeate flux because pectins in the wastewater were reduced by 92%. The concentrated wastewater after FO was treated by ultrafiltration. UF permeate was rich in low molecular biophenols and used as FS in a second FO with $MgCl_2$ as DS. Here, FO permeate flux was 5 L/(m²·h) and volume reduction was 64%. Figure 12 illustrates the proposed treatment chain.
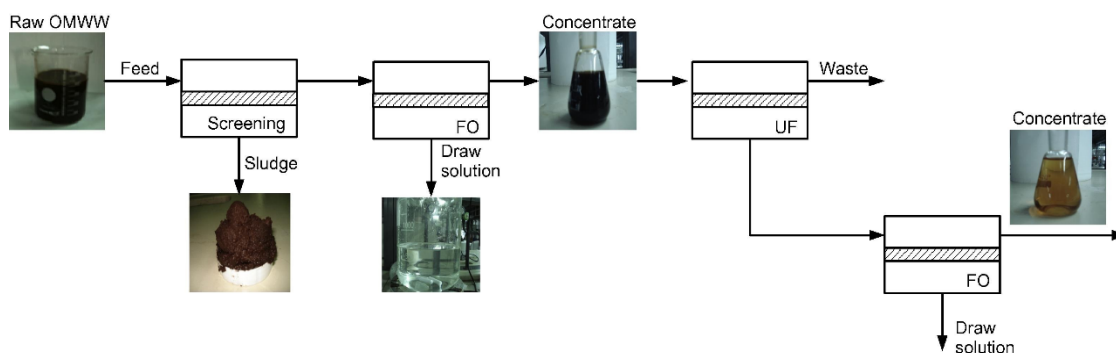
Figure 12. FO application for the treatment of olive mill wastewater (reprinted from [117] with permission from Elsevier).

Singh et al. examined the FO concentration of distillery wastewater [118]. They used real wastewater from sugarcane molasses distillery as FS and $MgCl_2$ as DS. FO permeate flux was only 2.8 L/(m²·h), which is low compared to the permeate fluxes with olive mill wastewater mentioned above. Still, water recovery after 24 h was 70%, which would be higher than with RO (35–40%). Rejection and permeate flux was stable over five 24 h experiments with the same membrane that was rinsed with water in between.

Salih et al. used wastewater from a grain processing plant as FS in FO process [119]. This wastewater was first treated biologically and by dissolved air flotation. The DS was hypersaline brine from a potential CO_2 sequestration site. FO permeate fluxes were between 10 and 15 kg/(m²·h). The brine produced higher FO permeate flux than 20% $MgSO_4$ as DS but also higher reverse salt flux. Different treatment options for both wastewater and brine were evaluated (Figure 13). FO or MD (either with or without pre-filtration) concentrated grain processing wastewater. Purified water from the brine was gained by MD or FO-MD (brine being the DS regenerated by MD). Treatment options with FO had the advantage that fouling was reversible.
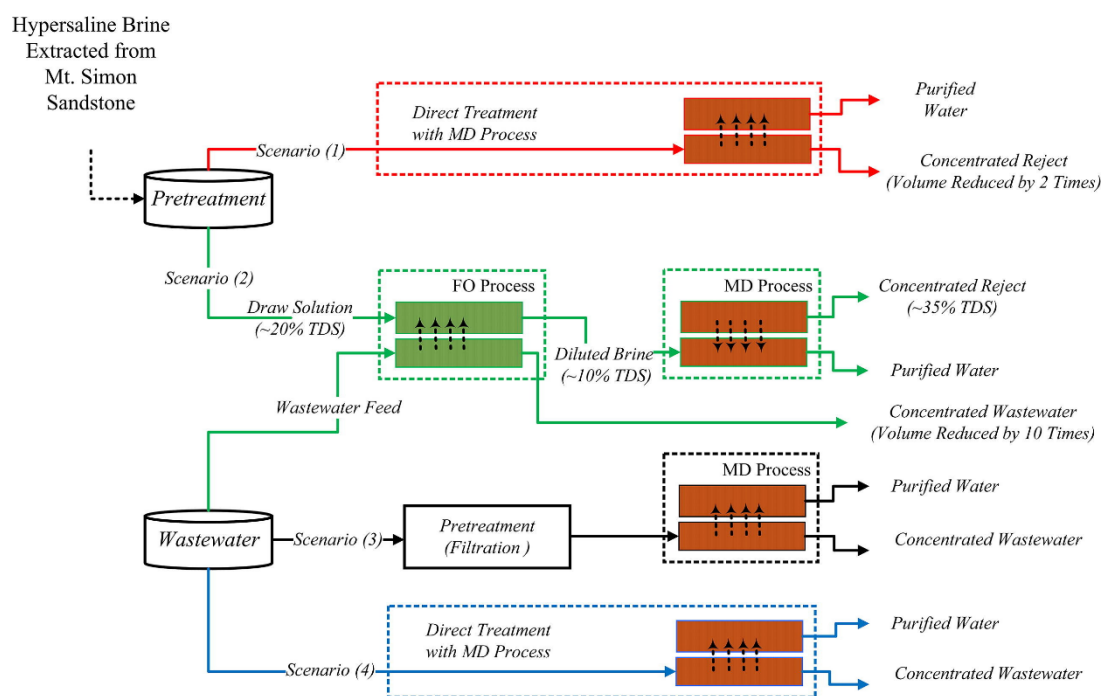
Figure 13. FO application and other treatment possibilities for grain processing wastewater and brine from CO_2 sequestration site (reprinted from [119] with permission from Elsevier).

FO can also be used to produce drinking water from seawater. In this application, seawater is the FS and a highly concentrated solution is the DS. A regeneration technology concentrates the diluted DS and produces drinking water. An overview about FO seawater desalination is provided in several reviews elsewhere [28–30,35].

2.3.3   Chemical Industry

Wünsch et al. investigated the FO treatment of secondary effluent from an industrial wastewater treatment plant [57]. Based on the list of co-authors it is likely that the wastewater originates from chemical industry. The secondary effluent was first concentrated by UF (85%) and RO (50%). Afterwards a softening step was applied (soda ash treatment). The resulting wastewater was then used as FS in in lab-scale FO

experiment. Here, three different DS were evaluated (NaCl, Na_2SO_4, $MgCl_2$) all having the same concentration (1 mol/L). Thus in the FO experiment, the osmotic pressure difference was not equal but was 115 bar, 33.4 bar, and 35.1 bar with $MgCl_2$, Na_2SO_4, and NaCl, respectively. Permeate fluxes for 67% water recovery were interpolated from measured data. They were 13.0 L/(m²·h), 8.08 L/(m²·h), and 9.63 L/(m²·h) with $MgCl_2$, Na_2SO_4, and NaCl, respectively. $MgCl_2$ was the best DS because it delivered the highest permeate flux and lowest reverse salt flux.

Wastewater from esterification was treated in another study [120]. It was pretreated and used as FS in FO experiments with different self-manufactured CTA FO membranes. Within the first 5 h, permeate flux declined from 9.56 L/(m²·h) to 6.0 L/(m²·h). Afterwards, it declined slower which is probably due to a stable fouling layer on the membrane surface. TOC rejection was very high (>96%) and water recovery was 57.1%.

Two studies used wastewater from industrial ammonia absorption processes as DS in FO process [87, 121]. This wastewater has high sulfate and ammonia concentrations and therefore a high osmotic pressure. The acidic pH was adjusted to pH 7 or pH 4 so that the membrane in the lab-scale experiments was not damaged. In one of the studies, anaerobically digested sludge centrate from a municipal wastewater treatment plant was used as FS [121]. Permeate fluxes here were between 2 and 5 L/(m²·h) (Figure 14a). Nitrogen in the sludge centrate could be concentrated successfully. Phosphorus concentration, however, was not successful because it precipitated as calcium phosphate. In the other study, an osmotic bioreactor was simulated and activated sludge was the FS in the FO process [87]. Permeate fluxes were between 1 und 3 L/(m²·h) (Figure 14b). Osmotic backwash was applied regularly to clean the membrane. In both cases, wastewater from ammonia absorption was a good DS.
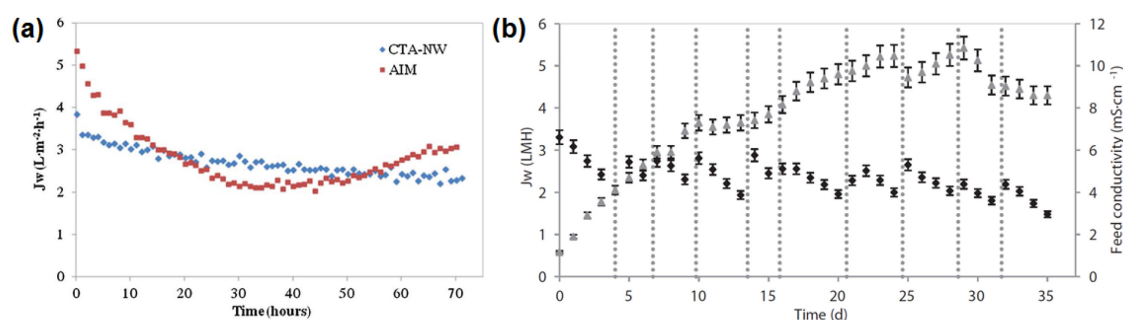
Figure 14. FO permeate flux with wastewater from ammonia absorption as DS and (**a**) anaerobically digested sludge centrate as FS [121] or (**b**) activated sludge as FS (OMBR) [87] (reprinted with permission from Elsevier).

An interesting FO application is proposed by Takahashi et al. [48]. They use FO to dehydrate polyvinyl chloride (PVC) latex before it is dried. Unlike in most other lab-scale FO experiments, the FS was not circulated through the membrane test cell but was placed in a reservoir above the membrane (Figure 6). Synthetic seawater (0.8–1.8 M NaCl) was

the DS. Permeate fluxes in the beginning of the experiments were 8 and 4.5 L/(m²·h) depending on the membrane type. After 24 h the PVC latex concentration reached 75 wt %. However, cake layer formation occurred in the end. For this reason, a final PVC concentration of 60 to 64 wt % is proposed.

The application of forward osmosis combined with biological fermentation processes was subject in many studies. Law et al. used succinic acid as FS combined with seawater as DS [122]. Succinic acid is raw material for many chemical production processes and is traditionally produced from petroleum. Another way to obtain succinic acid is fermentation. Here, the succinic acid has to be eliminated from the fermentation broth and further concentrated. FO was examined to concentrate succinic acid depending on its pH. Furthermore, real seawater was used as DS. Figure 15 shows the permeate fluxes which were between 0 and 4.8 L/(m²·h). A patent was issued on the FO concentration of fermentation broths [123]. Here, succinic acid (67 g/L) was the FS and NaCl (30 wt %) was the DS. FO application in fermentation broth treatment was also investigated in another study [124]. In this case, butyric acid was used as FS and $MgCl_2$ as DS. Permeate flux varied between 16 and 18 L/(m²·h).
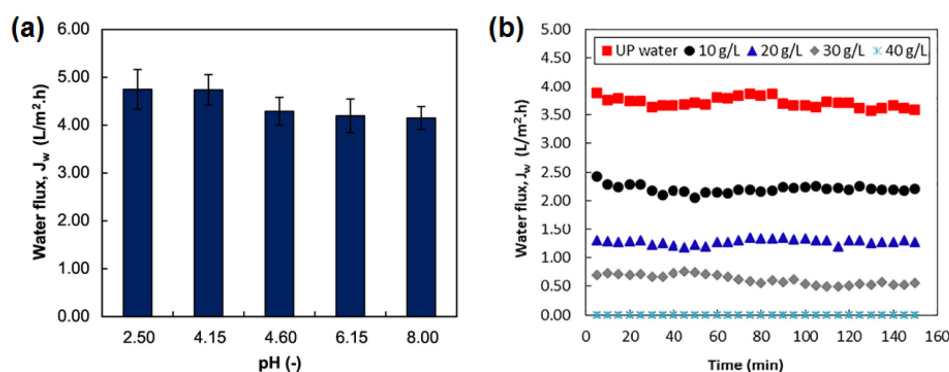
Figure 15. FO permeate fluxes with (**a**) 20 g/L succinic acid as FS and 1 M NaCl as FS; (**b**) succinic acid as FS (pH 6.9) and real seawater as DS (reprinted from [122] with permission from Elsevier).

Ihalainen describes in her master thesis the FO treatment of lactic acid [125]. Lactic acid, like succinic acid, can be produced by fermentation requiring post-treatment e.g., concentration. FO experiments were conducted with lactic acid and glucose as FS and DS, respectively. In the long-term experiment, the permeate flux was 12 L/(m²·h) corresponding to 84% water recovery. However, lactic acid rejection was only 56% meaning that valuable product is lost. The diluted glucose solution can be used as carbohydrate source for the fermentation process (Figure 16). Thus, no DS regeneration is necessary for this application.

A similar FO application concept was proposed by Kalafatakis et al. [126]. Crude glycerol as well as pretreated and enzymatically hydrolysed wheat straw (PHWS) were the investigated DS. After dilution in FO process, they are transferred in the fermentation

reactor as feedstock. DS regeneration is not necessary. The corresponding FS is the fermentation broth, which is concentrated in the FO process (Figure 17). In the experiments, however, FS was created by using the same substance as the DS highly diluted with deionized water. With crude glycerol (100%) as DS, permeate fluxes were 8.4, 9.0 and 10.5 L/(m²·h) with FS glycerol concentrations of 5, 2, and 1%, respectively. When 100% PHWS was the DS, permeate fluxes were 1.3, 5.4, and 6.2 L/(m²·h) with FS PHWS concentration being 20, 5, and 0%, respectively. Permeate fluxes were calculated from the first 30 min of the experiments. In addition to the lab-scale experiments, the usage of crude glycerol as DS and its fermentation to produce butanol was economically evaluated. As a result, they showed that 50% water reclamation could reduce butanol purification costs by 50%.
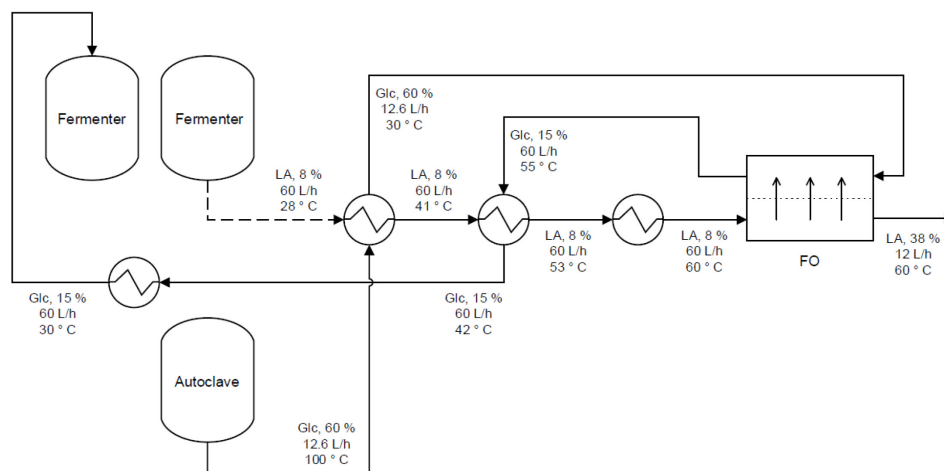
Figure 16. Proposed FO application with glucose (Glc.) as DS in production of lactic acid (LA) by fermentation (reprinted from [125] with permission from author).
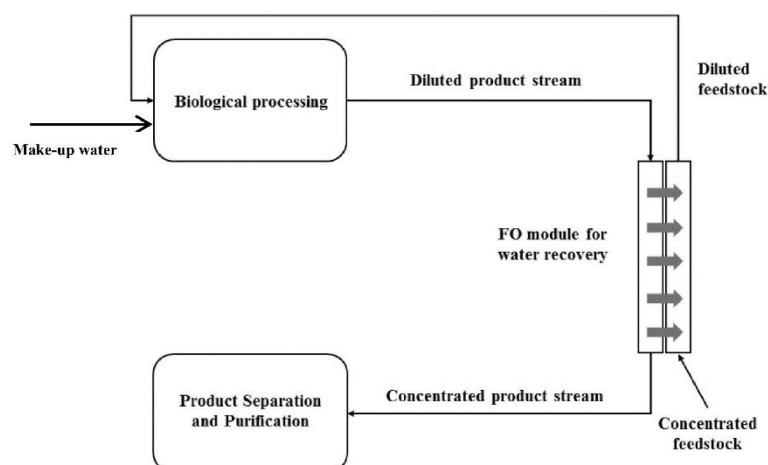
Figure 17. Proposed FO application with fermentation feedstock concentrate as DS and fermentation product as FS (reprinted from [126] with permission from Elsevier).

So far, FO was applied to concentrate the fermentation product stream. Shibuya et al. investigated FO to concentrate the fermentation feedstock [127, 128]. In both studies,

ethanol was produced by fermentation from lignocellulose biomass. The sugar-containing liquid fraction from rice straw pretreated with hot water was used as FS or simulated by using a synthetic sugar solution. Before FO, the liquid was filtered. So-called switchable polarity solvents (SPS) were used as DS. SPS can be mixed with water when CO_2 is present. In the absence of CO_2, they separate from water. Thus, DS regeneration can be accomplished easily.

In the first study, FO successfully concentrated the sugar solution as well as the liquid fraction of the pretreated rice straw. Nevertheless, fermentation inhibitors were also concentrated [127]. For this reason, different treatment technologies were combined and investigated in the second study [128]. Here, the sugar containing solution was to be concentrated whereas the inhibitors were supposed to be removed. NF concentration with water addition was performed before enzymatic hydrolysis and FO treatment. Experiments showed that this treatment chain delivered a high ethanol yield in the fermentation process. Permeate fluxes varied between 0.8 and 9 L/(m²·h) (Figure 18).
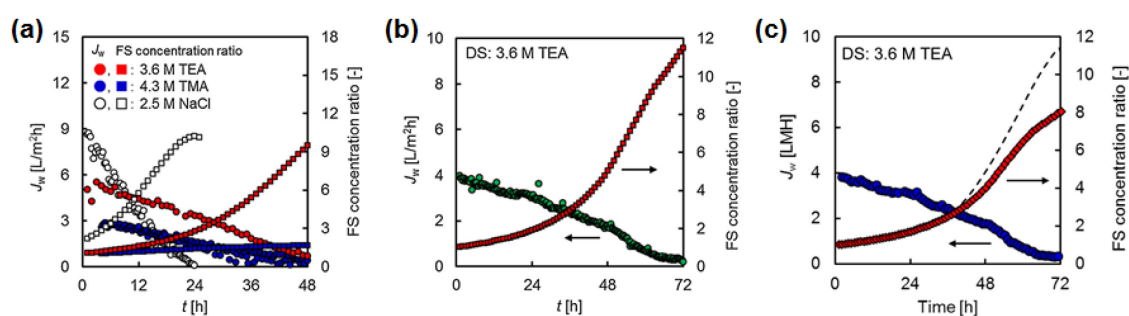
Figure 18. FO permeate flux with FS being model sugar solution (**a**), liquid fraction of pretreated rice straw after filtration (**b**) and filtration and enzymatic hydrolysis (**c**) (reprinted from [127, 128] with permission from Elsevier).

Several researchers focused on the FO treatment of acids. In one study, different carboxylic acids were concentrated by FO [129]. These acids are utilized in many chemical processes. For this reason, they are likely to be contained in the wastewater. Acetic, butyric, valeric, and lactic acid (concentration 10 mM) were the FS in the FO experiments. Ammonium chloride was the DS. A model was developed to simulate the FO experiments. The comparison of the results showed that they matched well proving the correctness of the proposed model. Taken the average weight change of approximately 0.6 kg within the 30-h experiment and a membrane surface area of 42 cm², the permeate flux was 4.8 L/(m²·h) for all tested acids.

2.3.4   Pharmaceutical Industry

Closely related to the chemical industry is the pharmaceutical industry. Two research papers published results from forward osmosis experiments treating pharmaceutical liquids. Cui et al., (2018) reported about FO experiments in which they used typical pharmaceutical solvents as FS, which usually contain pharmaceutical active ingredients (API) [130]. The aim was to recover the organic solvents and reject the API. So, in this case, not water but organic solvents were supposed to pass through the membrane and dilute the DS. Ethanol, isopropanol, and hexane were the tested FS, in some cases with dissolved tetracycline and triglycerides. DS were lithium chloride, methyl palmitate, citric acid, polyethylene glycol, and diethanolamine. Average solvent fluxes were between 0.32 ± 0.07 and 3.82 ± 0.37 L/(m²·h). API rejection was >98%.

Wang et al., (2011) investigated the concentration of protein solutions by forward osmosis [161]. They used bovine serum albumin (BSA) solution as FS and NaCl as DS. Membrane distillation was applied for DS regeneration and self-manufactured hollow-fibre membranes were used for FO and MD. Initial permeate fluxes were 2.7 and 5.3 L/(m²·h) with 0.5 and 2 M NaCl, respectively.

2.3.5   Coal Processing

FO is potentially applicable for the treatment of wastewater from mining [80]. A further step would be to investigate FO application in coal processing industry. Kumar et al. investigated a hybrid system of FO and NF to recycle coke-oven wastewater [131]. The wastewater came from a factory that produces coke for steel manufacturing. Coke-oven wastewater usually contains toxic substances [132]. For this reason, it has to be treated before disposal. According to Kumar et al. biological treatment, adsorption, coagulation, wet oxidation, and advanced oxidation processes have been examined as treatment technologies so far [131]. However, all of these technologies are either technically or economically difficult. In lab-scale forward osmosis experiments, Kumar et al. used real coke-oven wastewater as FS. NaCl, $MgSO_4$, and $CaCl_2 \cdot H_2O$ (0.4–2.5 M) were the DS. FO permeate fluxes were 42–46 L/(m²·h) and substance rejection exceeded 97%. NF was operated simultaneously to concentrate and recycle the DS. Overall, the hybrid system worked well. Occuring fouling proved to be reversible. Economic calculations showed that FO-NF would be an economic alternative to other treatment options. Fenton oxidation processes or struvite precipitation could further treat concentrated coke-oven wastewater after FO.

The treatment of coal gasification wastewater with FO was investigated in a different study [133]. This wastewater is hard to treat because it contains toxic phenolic compounds. In FO experiments, three types of artificial coal gasification wastewater (100 mg/L of three

phenolic compounds, various pH-values) and sodium chloride (1.75–10.5%) were the FS and DS, respectively. It was found that coal gasification wastewater could be concentrated by FO. Rejection of phenolic compounds was better with alkaline pH-values and higher DS concentration, which also increased the permeate water flux. Permeate water fluxes varied between approximately 8.5 and 10.5 L/(m²·h). The authors of the study also developed a model to represent their experiments. Simulated results and experimental results matched well supporting the established model. The focus of this study was the rejection of phenolic compounds by FO membrane. Regarding further treatment technologies, e.g., the concentrated coal gasification wastewater or the diluted NaCl solution, no suggestions are made.

Another study investigated the rejection of phenol by different forward osmosis membranes [74]. The FS was an artificial wastewater from oil and gas industry. It contained phenol and sodium chloride. Sodium chloride (0.5–4 mol/L) was the DS. The sorption and the rejection of phenol varied depending on the operation conditions and on the three different membrane types used. Furthermore, a model was established and validated. In general, the results of this study correspond to the ones mentioned above [133].

2.3.6 Micro Algae Cultivation

Algal biomass has drawn raising attention because it provides multiple benefits. Microalgae are considered a renewable energy source, e.g., for biofuel production [134]. Furthermore, industries like food and cosmetic industries use microalgae as raw material for their products [135]. During the cultivation of microalgae, a large quantity of substances in the surrounding water is consumed and CO_2 can be captured [136]. For this reason, microalgae cultivation not only provides a valuable product but can also be used for wastewater treatment. However, the separation of microalgae from water is an economically critical issue. Different treatment methods have been investigated including centrifugation, flotation, flocculation, sedimentation, and pressure-driven membrane processes [137, 138]. Forward osmosis might be an alternative treatment technology here.

Larronde-Larretche et al. concentrated different microalgae solutions with FO [139]. Three different DS were used: sea salt solution, $MgCl_2$, and $CaCl_2$. DS concentration was set to provide the same initial permeate flux of 7 L/(m²·h). FO experiments were conducted until permeate volume was 75% of initial FS volume. Permeate flux declined in the course of the experiments. The extent of this flux loss varied between 5 and 71% depending on the microalgae species and the used DS. Algae dewatering efficiency was between 59 and 80%. For technical application, the usage of seawater as DS was proposed

either before seawater desalination to facilitate desalination reverse osmosis or after seawater desalination to dilute RO concentrate before sea disposal. In this case, DS regeneration is not necessary.

In a previous study, Larronde-Larretche et al. also investigated FO concentration of microalgae [140]. One microalgae species solution was the FS. The DS were sea salt solution, NaCl, MgCl$_2$, and CaCl$_2$. It was shown that ALFS membrane orientation was more suitable because permeate flux loss was lower than in ALDS membrane orientation and fouling layers were easily removable by rinsing with deionized water. NaCl was the best DS followed by MgCl$_2$. If calcium was present in the DS more severe fouling occurred and permeate flux decreased a lot. Permeate fluxes in the beginning of the experiment were 6.7–8.2 L/(m²·h), after 75% permeate volume they were 1.5–5.9 L/(m²·h). Permeate flux losses were between 10 and 59% (Figure 19).
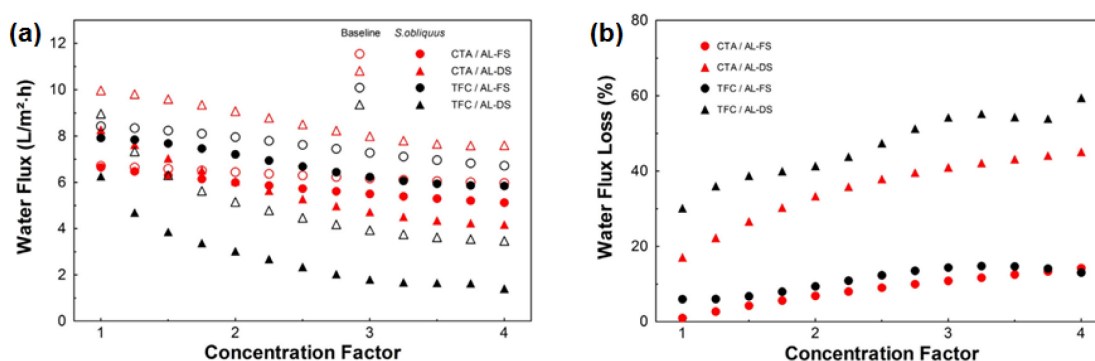
Figure 19. FO permeate flux (a) and permeate flux loss (b) with 0.2 g/L microalgae suspension as FS and 70 g/L sea salt solution as DS (reprinted from [140] with permission from Elsevier).

If FO is used for microalgae concentration, fouling is a critical point to be considered. In the studies mentioned above, fouling occurred resulting in permeate flux loss. However, it is mentioned that fouling could be minimized by choosing proper microalgae species and DS type. Furthermore, fouling was reversible. These facts are supported by other studies [141,142]. Here, it was shown that magnesium ions in the DS enhance fouling formation and make it harder to be removed. With NaCl as DS less fouling occurred and was also reversible. Spacers in the FS feed channel further reduced the negative impact of fouling on FO performance.

Buckwalter et al. proposed a different algae cultivation method [143]. Algae were not cultivated inside a bioreactor but inside a membrane bag filled with nutrient solution. The bags were stored in the sea. This way, microalgae growth and concentration by FO process took place at the same time. The bags were taken out of the sea and algae were harvested. The membrane bags were based on the so-called hydration bags and made of FO CTA membrane from HTI. The nutrient-algae solution inside the bags was the FS and seawater the DS in FO process. Average permeate flux was 2 L/(m²·h). Fouling occurred but did not

affect algae dewatering. However, membrane bags were damaged in long-term experiments in the ocean.

2.3.7   Textile Industry

Manufacturing of textiles is an industry with a high water demand of 200 to 400 L per kg produced fabric [144]. Especially, dying and conditioning technologies use large amounts of water and produce wastewater that has to be treated [145]. Wastewater treatment and water recycling can enable a more sustainable production process. Physico-chemical processes (coagulation, flotation, chemical oxidation, and biodegradation) as well as advanced treatment technologies (adsorption, ozonation, photocatalysis, and membrane processes) have been investigated for textile wastewater treatment [146].

Han et al. propose the application of forward osmosis to treat textile wastewater [147]. FO shall concentrate the dye-containing wastewater as FS. Subsequently, the concentrate is to be treated by coagulation and flocculation. In lab-scale experiments, different synthetic dye wastewaters were tested. DS was sodium chloride (2 mol/L). Dye retention was almost 100%. Permeate flux in the beginning was 36 L/(m²·h), decreased to 12 L/(m²·h), and was maintained at this level. Fouling occurred but was reversible by rinsing with water (Figure 20).
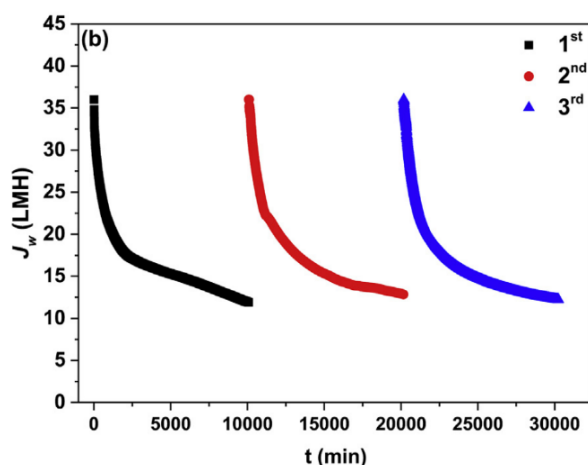
Figure 20. Results of FO experiment with synthetic textile wastewater as FS and 2 M NaCl as DS (TFC-FO-membrane, self-manufactured; ALFS; membrane flushed with DI water between test runs) (reprinted from [147] with permission from Elsevier).

Other studies also investigated the FO application to concentrate dye-containing textile wastewater focusing on the type of draw solution. Polyelectrolytes and brown coal slurry were tested [50, 148, 149]. Huang et al. [148] used different polyelectrolytes as DS and dye containing wastewater as FS (50 ppm Congo red aqueous solution). They showed that polyelectrolyte P(SSA-co-MA)-Na-1 as DS has the advantage—besides its high osmotic

pressure—to be regenerated easily by nanofiltration because of its large molecular size. Rejection rate of Congo red was high, although TOC in the DS increased a little bit. Average permeate flux in the 2 h FO experiment with the mentioned FS and DS was ca. 3 L/(m²·h) (Figure 21a). Ge et al. also used polyelectrolyte as DS [149]. This PAA-Na-solution was successfully regenerated by membrane distillation. Dye-containing wastewater was simulated with a 50 ppm Orange-Acid-8-solution, which was the FS. Permeate flux in experiments without DS regeneration decreased from 25 to 15.5 L/(m²·h) within the 2 h experiment (Figure 21b).
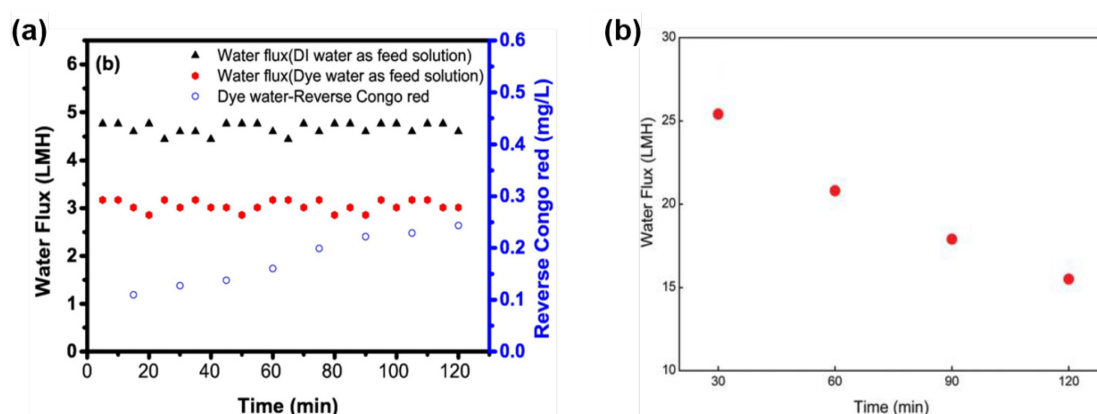
Figure 21. Results of FO experiment with (**a**) DI water or dye water (50 ppm Congo red aqueous solution) as FS and 0.25 g/mL P(SSA-co-MA)-Na-1 as DS (TFC-FO-membrane from HTI; ALFS) (reprinted from [148] with permission from Elsevier) and (**b**) dye water (50 ppm Acid Orange 8 aequeous solution) as FS and 0.48 g/mL mL PAA-Na as DS (self-manufactured hollow fiber FO membrane; ALDS) (reprinted from [149] with permission from American Chemical Society).

Gu et al. investigated brown coal powder as DS to concentrate dye-containing textile wastewater [50]. Permeate fluxes were 0.979 and 0.900 L/(m²·h). The moistened brown coal after FO is supposed to be mixed further with water to create coal water slurry. This coal water slurry can then be used as a substitute for fossil fuel in gasification and chemical synthesis processes. Dye-containing wastewater would be concentrated facilitating further treatment. No DS regeneration is necessary in this application.

Three different dye solutions were investigated as FS for forward osmosis in another study [146]. Real seawater was the DS. Permeate fluxes were between 1.62 and 3.47 L/(m²·h) depending on the dye concentration, membrane orientation and experiment duration. Dye rejection was almost 100%. FO performance was compared to NF that obtained permeate fluxes around 30 L/(m2·h) and dye rejection of more than 99%. As conclusion a textile wastewater treatment was proposed: (1) NF to treat textile wastewater; (2) FO with NF concentrate as FS and RO brine from seawater desalination as DS (Figure 22).

In another study, FO experiments were conducted with polayacrylamide (PAM) as DS [150]. Dye-containing wastewater was the FS. Permeate fluxes were between 2.65 and

5.14 L/(m²·h) depending on membrane orientation and experiment duration. Membrane fouling occurred with dye wastewater but was found out to be neglectable. Dye rejection was almost 100% regardless which membrane orientation was used. PAM was compared to KCl representing a conventional DS. Permeate water fluxes were more stable and reverse salt flux was lower with PAM. It was proposed that the diluted PAM solution could either be used in oil field extraction or be regenerated and recycled by UF, MD or heating processes.
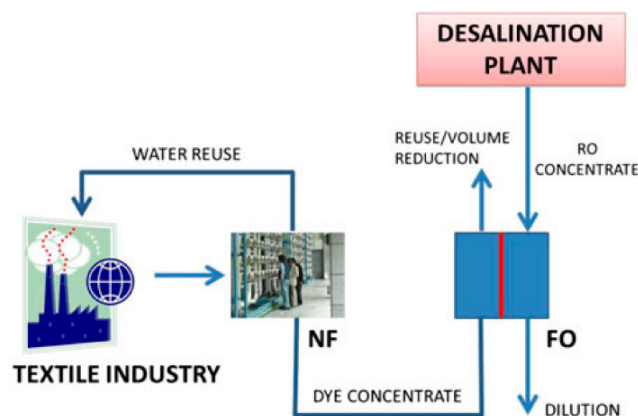
Figure 22. Proposed treatment scenario of dye-containing wastewater (reprinted from [146] with permission of Balaban Publishers – Desalination Publications).

2.3.8   Pulp and Paper Production

To the authors' knowledge, only little FO research is done regarding the pulp and paper industry. Duan et al. evaluated sodium lignin sulfonate (NaLS), a waste product from pulp production, as draw solution [151]. The diluted solution could be used for desert restoration to stabilize sand (Figure 23). Moreover, NaLS is a good substrate for plant growing.
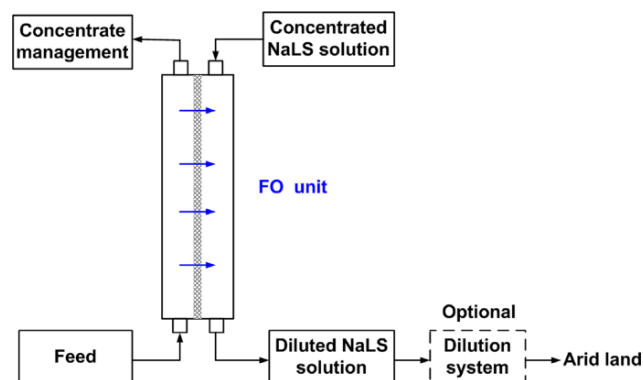
Figure 23. FO application scenario with usage of NaLS (waste product from pulp manufacturing) as DS (reprinted from [151] with permission from Elsevier).

In their experiments, Duan et al. used DI water and saline water as FS. As a result, permeate flux was 15 and 10 L/(m²·h) for the two membranes with deionized water as FS (600 g/kg NaLS solution as DS, ALDS membrane orientation). In this case, the osmotic pressure difference was 78 bar. The same DS combined with 30,000 mg/L NaCl as FS resulted in 5 and 2 L/(m²·h) permeate flux (ALFS membrane orientation). The lower permeate fluxes can be explained by the lower osmotic pressure difference. The FO application for NaLS dilution is similar to the FO application in fertigation. To use the NaLS solution for sand stabilization, a dilution down to 1–2% is necessary which is equivalent to an osmotic pressure of 1.3–2.7 bar. Only brakish water (2000 mg/L NaCl equal to an osmotic pressure of 1.5 bar) or less saline waters as FS could result in a NaLS solution that was directly applicable. If for example sea water (30,000 mg/L NaCl, π = 23 bar) is used as FS, the NaLS DS can be diluted down to 17% only. Thus, another dilution step would be necessary. Nevertheless, a promising FO application scenario is proposed.

2.3.9   Electronic Industry

In electronic industry, wastewater streams occur that contain valuable substances, e.g., heavy metals. However, these substances are often toxic or harmful and have to be removed from the wastewater. At the same time, this removal offers the chance to regain and recycle these substances back into the production process.

Gwak et al. utilized forward osmosis to treat wastewater from a printed circuit board (PCB) manufacturing (Figure 24) [152]. Palladium containing wastewater as FS was concentrated up to 90%. This way, palladium could be regained efficiently by electrowinning. Nickel containing wastewater from electroless nickel plating was the DS. The diluted DS could be disposed to a wastewater treatment plant. No DS regeneration process is necessary in this case. Gwak et al. [153] mention that inorganic fouling occurred on the FS side and needed more investigation. However, they also say that in PCB manufacturing, other high conductivity waste streams are available. Further FO steps using these waste streams as DS could increase the palladium concentration even more.
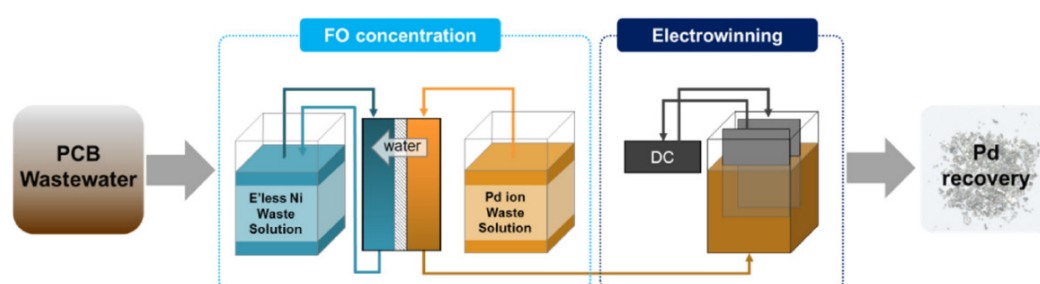
Figure 24. Forward osmosis application scenario at a PCB plant for palladium recovery (reprinted from [153] with permission from author).

Nguyen et al. describe lab-scale experiments in which they examined forward osmosis treatment for two wastewaters from a thin film transistor liquid crystal display (TFT-LCD) plant [154]. They used potassium iodide wastewater from the polarizer process as FS. Potassium hydroxide wastewater was applied as DS originating from the developing process. The iodide concentration in the FS increased from 0.6 to 6.9% during 120 h FO treatment enabling a recycling. Here, FO could replace conventional technologies like thermal distillation and reverse osmosis. The diluted DS could also be reused in the manufacturing process. Thus, a DS regeneration is not necessary.

2.3.10   Car Manufacturing Wastewater

Different wastewaters from car manufacturing industry were used for FO experiments [115]. The wastewaters were either used as FS or DS. If the tested wastewater was not combined with another wastewater, deionized water and 1 mol/L NaCl were used as FS and DS, respectively. Automobile cooling tower water and wastewater from cathodic dip painting were the tested DS. However, permeate fluxes were below 1.1 L/(m²·h). Rinsing water and wastewater from automobile cathodic dip painting as well as wastewater from automobile paint shop pre-treatment were the tested FS and showed good performance regarding the permeate flux between 7.5 and 19.4 L/(m²·h).

2.3.11   General Industrial Application

Several researchers who conducted FO experiment focused on the behaviour of single chemical elements during FO process, e.g., heavy metals [155, 156]. Sometimes these studies examined also other points of interest like the performance of a newly developed FO membrane [49, 157] or wastewater treatment [158, 159]. In regard of the chosen elements, deposition on the membrane, diffusion through the membrane, and rejection by the membrane were investigated. Table 2 shows which heavy metals were studied.

The early FO research used a FO set-up without circulation and commercial RO membranes. Here, permeate flux did not exceed 4.5 L/(m²·h) and high diffusion rates for both DS substances and heavy metals were observed. In the recent studies, flat-sheet FO membranes, either commercial or self-manufactured, were applied and a circulation lab-scale set-up was used as described before [49, 155–159]. Heavy metal rejection was high between 85 and 99.9%. Permeate fluxes ranged from 4 to 69 L/(m²·h).

Table 2. Investigated heavy metals for FO treatment.

As	Cd	Cr	Cu	Hg	Ni	Pb	Zn	Ref.
	☑		☑			☑		[155]
	☑		☑		☑	☑	☑	[49]
	☑		☑			☑	☑	[157]
				☑				[159]
					☑			[158]
☑	☑		☑	☑		☑		[156]
		☑	☑					[42, 43]

To control process temperatures, many manufacturing industries use large amounts of cooling water, which are often recirculated in closed cooling loops. Due to evaporation losses, this cooling water is concentrated and has to be diluted with fresh water intermittently. This water is called make-up water. Furthermore, to remove substances from this cooling water loop, a certain amount of concentrated cooling water is discharged regularly.

Wang et al. investigated the usage of rainwater as make-up water [160]. They conducted FO experiments with rainwater as FS and cooling water from a steam plant as DS. This way, pure water was transported into the cooling water. The average flux was 1.75 L/(m²·h) at 23 °C. Increasing DS temperature from 3 to 50 °C lead to a 10 times higher FO permeate flux. Fouling did not show negative impact on the FO process.

Cooling tower water from automobile industry was the DS in other FO experiments [115]. Here, deionized water and wastewater from paintshop pre-treatment were the corresponding FS producing only low average permeate fluxes of 1.1 and 0.1 L/(m²·h), respectively.

2.4   Concluding Remarks

Forward osmosis is a promising solution for the energy-efficient water usage in manufacturing industries. In this paper, 51 original research articles were evaluated in which forward osmosis application in industries was investigated. So far, research was conducted on FO application in food and beverage industry, chemical industry, pharmaceutical industry, coal processing, micro algae cultivation, textile industry, pulp and paper industry, electronic industry, and car manufacturing. Articles were also published about heavy metal elimination and cooling water treatment; both of which might be related to industries. Forward osmosis was either applied for wastewater treatment, for the dilution of a fluid product or the concentration of a fluid product.

Unfortunately, it is not possible to compare the efficiency of the different application experiments due to varying experimental set-ups, operation conditions, and data interpretation. For this reason, it is also difficult to evaluate the potential of FO application

in the industrial sectors. Certainly, one approach is the comparison of the obtained permeate fluxes: If the permeate flux is low, FO might not be a suitable treatment technology. However, the given permeate fluxes cannot be compared as they range from initial short-time permeate fluxes to long-time average permeate fluxes. Furthermore, the FO potential has to be evaluated individually for each application scenario because more aspects require consideration. These aspects are, for example, economic benefits, alternative treatment technologies, and legal requirements.

The general principle of forward osmosis is not questioned in the evaluated research papers. Full-scale implementation of forward osmosis in seawater desalination shows that forward osmosis is an applicable treatment technology. In regard to the industrial applications only basic proof-of-principle studies were conducted in lab-scale. The up-scaling on pilot- or full-scale will be the next step to optimize the operation and implement FO in industrial water and wastewater treatment. To further promote forward osmosis in industries, more research needs to be done. Crucial points are illustrated in Figure 25.
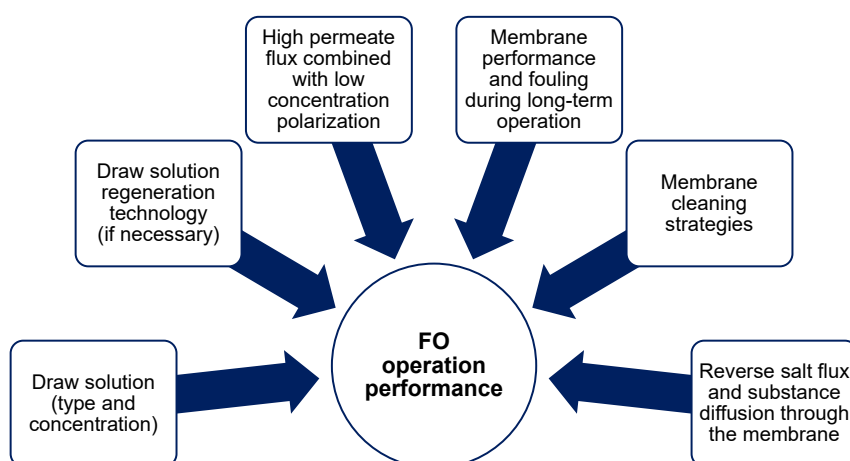
Figure 25. Crucial points for forward osmosis operation performance.

By conducting more research, it should be possible to establish forward osmosis as a treatment technology in manufacturing industries. It should also be possible to find more application scenarios. Advantageous would be the combined treatment of two streams where no synthetic draw solution would be necessary. So far, most research papers investigated FO application in one industry only. However, in order to benefit from the simultaneous treatment of two fluids in the forward osmosis process, water and wastewater streams in industrial parks with numerous industry branches should be investigated. Besides the technical applicability, energetic and economic benefits of forward osmosis need to be critically evaluated for each application scenario before full-scale implementation.

Supplementary Materials: Table S1: Lab-scale set-ups used for investigation of forward osmosis application in manufacturing industries.

References of Chapter 2

1. United Nations. *Transforming Our World: The 2030 Agenda for Sustainable Development (A/RES/70/1)*; United Nations: New York, NY, USA, 2015.

2. Ait-Kadi, M. Water for Development and Development for Water: Realizing the Sustainable Development Goals (SDGs) Vision. *Aquat. Procedia* **2016**, *6*, 106–110, doi:10.1016/j.aqpro.2016.06.013.

3. WWAP. *The United Nations World Water Development Report 2017: Wastewater, The Untapped Resource*; WWAP (United Nations World Water Assessment Programme); UNESCO: Paris, France, 2017.

4. Cath, T.Y.; Childress, A.E.; Elimelech, M. Forward osmosis: Principles, applications, and recent developments. *J. Membr. Sci.* **2006**, *281*, 70–87, doi:10.1016/j.memsci.2006.05.048.

5. Mazlan, N.M.; Peshev, D.; Livingston, A.G. Energy consumption for desalination—A comparison of forward osmosis with reverse osmosis, and the potential for perfect membranes. *Desalination* **2016**, *377*, 138–151, doi:10.1016/j.desal.2015.08.011.

6. Wu, Z.; Zou, S.; Zhang, B.; Wang, L.; He, Z. Forward osmosis promoted in-situ formation of struvite with simultaneous water recovery from digested swine wastewater. *Chem. Eng. J.* **2018**, *342*, 274–280, doi:10.1016/j.cej.2018.02.082.

7. Fodi, T.; Didaskalou, C.; Kupai, J.; Balogh, G.T.; Huszthy, P.; Szekely, G. Nanofiltration-Enabled In Situ Solvent and Reagent Recycle for Sustainable Continuous-Flow Synthesis. *ChemSusChem* **2017**, *10*, 3435–3444, doi:10.1002/cssc.201701120.

8. Schaepertoens, M.; Didaskalou, C.; Kim, J.F.; Livingston, A.G.; Szekely, G. Solvent recycle with imperfect membranes: A semi-continuous workaround for diafiltration. *J. Membr. Sci.* **2016**, *514*, 646–658, doi:10.1016/j.memsci.2016.04.056.

9. Chávez-Castilla, L.R.; Aguilar, O. An integrated process for the in situ recovery of prodigiosin using micellar ATPS from a culture of Serratia marcescens. *J. Chem. Technol. Biotechnol.* **2016**, *91*, 2896–2903, doi:10.1002/jctb.4906.

10. Zhao, S.; Zou, L.; Tang, C.Y.; Mulcahy, D. Recent developments in forward osmosis: Opportunities and challenges. *J. Membr. Sci.* **2012**, *396*, 1–21, doi:10.1016/j.memsci.2011.12.023.

11. Sreedhar, I.; Khaitan, S.; Gupta, R.; Reddy, B.M.; Venugopal, A. An odyssey of process and engineering trends in forward osmosis. *Environ. Sci. Water Res. Technol.* **2018**, *4*, 129–168, doi:10.1039/C7EW00507E.

12. McCutcheon, J.R. Forward osmosis: A technology platform here to stay. *Desalination* **2017**, *421*, 1–2, doi:10.1016/j.desal.2017.08.017.

13. Chung, T.-S.; Luo, L.; Wan, C.F.; Cui, Y.; Amy, G. What is next for forward osmosis (FO) and pressure retarded osmosis (PRO). *Sep. Purif. Technol.* **2015**, *156*, 856–860, doi:10.1016/j.seppur.2015.10.063.

14. Nasr, P.; Sewilam, H. Forward osmosis: An alternative sustainable technology and potential applications in water industry. *Clean Technol. Environ. Policy* **2015**, *17*, 2079–2090, doi:10.1007/s10098-015-0927-8.

15. Shaffer, D.L.; Werber, J.R.; Jaramillo, H.; Lin, S.; Elimelech, M. Forward osmosis: Where are we now? *Desalination* **2015**, *356*, 271–284, doi:10.1016/j.desal.2014.10.031.

16. Chung, T.-S.; Zhang, S.; Wang, K.Y.; Su, J.; Ling, M.M. Forward osmosis processes: Yesterday, today and tomorrow. *Desalination* **2012**, *287*, 78–81, doi:10.1016/j.desal.2010.12.019.

17. Hoover, L.A.; Phillip, W.A.; Tiraferri, A.; Yip, N.Y.; Elimelech, M. Forward with Osmosis: Emerging Applications for Greater Sustainability. *Environ. Sci. Technol.* **2011**, *45*, 9824–9830, doi:10.1021/es202576h.

18. Chun, Y.; Mulcahy, D.; Zou, L.; Kim, I.S. A Short Review of Membrane Fouling in Forward Osmosis Processes. *Membranes* **2017**, *7*, 30, doi:10.3390/membranes7020030.

19. Li, L.; Liu, X.; Li, H. A review of forward osmosis membrane fouling: Types, research methods and future prospects. *Environ. Technol. Rev.* **2017**, *6*, 26–46, doi:10.1080/21622515.2016.1278277.

20. She, Q.; Wang, R.; Fane, A.G.; Tang, C.Y. Membrane fouling in osmotically driven membrane processes: A review. *J. Membr. Sci.* **2016**, *499*, 201–233, doi:10.1016/j.memsci.2015.10.040.

21. Kim, B.; Gwak, G.; Hong, S. Review on methodology for determining forward osmosis (FO) membrane characteristics: Water permeability (A), solute permeability (B), and structural parameter (S). *Desalination* **2017**, *422*, 5–16, doi:10.1016/j.desal.2017.08.006.

22. Johnson, D.J.; Suwaileh, W.A.; Mohammed, A.W.; Hilal, N. Osmotic's potential: An overview of draw solutes for forward osmosis. *Desalination* **2018**, *434*, 100–120, doi:10.1016/j.desal.2017.09.017.

23. Cai, Y.; Hu, X. 'Matthew' A critical review on draw solutes development for forward osmosis. *Desalination* **2016**, *391*, 16–29, doi:10.1016/j.desal.2016.03.021.

24. Luo, H.; Wang, Q.; Zhang, T.C.; Tao, T.; Zhou, A.; Chen, L.; Bie, X. A review on the recovery methods of draw solutes in forward osmosis. *J. Water Process Eng.* **2014**, *4*, 212–223, doi:10.1016/j.jwpe.2014.10.006.

25. Blandin, G.; Verliefde, A.R.D.; Comas, J.; Rodriguez-Roda, I.; Le-Clech, P. Efficiently Combining Water Reuse and Desalination through Forward Osmosis—Reverse Osmosis (FO-RO) Hybrids: A Critical Review. *Membranes* **2016**, *6*, 37, doi:10.3390/membranes6030037.

26. Chekli, L.; Phuntsho, S.; Kim, J.E.; Kim, J.; Choi, J.Y.; Choi, J.-S.; Kim, S.; Kim, J.H.; Hong, S.; Sohn, J.; et al. A comprehensive review of hybrid forward osmosis systems: Performance, applications and future prospects. *J. Membr. Sci.* **2016**, *497*, 430–449, doi:10.1016/j.memsci.2015.09.041.

27. Abou El-Nour, F.H. Water Desalination Studies Using Forward Osmosis Technology, a Review. *Arab J. Nucl. Sci. Appl.* **2016**, *49*, 167–176.

28. Qasim, M.; Darwish, N.A.; Sarp, S.; Hilal, N. Water desalination by forward (direct) osmosis phenomenon: A comprehensive review. *Desalination* **2015**, *374*, 47–69, doi:10.1016/j.desal.2015.07.016.

29. Akther, N.; Sodiq, A.; Giwa, A.; Daer, S.; Arafat, H.A.; Hasan, S.W. Recent advancements in forward osmosis desalination: A review. *Chem. Eng. J.* **2015**, *281*, 502–522, doi:10.1016/j.cej.2015.05.080.

30. Valladares Linares, R.; Li, Z.; Sarp, S.; Bucs, S.S.; Amy, G.; Vrouwenvelder, J.S. Forward osmosis niches in seawater desalination and wastewater reuse. *Water Res.* **2014**, *66*, 122–139, doi:10.1016/j.watres.2014.08.021.

31. Qin, J.-J.; Lay, W.C.L.; Kekre, K.A. Recent developments and future challenges of forward osmosis for desalination: A review. *Desalination Water Treat.* **2012**, *39*, 123–136, doi:10.1080/19443994.2012.669167.

32. Lutchmiah, K.; Verliefde, A.R.D.; Roest, K.; Rietveld, L.C.; Cornelissen, E.R. Forward osmosis for application in wastewater treatment: A review. *Water Res.* **2014**, *58*, 179–197, doi:10.1016/j.watres.2014.03.045.

33. Munirasu, S.; Haija, M.A.; Banat, F. Use of membrane technology for oil field and refinery produced water treatment—A review. *Process Saf. Environ. Prot.* **2016**, *100*, 183–202, doi:10.1016/j.psep.2016.01.010.

34. Coday, B.D.; Xu, P.; Beaudry, E.G.; Herron, J.; Lampi, K.; Hancock, N.T.; Cath, T.Y. The sweet spot of forward osmosis: Treatment of produced water, drilling wastewater, and other complex and difficult liquid streams. *Desalination* **2014**, *333*, 23–35, doi:10.1016/j.desal.2013.11.014.

35. Rastogi, N.K. Opportunities and Challenges in Application of Forward Osmosis in Food Processing. *Crit. Rev. Food Sci. Nutr.* **2016**, *56*, 266–291, doi:10.1080/10408398.2012.724734.

36. Ansari, A.J.; Hai, F.I.; Price, W.E.; Drewes, J.E.; Nghiem, L.D. Forward osmosis as a platform for resource recovery from municipal wastewater—A critical assessment of the literature. *J. Membr. Sci.* **2017**, *529*, 195–206, doi:10.1016/j.memsci.2017.01.054.

37. Wang, X.; Chang, V.W.C.; Tang, C.Y. Osmotic membrane bioreactor (OMBR) technology for wastewater treatment and reclamation: Advances, challenges, and prospects for the future. *J. Membr. Sci.* **2016**, *504*, 113–132, doi:10.1016/j.memsci.2016.01.010.

38. McCutcheon, J.R.; Elimelech, M. Influence of concentrative and dilutive internal concentration polarization on flux behavior in forward osmosis. *J. Membr. Sci.* **2006**, *284*, 237–247, doi:10.1016/j.memsci.2006.07.049.

39. Yangali-Quintanilla, V.; Li, Z.; Valladares, R.; Li, Q.; Amy, G. Indirect desalination of Red Sea water with forward osmosis and low pressure reverse osmosis for water reuse. *Desalination* **2011**, *280*, 160–166, doi:10.1016/j.desal.2011.06.066.

40. McGinnis, R.L.; Elimelech, M. Energy requirements of ammonia–carbon dioxide forward osmosis desalination. *Desalination* **2007**, *207*, 370–382, doi:10.1016/j.desal.2006.08.012.

41. Nicoll, P.G. Forward Osmosis a Brief Introduction. In *Proceedings IDA World Congress on Desalination and Water Reuse*; IDA (International Desalination Association): Tianjin, China, 2013.

42. Votta, F.; Barnett, S.M.; Anderson, D.K. Concentration of industrial waste by direct osmosis. In *Completion Report*; University of Rhode Island: Kingston, RI, USA, 1974.

43. Anderson, D.K. Concentration of Dilute Industrial Wastes by Direct Osmosis. Master's Thesis, University of Rhode Island, Kingston, RI, USA, 1977.

44. Lee, K.P.; Arnot, T.C.; Mattia, D. A review of reverse osmosis membrane materials for desalination—Development to date and future potential. *J. Membr. Sci.* **2011**, *370*, 1–22, doi:10.1016/j.memsci.2010.12.036.

45. Li, D.; Yan, Y.; Wang, H. Recent advances in polymer and polymer composite membranes for reverse and forward osmosis processes. *Prog. Polym. Sci.* **2016**, *61*, 104–155, doi:10.1016/j.progpolymsci.2016.03.003.

46. Xu, W.; Chen, Q.; Ge, Q. Recent advances in forward osmosis (FO) membrane: Chemical modifications on membranes for FO processes. *Desalination* **2017**, *419*, 101–116, doi:10.1016/j.desal.2017.06.007.

47. Razali, M.; Kim, J.F.; Attfield, M.; Budd, P.M.; Drioli, E.; Lee, Y.M.; Szekely, G. Sustainable wastewater treatment and recycling in membrane manufacturing. *Green Chem.* **2015**, *17*, 5196–5205, doi:10.1039/C5GC01937K.

48. Takahashi, T.; Yasukawa, M.; Matsuyama, H. Highly condensed polyvinyl chloride latex production by forward osmosis: Performance and characteristics. *J. Membr. Sci.* **2016**, *514*, 547–555, doi:10.1016/j.memsci.2016.04.012.

49. Liu, C.; Lei, X.; Wang, L.; Jia, J.; Liang, X.; Zhao, X.; Zhu, H. Investigation on the removal performances of heavy metal ions with the layer-by-layer assembled forward osmosis membranes. *Chem. Eng. J.* **2017**, *327*, 60–70, doi:10.1016/j.cej.2017.06.070.

50. Gu, W.-X.; Low, Z.-X.; Feng, Y.; Wei, J.; Wang, H. Investigating forward osmosis process for simultaneous preparation of brown coal slurry and wastewater reclamation. *Fuel Process. Technol.* **2015**, *131*, 414–420, doi:10.1016/j.fuproc.2014.11.041.

51. Phuntsho, S.; Kim, J.E.; Johir, M.A.H.; Hong, S.; Li, Z.; Ghaffour, N.; Leiknes, T.; Shon, H.K. Fertiliser drawn forward osmosis process: Pilot-scale desalination of mine impaired water for fertigation. *J. Membr. Sci.* **2016**, *508*, 22–31, doi:10.1016/j.memsci.2016.02.024.

52. Kim, J.; Blandin, G.; Phuntsho, S.; Verliefde, A.; Le-Clech, P.; Shon, H. Practical considerations for operability of an 8" spiral wound forward osmosis module: Hydrodynamics, fouling behaviour and cleaning strategy. *Desalination* **2017**, *404*, 249–258, doi:10.1016/j.desal.2016.11.004.

53. Kim, J.E.; Phuntsho, S.; Lotfi, F.; Shon, H.K. Investigation of pilot-scale 8040 FO membrane module under different operating conditions for brackish water desalination. *Desalination Water Treat.* **2015**, *53*, 2782–2791, doi:10.1080/19443994.2014.931528.

54. Song, M.; Im, S.-J.; Jeong, S.; Jang, A. Evaluation of an element-scale plate-type forward osmosis: Effect of structural parameters and operational conditions. *Desalination* **2018**, *430*, 15–23, doi:10.1016/j.desal.2017.12.010.

55. Lee, S.; Kim, Y.C. Performance analysis of plate-and-frame forward osmosis membrane elements and implications for scale-up design. *J. Membr. Sci.* **2018**, *550*, 219–229, doi:10.1016/j.memsci.2017.12.080.

56. Kazner, C.; Wünsch, R.; Remmen, K.; Wintgens, T. Membranbasierte Behandlungsverfahren für hoch-belastete Abwässer in der Chemieindustrie mit dem Ziel Zero-Liquid-Discharge. Presentation at 89. Darmstädter Seminar Abwassertechnik, Darmstadt, Germany, 18 January 2018.

57. Wünsch, R.; Remmen, K.; Pătruţ, C.; Dijk, L.; Moerland, M.; Palacin, J.; Kochan, J.; Kazner, C. Water Recovery by Forward Osmosis from Challenging Industrial Effluents towards Zero Liquid Discharge: Selection of a Suitable Draw Solution. In Proceedings of the 12. Aachener Tagung Wassertechnologie, Aachen, Germany, 24–25 October 2017.

58. INSPIREWATER—Innovative Solutions in the Process Industry for Next Generation Resource Efficient Water Management|SPIRE. Available online: https://www.spire2030.eu/inspirewater (accessed on 8 June 2018).

59. Aquaporin|Singapore Is Increasing Its Waste Water Reuse. Available online: https://aquaporin.dk/2017/07/10/singapore-is-increasing-its-waste-water-reuse/ (accessed on 8 June 2018).

60. Milk Concentration with Porifera. Available online: https://www.porifera.com/food-and-beverage/ (accessed on 8 June 2018).

61. Aquaporin|Arla Featuring Aquaporin Inside™ in the Dairy Industry. Available online: https://aquaporin.dk/2017/09/20/arla-featuring-aquaporin-inside-in-the-dairy-industry/ (accessed on 8 June 2018).

62. Modern Water Modern Water secures sale of FO system to China's Hangzhou Water. *Membr. Technol.* **2017**, *2017*, 5–6, doi:10.1016/S0958-2118(17)30111-8. Available online: https://www.sciencedirect.com/science/article/pii/S0958211817301118 (accessed on 22 July 2018).

63. Modern Water makes first forward osmosis technology sale in China. *Pump Ind. Anal.* **2017**, *2017*, 2, doi:10.1016/S1359-6128(17)30126-X. Available online: https://www.sciencedirect.com/science/article/pii/S135961281730126X (accessed on 22 July 2018).

64. Modern Water makes first FO technology sale in China. *Filtr. Sep.* **2017**, *54*, 4, doi:10.1016/S0015-1882(17)30091-5.

65. Oasys Water—Case Study: Wastewater: Changxing. Available online: http://oasyswater.com/case-study-post/changxing/ (accessed on 8 June 2018).

66. Aquaporin launches commercial forward osmosis element. *Membr. Technol.* **2017**, *2017*, 2, doi:10.1016/S0958-2118(17)30160-X.

67. Aquaporin sets up first full-scale production plant at its headquarters. *Membr. Technol.* **2017**, *2017*, 5, doi:10.1016/S0958-2118(17)30052-6.

68. Aquaporin Asia receives first prototypes of spiral-wound FO elements. *Membr. Technol.* **2017**, *2017*, 1, doi:10.1016/S0958-2118(17)30001-0.

69. Aquaporin and WOG study FO as a pre-concentration step for ZLD. *Membr. Technol.* **2016**, *2016*, 2–3, doi:10.1016/S0958-2118(16)30240-3.

70. Remmen, K.; Wünsch, R.; Heisele, A.; Dijk, L.; Schwantes, R.; Wintgens, T.; Kazner, C. Optimization of Forward Osmosis in challenging environmental applications. In Proceedings of the 11th IWA International Conference on Water Reclamation and Reuse, Long Beach, CA, USA, 23–27 July 2017.

71. Aquaporin and Darco pilot low-energy ZLD systems based on FO technology. *Membr. Technol.* **2016**, *2016*, 16, doi:10.1016/S0958-2118(16)30133-1.

72. Darco collaborates with Aquaporin on FO project. *Pump Ind. Anal.* **2016**, *2016*, 4, doi:10.1016/S1359-6128(16)70056-5.

73. Atkinson, S. De.mem adds membrane technology with large market potential to its proprietary technology portfolio. *Membr. Technol.* **2018**, *2018*, 9, doi:10.1016/S0958-2118(18)30100-9.

74. Xiao, T.; Nghiem, L.D.; Song, J.; Bao, R.; Li, X.; He, T. Phenol rejection by cellulose triacetate and thin film composite forward osmosis membranes. *Sep. Purif. Technol.* **2017**, *186*, 45–54, doi:10.1016/j.seppur.2017.05.047.

75. Growth of activity in China expands commercialisation of Oasys' FO-based ZLD technology. *Membr. Technol.* **2016**, *2016*, 1–16, doi:10.1016/S0958-2118(16)30197-5.

76. Oasys enhances its ClearFlo technology platform. *Membr. Technol.* **2017**, *2017*, 2–3, doi:10.1016/S0958-2118(17)30004-6.

77. Trevi Systems reports "lowest energy use" from forward osmosis desalination trial in Abu Dhabi. *Water Wastewater International WWi*, 7 March 2017.

78. Loo, S.-L.; Fane, A.G.; Krantz, W.B.; Lim, T.-T. Emergency water supply: A review of potential technologies and selection criteria. *Water Res.* **2012**, *46*, 3125–3151, doi:10.1016/j.watres.2012.03.030.

79. Coday, B.D.; Hoppe-Jones, C.; Wandera, D.; Shethji, J.; Herron, J.; Lampi, K.; Snyder, S.A.; Cath, T.Y. Evaluation of the transport parameters and physiochemical properties of forward osmosis membranes after treatment of produced water. *J. Membr. Sci.* **2016**, *499*, 491–502, doi:10.1016/j.memsci.2015.09.031.

80. Thiruvenkatachari, R.; Francis, M.; Cunnington, M.; Su, S. Application of integrated forward and reverse osmosis for coal mine wastewater desalination. *Sep. Purif. Technol.* **2016**, *163*, 181–188, doi:10.1016/j.seppur.2016.02.034.

81. Zhao, S.; Minier-Matar, J.; Chou, S.; Wang, R.; Fane, A.G.; Adham, S. Gas field produced/process water treatment using forward osmosis hollow fiber membrane: Membrane fouling and chemical cleaning. *Desalination* **2017**, *402*, 143–151, doi:10.1016/j.desal.2016.10.006.

82. Zhang, S.; Wang, P.; Fu, X.; Chung, T.-S. Sustainable water recovery from oily wastewater via forward osmosis-membrane distillation (FO-MD). *Water Res.* **2014**, *52*, 112–121, doi:10.1016/j.watres.2013.12.044.

83. Chekli, L.; Kim, Y.; Phuntsho, S.; Li, S.; Ghaffour, N.; Leiknes, T.; Shon, H.K. Evaluation of fertilizer-drawn forward osmosis for sustainable agriculture and water reuse in arid regions. *J. Environ. Manag.* **2017**, *187*, 137–145, doi:10.1016/j.jenvman.2016.11.021.

84. Chekli, L.; Kim, J.E.; El Saliby, I.; Kim, Y.; Phuntsho, S.; Li, S.; Ghaffour, N.; Leiknes, T.; Kyong Shon, H. Fertilizer drawn forward osmosis process for sustainable water reuse to grow hydroponic lettuce using commercial nutrient solution. *Sep. Purif. Technol.* **2017**, *181*, 18–28, doi:10.1016/j.seppur.2017.03.008.

85. Kim, J.E.; Phuntsho, S.; Chekli, L.; Hong, S.; Ghaffour, N.; Leiknes, T.; Choi, J.Y.; Shon, H.K. Environmental and economic impacts of fertilizer drawn forward osmosis and nanofiltration hybrid system. *Desalination* **2017**, *416*, 76–85, doi:10.1016/j.desal.2017.05.001.

86. Wang, X.; Zhao, Y.; Li, X.; Ren, Y. Performance evaluation of a microfiltration-osmotic membrane bioreactor (MF-OMBR) during removing silver nanoparticles from simulated wastewater. *Chem. Eng. J.* **2017**, *313*, 171–178, doi:10.1016/j.cej.2016.12.077.

87. Luján-Facundo, M.J.; Soler-Cabezas, J.L.; Mendoza-Roca, J.A.; Vincent-Vela, M.C.; Bes-Piá, A.; Doñate-Hernández, S. A study of the osmotic membrane bioreactor process using a sodium chloride solution and an industrial effluent as draw solutions. *Chem. Eng. J.* **2017**, *322*, 603–610, doi:10.1016/j.cej.2017.04.062.

88. Blandin, G.; Gautier, C.; Sauchelli Toran, M.; Monclús, H.; Rodriguez-Roda, I.; Comas, J. Retrofitting membrane bioreactor (MBR) into osmotic membrane bioreactor (OMBR): A pilot scale study. *Chem. Eng. J.* **2018**, *339*, 268–277, doi:10.1016/j.cej.2018.01.103.

89. Cornelissen, E.R.; Harmsen, D.; de Korte, K.F.; Ruiken, C.J.; Qin, J.-J.; Oo, H.; Wessels, L.P. Membrane fouling and process performance of forward osmosis membranes on activated sludge. *J. Membr. Sci.* **2008**, *319*, 158–168, doi:10.1016/j.memsci.2008.03.048.

90. Xie, M.; Nghiem, L.D.; Price, W.E.; Elimelech, M. Toward Resource Recovery from Wastewater: Extraction of Phosphorus from Digested Sludge Using a Hybrid Forward Osmosis–Membrane Distillation Process. *Environ. Sci. Technol. Lett.* **2014**, *1*, 191–195, doi:10.1021/ez400189z.

91. Holloway, R.W.; Childress, A.E.; Dennett, K.E.; Cath, T.Y. Forward osmosis for concentration of anaerobic digester centrate. *Water Res.* **2007**, *41*, 4005–4014, doi:10.1016/j.watres.2007.05.054.

92. Wu, S.; Zou, S.; Yang, Y.; Qian, G.; He, Z. Enhancing the performance of an osmotic microbial fuel cell through self-buffering with reverse-fluxed sodium bicarbonate. *Chem. Eng. J.* **2018**, *349*, 241–248, doi:10.1016/j.cej.2018.05.086.

93. Qin, M.; Hynes, E.A.; Abu-Reesh, I.M.; He, Z. Ammonium removal from synthetic wastewater promoted by current generation and water flux in an osmotic microbial fuel cell. *J. Clean. Prod.* **2017**, *149*, 856–862, doi:10.1016/j.jclepro.2017.02.169.

94. Yang, Y.; Qin, M.; Yang, X.; He, Z. Sustainable operation of osmotic microbial fuel cells through effective reproduction of polyelectrolyte draw solutes facilitated by cathodic pH increase. *J. Clean. Prod.* **2017**, *168*, 1143–1149, doi:10.1016/j.jclepro.2017.09.107.

95. Yang, E.; Chae, K.-J.; Alayande, A.B.; Kim, K.-Y.; Kim, I.S. Concurrent performance improvement and biofouling mitigation in osmotic microbial fuel cells using a silver nanoparticle-polydopamine coated forward osmosis membrane. *J. Membr. Sci.* **2016**, *513*, 217–225, doi:10.1016/j.memsci.2016.04.028.

96. Al-Mamun, A.; Baawain, M.S.; Dhar, B.R.; Kim, I.S. Improved recovery of bioenergy and osmotic water in an osmotic microbial fuel cell using micro-diffuser assisted marine aerobic biofilm on cathode. *Biochem. Eng. J.* **2017**, *128*, 235–242, doi:10.1016/j.bej.2017.09.020.

97. Liu, J.; Wang, X.; Wang, Z.; Lu, Y.; Li, X.; Ren, Y. Integrating microbial fuel cells with anaerobic acidification and forward osmosis membrane for enhancing bio-electricity and water recovery from low-strength wastewater. *Water Res.* **2017**, *110*, 74–82, doi:10.1016/j.watres.2016.12.012.

98. Zhang, F.; Brastad, K.S.; He, Z. Integrating Forward Osmosis into Microbial Fuel Cells for Wastewater Treatment, Water Extraction and Bioelectricity Generation. *Environ. Sci. Technol.* **2011**, *45*, 6690–6696, doi:10.1021/es201505t.

99. Xie, M.; Luo, W.; Guo, H.; Nghiem, L.D.; Tang, C.Y.; Gray, S.R. Trace organic contaminant rejection by aquaporin forward osmosis membrane: Transport mechanisms and membrane stability. *Water Res.* **2018**, *132*, 90–98, doi:10.1016/j.watres.2017.12.072.

100. Alturki, A.A.; McDonald, J.A.; Khan, S.J.; Price, W.E.; Nghiem, L.D.; Elimelech, M. Removal of trace organic contaminants by the forward osmosis process. *Sep. Purif. Technol.* **2013**, *103*, 258–266, doi:10.1016/j.seppur.2012.10.036.

101. Xie, M.; Price, W.E.; Nghiem, L.D.; Elimelech, M. Effects of feed and draw solution temperature and transmembrane temperature difference on the rejection of trace organic contaminants by forward osmosis. *J. Membr. Sci.* **2013**, *438*, 57–64, doi:10.1016/j.memsci.2013.03.031.

102. Xie, M.; Nghiem, L.D.; Price, W.E.; Elimelech, M. Comparison of the removal of hydrophobic trace organic contaminants by forward osmosis and reverse osmosis. *Water Res.* **2012**, *46*, 2683–2692, doi:10.1016/j.watres.2012.02.023.

103. Hancock, N.T.; Xu, P.; Heil, D.M.; Bellona, C.; Cath, T.Y. Comprehensive Bench- and Pilot-Scale Investigation of Trace Organic Compounds Rejection by Forward Osmosis. *Environ. Sci. Technol.* **2011**, *45*, 8483–8490, doi:10.1021/es201654k.

104. Valladares Linares, R.; Yangali-Quintanilla, V.; Li, Z.; Amy, G. Rejection of micropollutants by clean and fouled forward osmosis membrane. *Water Res.* **2011**, *45*, 6737–6744, doi:10.1016/j.watres.2011.10.037.

105. Carvalho, F.; Prazeres, A.R.; Rivas, J. Cheese whey wastewater: Characterization and treatment. *Sci. Total Environ.* **2013**, *445*, 385–396, doi:10.1016/j.scitotenv.2012.12.038.

106. Aydiner, C.; Sen, U.; Koseoglu-Imer, D.Y.; Can Dogan, E. Hierarchical prioritization of innovative treatment systems for sustainable dairy wastewater management. *J. Clean. Prod.* **2016**, *112*, 4605–4617, doi:10.1016/j.jclepro.2015.08.107.

107. Aydiner, C.; Sen, U.; Topcu, S.; Ekinci, D.; Altinay, A.D.; Koseoglu-Imer, D.Y.; Keskinler, B. Techno-economic viability of innovative membrane systems in water and mass recovery from dairy wastewater. *J. Membr. Sci.* **2014**, *458*, 66–75, doi:10.1016/j.memsci.2014.01.058.

108. Aydiner, C.; Sen, U.; Topcu, S.; Sesli, D.; Ekinci, D.; Altınay, A.D.; Ozbey, B.; Koseoglu-Imer, D.Y.; Keskinler, B. Techno-economic investigation of water recovery and whey powder production from whey using UF/RO and FO/RO integrated membrane systems. *Desalination Water Treat.* **2014**, *52*, 123–133, doi:10.1080/19443994.2013.786655.

109. Aydiner, C.; Topcu, S.; Tortop, C.; Kuvvet, F.; Ekinci, D.; Dizge, N.; Keskinler, B. A novel implementation of water recovery from whey: "Forward–reverse osmosis" integrated membrane system. *Desalination Water Treat.* **2013**, *51*, 786–799, doi:10.1080/19443994.2012.693713.

110. Seker, M.; Buyuksari, E.; Topcu, S.; Babaoglu, D.S.; Celebi, D.; Keskinler, B.; Aydiner, C. Effect of pretreatment and membrane orientation on fluxes for concentration of whey with high foulants by using NH_3/CO_2 in forward osmosis. *Bioresour. Technol.* **2017**, *243*, 237–246, doi:10.1016/j.biortech.2017.06.101.

111. Seker, M.; Buyuksari, E.; Topcu, S.; Sesli, D.; Celebi, D.; Keskinler, B.; Aydiner, C. Effect of process parameters on flux for whey concentration with NH_3/CO_2 in forward osmosis. *Food Bioprod. Process.* **2017**, *105*, 64–76, doi:10.1016/j.fbp.2017.05.006.

112. Wang, Y.-N.; Wang, R.; Li, W.; Tang, C.Y. Whey recovery using forward osmosis—Evaluating the factors limiting the flux performance. *J. Membr. Sci.* **2017**, *533*, 179–189, doi:10.1016/j.memsci.2017.03.047.

113. Pal, P.; Nayak, J. Development and analysis of a sustainable technology in manufacturing acetic acid and whey protein from waste cheese whey. *J. Clean. Prod.* **2016**, *112*, 59–70, doi:10.1016/j.jclepro.2015.07.085.

114. Song, H.; Xie, F.; Chen, W.; Liu, J. FO/MD hybrid system for real dairy wastewater recycling. *Environ. Technol.* **2017**, 1–11, doi:10.1080/09593330.2017.1377771.

115. Haupt, A.; Lerch, A. Forward osmosis treatment of effluents from dairy and automobile industry—Results from short-term experiments to show general applicability. *Water Sci. Technol.* **2018**, in press.

116. Marques, M.P.; Alves, V.D.; Coelhoso, I.M. Concentration of Tea Extracts by Osmotic Evaporation: Optimisation of Process Parameters and Effect on Antioxidant Activity. *Membranes* **2016**, *7*, 1, doi:10.3390/membranes7010001.

117. Gebreyohannes, A.Y.; Curcio, E.; Poerio, T.; Mazzei, R.; Di, P.; Drioli, E.; Giorno, L. Treatment of Olive Mill Wastewater by Forward Osmosis. *Sep. Purif. Technol.* **2015**, *147*, 292–302, doi:10.1016/j.seppur.2015.04.021.

118. Singh, N.; Petrinic, I.; Hélix-Nielsen, C.; Basu, S.; Balakrishnan, M. Concentrating molasses distillery wastewater using biomimetic forward osmosis (FO) membranes. *Water Res.* **2018**, *130*, 271–280, doi:10.1016/j.watres.2017.12.006.

119. Salih, H.H.; Dastgheib, S.A. Treatment of a hypersaline brine, extracted from a potential CO_2 sequestration site, and an industrial wastewater by membrane distillation and forward osmosis. *Chem. Eng. J.* **2017**, *325*, 415–423, doi:10.1016/j.cej.2017.05.075.

120. Ji, Q.; Lv, Z.; Yun, Y.; Li, J.; Li, C.; Zhu, S. Preparation of cellulose triacetate forward osmosis membranes for treating esterification wastewater. *Desalination Water Treat.* **2017**, *61*, 88–97, doi:10.5004/dwt.2016.0129.

121. Soler-Cabezas, J.L.; Mendoza-Roca, J.A.; Vincent-Vela, M.C.; Luján-Facundo, M.J.; Pastor-Alcañiz, L. Simultaneous concentration of nutrients from anaerobically digested sludge centrate and pre-treatment of industrial effluents by forward osmosis. *Sep. Purif. Technol.* **2018**, *193*, 289–296, doi:10.1016/j.seppur.2017.10.058.

122. Law, J.Y.; Mohammad, A.W. Osmotic concentration of succinic acid by forward osmosis: Influence of feed solution pH and evaluation of seawater as draw solution. *Chin. J. Chem. Eng.* **2018**, *26*, 976–983, doi:10.1016/j.cjche.2017.10.003.

123. Chang, H.N.; Choi, J.; Lee, S.Y.; Lee, J.W.; Park, S.; Kim, W.; Kim, T.-W.; Jung, K.; Park, G.; Kong, W.; et al. Method of Concentrating Low Titer Fermentation Broths Using Forward Osmosis. U.S. Patent 20120118827A1, 17 May 2012.

124. Cho, Y.H.; Lee, H.D.; Park, H.B. Integrated Membrane Processes for Separation and Purification of Organic Acid from a Biomass Fermentation Process. *Ind. Eng. Chem. Res.* **2012**, *51*, 10207–10219, doi:10.1021/ie301023r.

125. Ihalainen, H. Concentration of Lactic Acid by Forward Osmosis. Master's Thesis, Lappeenranta University of Technology, Lappeenranta, Finland, 2016.

126. Kalafatakis, S.; Braekevelt, S.; Carlsen, V.; Lange, L.; Skiadas, I.V.; Gavala, H.N. On a novel strategy for water recovery and recirculation in biorefineries through application of forward osmosis membranes. *Chem. Eng. J.* **2017**, *311*, 209–216, doi:10.1016/j.cej.2016.11.092.

127. Shibuya, M.; Yasukawa, M.; Sasaki, K.; Tanaka, Y.; Takahashi, T.; Kondo, A.; Matsuyama, H. Up-concentration of sugars in pretreated-rice straw by an osmotic pressure-driven method. *Biochem. Eng. J.* **2017**, *121*, 13–16, doi:10.1016/j.bej.2017.01.012.

128. Shibuya, M.; Sasaki, K.; Tanaka, Y.; Yasukawa, M.; Takahashi, T.; Kondo, A.; Matsuyama, H. Development of combined nanofiltration and forward osmosis process for production of ethanol from pretreated rice straw. *Bioresour. Technol.* **2017**, *235*, 405–410, doi:10.1016/j.biortech.2017.03.158.

129. Ruprakobkit, T.; Ruprakobkit, L.; Ratanatamskul, C. Carboxylic acid concentration by forward osmosis processes: Dynamic modeling, experimental validation and simulation. *Chem. Eng. J.* **2016**, *306*, 538–549, doi:10.1016/j.cej.2016.07.091.

130. Cui, Y.; Chung, T.-S. Pharmaceutical concentration using organic solvent forward osmosis for solvent recovery. *Nat. Commun.* **2018**, *9*, 1426, doi:10.1038/s41467-018-03612-2.

131. Kumar, R.; Pal, P. A novel forward osmosis-nano filtration integrated system for coke-oven wastewater reclamation. *Chem. Eng. Res. Des.* **2015**, *100*, 542–553, doi:10.1016/j.cherd.2015.05.012.

132. Pal, P.; Kumar, R. Treatment of Coke Wastewater: A Critical Review for Developing Sustainable Management Strategies. *Sep. Purif. Rev.* **2014**, *43*, 89–123, doi:10.1080/15422119.2012.717161.

133. Zhang, X.; Li, Q.; Wang, J.; Li, J.; Zhao, C.; Hou, D. Effects of feed solution pH and draw solution concentration on the performance of phenolic compounds removal in forward osmosis process. *J. Environ. Chem. Eng.* **2017**, *5*, 2508–2514, doi:10.1016/j.jece.2017.03.030.

134. Leite, G.B.; Abdelaziz, A.E.M.; Hallenbeck, P.C. Algal biofuels: Challenges and opportunities. *Bioresour. Technol.* **2013**, *145*, 134–141, doi:10.1016/j.biortech.2013.02.007.

135. Markou, G.; Nerantzis, E. Microalgae for high-value compounds and biofuels production: A review with focus on cultivation under stress conditions. *Biotechnol. Adv.* **2013**, *31*, 1532–1542, doi:10.1016/j.biotechadv.2013.07.011.

136. Razzak, S.A.; Hossain, M.M.; Lucky, R.A.; Bassi, A.S.; de Lasa, H. Integrated CO_2 capture, wastewater treatment and biofuel production by microalgae culturing—A review. *Renew. Sustain. Energy Rev.* **2013**, *27*, 622–653, doi:10.1016/j.rser.2013.05.063.

137. Mo, W.; Soh, L.; Werber, J.R.; Elimelech, M.; Zimmerman, J.B. Application of membrane dewatering for algal biofuel. *Algal Res.* **2015**, *11*, 1–12, doi:10.1016/j.algal.2015.05.018.

138. Bilad, M.R.; Arafat, H.A.; Vankelecom, I.F.J. Membrane technology in microalgae cultivation and harvesting: A review. *Biotechnol. Adv.* **2014**, *32*, 1283–1300, doi:10.1016/j.biotechadv.2014.07.008.

139. Larronde-Larretche, M.; Jin, X. Microalgal biomass dewatering using forward osmosis membrane: Influence of microalgae species and carbohydrates composition. *Algal Res.* **2017**, *23*, 12–19, doi:10.1016/j.algal.2016.12.020.

140. Larronde-Larretche, M.; Jin, X. Microalgae (*Scenedesmus obliquus*) dewatering using forward osmosis membrane: Influence of draw solution chemistry. *Algal Res.* **2016**, *15*, 1–8, doi:10.1016/j.algal.2016.01.014.

141. Zou, S.; Wang, Y.-N.; Wicaksana, F.; Aung, T.; Wong, P.C.Y.; Fane, A.G.; Tang, C.Y. Direct microscopic observation of forward osmosis membrane fouling by microalgae: Critical flux and the role of operational conditions. *J. Membr. Sci.* **2013**, *436*, 174–185, doi:10.1016/j.memsci.2013.02.030.

142. Zou, S.; Gu, Y.; Xiao, D.; Tang, C.Y. The role of physical and chemical parameters on forward osmosis membrane fouling during algae separation. *J. Membr. Sci.* **2011**, *366*, 356–362, doi:10.1016/j.memsci.2010.10.030.

143. Buckwalter, P.; Embaye, T.; Gormly, S.; Trent, J.D. Dewatering microalgae by forward osmosis. *Desalination* **2013**, *312*, 19–22, doi:10.1016/j.desal.2012.12.015.

144. Marcucci, M.; Nosenzo, G.; Capannelli, G.; Ciabatti, I.; Corrieri, D.; Ciardelli, G. Treatment and reuse of textile effluents based on new ultrafiltration and other membrane technologies. *Desalination* **2001**, *138*, 75–82, doi:10.1016/S0011-9164(01)00247-8.

145. Holkar, C.R.; Jadhav, A.J.; Pinjari, D.V.; Mahamuni, N.M.; Pandit, A.B. A critical review on textile wastewater treatments: Possible approaches. *J. Environ. Manag.* **2016**, *182*, 351–366, doi:10.1016/j.jenvman.2016.07.090.

146. Ammar, A.; Dofan, I.; Jegatheesan, V.; Muthukumaran, S.; Shu, L. Comparison between nanofiltration and forward osmosis in the treatment of dye solutions. *Desalination Water Treat.* **2015**, *54*, 853–861, doi:10.1080/19443994.2014.908419.

147. Han, G.; Liang, C.-Z.; Chung, T.-S.; Weber, M.; Staudt, C.; Maletzko, C. Combination of forward osmosis (FO) process with coagulation/flocculation (CF) for potential treatment of textile wastewater. *Water Res.* **2016**, *91*, 361–370, doi:10.1016/j.watres.2016.01.031.

148. Huang, J.; Long, Q.; Xiong, S.; Shen, L.; Wang, Y. Application of poly (4-styrenesulfonic acid-co-maleic acid) sodium salt as novel draw solute in forward osmosis for dye-containing wastewater treatment. *Desalination* **2017**, *421*, 40–46, doi:10.1016/j.desal.2017.01.039.

149. Ge, Q.; Wang, P.; Wan, C.; Chung, T.-S. Polyelectrolyte-Promoted Forward Osmosis–Membrane Distillation (FO–MD) Hybrid Process for Dye Wastewater Treatment. *Environ. Sci. Technol.* **2012**, *46*, 6236–6243, doi:10.1021/es300784h.

150. Zhao, P.; Gao, B.; Xu, S.; Kong, J.; Ma, D.; Shon, H.K.; Yue, Q.; Liu, P. Polyelectrolyte-promoted forward osmosis process for dye wastewater treatment—Exploring the feasibility of using polyacrylamide as draw solute. *Chem. Eng. J.* **2015**, *264*, 32–38, doi:10.1016/j.cej.2014.11.064.

151. Duan, J.; Litwiller, E.; Choi, S.-H.; Pinnau, I. Evaluation of sodium lignin sulfonate as draw solute in forward osmosis for desert restoration. *J. Membr. Sci.* **2014**, *453*, 463–470, doi:10.1016/j.memsci.2013.11.029.

152. Gwak, G.; Kim, D.I.; Hong, S. New industrial application of forward osmosis (FO): Precious metal recovery from printed circuit board (PCB) plant wastewater. *J. Membr. Sci.* **2018**, *552*, 234–242, doi:10.1016/j.memsci.2018.02.022.

153. Gwak, G.; Kim, D.I.; Lim, J.A.; Hong, S. New Industrial Application of Forward Osmosis: Precious Metal Recovery. *J. Membr. Sci.* **2018**, *552*, 234–242.

154. Nguyen, N.C.; Chen, S.-S.; Weng, Y.-T.; Thi Nguyen, H.; Ray, S.S.; Li, C.-W.; Yan, B.; Wang, J. Iodide recovery from thin film transistor liquid crystal display plants by using potassium hydroxide—Driven forward osmosis. *J. Membr. Sci.* **2016**, *520*, 214–220, doi:10.1016/j.memsci.2016.07.062.

155. Zhao, X.; Liu, C. Efficient removal of heavy metal ions based on the optimized dissolution-diffusion-flow forward osmosis process. *Chem. Eng. J.* **2018**, *334*, 1128–1134, doi:10.1016/j.cej.2017.11.063.

156. Cui, Y.; Ge, Q.; Liu, X.-Y.; Chung, T.-S. Novel forward osmosis process to effectively remove heavy metal ions. *J. Membr. Sci.* **2014**, *467*, 188–194, doi:10.1016/j.memsci.2014.05.034.

157. You, S.; Lu, J.; Tang, C.Y.; Wang, X. Rejection of heavy metals in acidic wastewater by a novel thin-film inorganic forward osmosis membrane. *Chem. Eng. J.* **2017**, *320*, 532–538, doi:10.1016/j.cej.2017.03.064.

158. Zhao, P.; Gao, B.; Yue, Q.; Liu, S.; Shon, H.K. The performance of forward osmosis in treating high-salinity wastewater containing heavy metal Ni^{2+}. *Chem. Eng. J.* **2016**, *288*, 569–576, doi:10.1016/j.cej.2015.12.038.

159. Wu, C.-Y.; Mouri, H.; Chen, S.-S.; Zhang, D.-Z.; Koga, M.; Kobayashi, J. Removal of trace-amount mercury from wastewater by forward osmosis. *J. Water Process Eng.* **2016**, *14*, 108–116, doi:10.1016/j.jwpe.2016.10.010.

160. Wang, W.; Zhang, Y.; Esparra-Alvarado, M.; Wang, X.; Yang, H.; Xie, Y. Effects of pH and temperature on forward osmosis membrane flux using rainwater as the makeup for cooling water dilution. *Desalination* **2014**, *351*, 70–76, doi:10.1016/j.desal.2014.07.025.

161. Wang, K.Y.; Teoh, M.M.; Nugroho, A.; Chung, T.-S. Integrated forward osmosis–membrane distillation (FO–MD) hybrid system for the concentration of protein solutions. *Chem. Eng. Sci.* **2011**, *66*, 2421–2430, doi:10.1016/j.ces.2011.03.001.

.

3 Forward Osmosis Treatment of Effluents from Dairy and Automobile Industry – Results from Short-Term Experiments to Show General Applicability

Abstract

Forward osmosis (FO) is a potential membrane technology to treat wastewater energy-efficiently with low fouling. In lab-scale experiments, six effluents from a dairy and an automobile production plant were tested to find out if FO is an applicable treatment technology. Permeate flux and reverse salt flux were determined in nine test series with three subsequent 5 h experiments each. In between, the membrane was cleaned with deionised water. Membrane performance tests before each experiment were used to monitor membrane performance and fouling. Samples were analysed and the T/M-value was introduced to indicate which substances caused fouling. Dairy cheese brine was a suitable DS. Here, permeate fluxes were 21.0 and 15.1 L/(m²·h). Automobile cooling tower water and wastewater from cathodic dip painting were also used as DS. However, permeate fluxes were below 1.1 L/(m²·h). The tested FS, reverse osmosis concentrate from dairy wastewater treatment, rinsing water and wastewater from automobile cathodic dip painting as well as wastewater from automobile paint shop pre-treatment, showed good performance regarding the permeate flux between 7.9 and 19.4 L/(m²·h). Membrane performance test showed that some of the effluents lead to permeate flux reduction due to fouling. Different cleaning-in-place methods were examined. Eventually, permeate flux was restored.

Keywords: automobile industry, dairy, forward osmosis, industrial wastewater, membrane technology

3.1   Introduction

In 2015 the United Nations (UN) defined 17 sustainable development goals (SDG) (United Nations 2015). One of them is the "availability and sustainable management of water and sanitation for all". This goal, but also others, are directly linked to a sufficient water supply (Ait-Kadi 2016). Industry is consuming 19 % of worldwide freshwater, making it the second largest consumer behind agriculture (70 %) (WWAP 2017). In order to achieve all of the defined SDG, an efficient water usage in industrial production processes is therefore essential. Nowadays, modern treatment technologies are applied to clean industrial wastewater so that it can be recycled. That way, industrial water demand as well as wastewater amount is reduced. However, wastewater treatment consumes a lot of energy (McGinnis & Elimelech 2008). Thus, to obtain sustainability, energy-efficient wastewater treatment technologies need to be promoted.

Frequently used treatment processes for industrial wastewaters are membrane processes. Ultra-, micro-, and nanofiltration as well as reverse osmosis (RO) are state of the art. The driving force of these conventional processes is a transmembrane pressure difference, which is technically generated by pumping resulting in a high energy demand. This is necessary to overcome the flow and membrane resistances as well as the osmotic pressure increasing with high concentrations of dissolved water constituents. Another membrane process for water treatment is forward osmosis (FO): it uses the osmotic pressure directly as a natural driving force to overcome flow and membrane resistances. Water molecules pass through the membrane from a feed solution (FS) with low osmotic pressure into a draw solution (DS) with high osmotic pressure (Cath et al. 2006). Due to the low demand of external energy, FO offers potential for energy-efficient water treatment (Mazlan et al. 2016). Disadvantageous may be the fact that a second treatment step is necessary to obtain "pure" water out of the DS (Chekli et al. 2016; Luo et al. 2014). Another negative effect occurring during FO treatment is the so-called reverse salt flux. This term describes that substances from the DS diffuse into the FS through the membrane, possibly changing FS composition (Phillip et al. 2010). In pressure driven membrane processes, reverse salt flux is less severe due to the high physical operating pressure. Still, FO is a promising approach for further concentration of aqueous product and sewage streams e. g. in industries. FO might even be applicable for waters that are unsuitable for conventional membrane processes due to a high fouling potential (Zhao et al. 2012).

Forward osmosis has already been used successfully in various applications. One of them is seawater desalination to produce drinking water (Modern Water 2017). Furthermore, FO is applied for emergency water supply in so-called hydration bags where a sugar-based draw solution and a membrane is used to clean contaminated water. Here, the result is a sweet, mineral-containing drink (Loo et al. 2012). Another application field is the

treatment of wastewater from oil and gas production as well as from mining (Coday et al. 2016; Thiruvenkatachari et al. 2016; Zhao et al. 2017). Even agricultural use of FO is examined: Concentrated fertilizer solutions are used as DS, diluted and then used for irrigation. This combined process of irrigation and fertilization is called fertigation (Chekli et al. 2017; Kim et al. 2017). In biological wastewater treatment, the separation of activated sludge and cleaned wastewater may also be done by FO process in a so-called osmotic membrane bioreactor, though reverse salt flux and its influence on microbial activity seems to be a major issue here (Wang et al. 2016). As can be seen, different types of water are subject for FO application. However, so far there are few findings regarding the FO treatment of industrial effluents or wastewater. For this reason, laboratory tests were carried out to examine the FO application for the treatment of effluents from the dairy and automobile industry. In this paper, the results of 9 test series are presented.

3.2   Material and Methods

3.2.1   Experimental Set-Up

A closed-loop lab-scale FO system was used for the experiments (figure 1). The included flat-sheet test cell had an effective membrane area of 48 cm² with symmetric channel dimensions of 1200 mm in length, 40 mm in width, and 0.86 mm in depth on both sides of the membrane. FS as well as DS flow channel contained a 34 mil propylene spacer from Hydranautics – A Nitto Group Company (USA). FS and DS were pumped through the cell in counter-current mode throughout all experiments shown here. Pumps were from Micropump Inc. (USA) and GATHER Industrie GmbH (Germany). The flow rate was automatically measured and recorded so that the pumping rate could be manually adjusted to the desired flow rate.
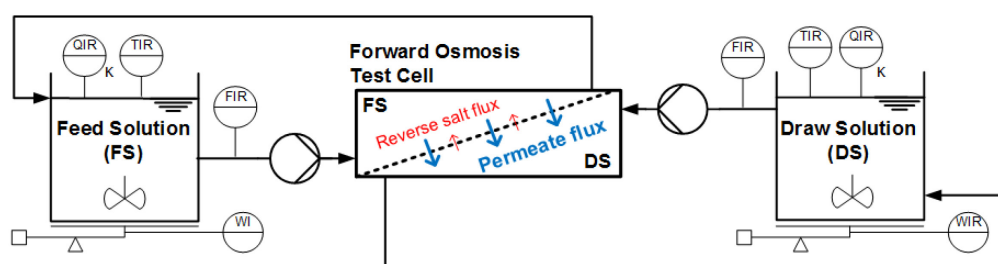
Figure 1. Lab-scale FO system with indication (I) and registration (R) of flow rate (F), quality parameter (Q) here electrical conductivity (κ), temperature (T), and weight (W)

The FS and DS tank were each placed on a digital scale (Sartorius AG and KERN & SOHN GmbH, Germany) and continuously stirred using a magnetic stirrer (Heidolph Instruments GmbH and IKA®-Werke GmbH & CO. KG, Germany). FS weight was measured continuously but only recorded manually if needed. DS weight was measured

continuously and recorded constantly using a data-logger (Delphin Technology AG, Germany). The recorded DS weight change was used to determine permeate flux. Meters in the FS and DS tank from Hach Lange GmbH (Germany) recorded the conductivity (κ) and temperature (T), which were used to calculate the reverse salt flux.

3.2.2   Membranes

Different FO membranes were used in the laboratory setup. Experiments with dairy effluents were conducted using a HTI OsMemTM TFC-ES membrane from Hydration Technology Innovations, LLC (HTI, USA); whereas experiments with automobile effluents were conducted with CSM forward osmosis membrane from Toray Chemical Korea Inc. (South Korea). The indicated standard permeate flux was 18 L/(m²·h) for the HTI membrane and 30±5 L/(m²·h) for the Toray membrane. The HTI membrane was stored in dry condition because the manufacturer had conserved the membrane with vegetable-based glycerine. The Toray membrane was stored in 1 % sodium bisulphite solution. Before the experiments, the membranes were cut to size and put in deionized water for at least 30 minutes. A new Toray membrane was used for each of the test series regarding automobile effluents. In the dairy experiments, one HTI membrane was used for all test series.

3.2.3   Experiments with Industrial Effluents as Feed and Draw Solutions

As a first step, data from a dairy and an automobile production site was evaluated. Possible FS and DS were determined. Criteria considered were above all the electrical conductivity and the desired dilution or further concentration of the effluent. Regarding the dairy, wastewater treatment RO concentrate and cheese brine were chosen for FO experiments. Four effluents were chosen from the automobile production site: they are cathodic dip painting rinsing water, cathodic dip painting wastewater, paint shop pre-treatment wastewater, and cooling tower circulation water.

The osmolality of the effluents was measured with a freezing-point microosmometer (Hermann Roebling Messtechnik, Germany). One sample of each effluent was used for three osmolality measurements. Afterward, the osmotic pressure was calculated applying equation 1 given in (Grattoni et al. 2008), where π is the osmotic pressure, c_{osm} the average osmolality, R the universal gas constant, and T the temperature.

$$\pi = c_{osm} \cdot R \cdot T \qquad (1)$$

Furthermore, all chosen effluents were analysed including the following parameters: pH, conductivity (κ), chemical oxygen demand (COD), total organic carbon (TOC), dissolved organic carbon (DOC), turbidity, total suspended solids (TSS), acid-base capacity ($K_{S4,3}$;

$K_{B8,2}$), aluminium, ammonium, lead, cadmium, calcium, chloride, iron, potassium, copper, magnesium, molybdenum, sodium, nickel, nitrate, nitrite, phosphate, silicon, and sulphate. From dairy, three samples of each effluent were analysed; from automobile industry, one sample of each effluent was analysed. Extracted information about the effluent composition and the osmotic pressure are provided in table 1.

Table 1. Composition and osmotic pressure of industrial effluents

Effluent	π (bar)	κ (mS/cm)	pH (-)	COD (mg/L)	TSS (mg/L)
Automobile effluents (one sample)					
Cathodic dip painting rinsing water	0.8	0.15	4.4	4190	588
Cathodic dip painting wastewater	2.1	4.53	2.1	890	0
Paint shop pre-treatment wastewater	1.0	1.01	3.1	91.1	18
Cooling tower circulation water	1.1	1.28	10.1	27.3	61
Dairy effluents (average value of three samples)					
Wastewater treatment RO concentrate	6.9	11.9	7.4	78.6	0
Cheese brine	158	214	4.9	11913	2491

FO experiments with industrial effluents were conducted in ALFS mode for 5 hours with an initial FS and DS volume of 1 L. The flow velocity on both sides of the membrane was 20 cm/s. First, the effluents were used as FS or DS and combined with 1 mol/L NaCl (DS) or deionized water (FS). Additionally, two combinations with an industrial effluent as FS and another industrial effluent as DS were tested. An overview of all test series can be found in table 2. Between the experiments of one test series, the membrane was kept in the test cell and rinsed with deionized water being pumped through FS and DS feed channel with a velocity of 20 cm/s.

Table 2. Conducted test series

	Feed solution (FS)	Draw solution (DS)	$\Delta\pi$ (bar)
Automobile effluents			
[A1]	*Cathodic dip painting rinsing water*	1 mol/L NaCl	44.8
[A2]	Deionized water	*Cooling tower circulation water*	1.1
[A3]	*Paint shop pre-treatment wastewater*	1 mol/L NaCl	44.5
[A4]	Deionized water	*Cathodic dip painting wastewater*	2.1
[A6]	*Cathodic dip painting wastewater*	1 mol/L NaCl	43.5
[A7]	*Paint shop pre-treatment wastewater*	*Cooling tower circulation water*	0.05
Dairy effluents			
[D1]	Deionized water	*Cheese brine*	158
[D2]	*Wastewater treatment RO concentrate*	1 mol/L NaCl	36.6
[D3]	*Wastewater treatment RO concentrate*	*Cheese brine*	151

During the experiments, FS weight, DS weight, FS conductivity, and DS conductivity were recorded either automatically via data-logger or manually. Moreover, the treated effluents after FO were analysed (only for automobile effluents to derive deposition processes, reverse salt flux concentration and composition). Based on these measurements,

permeate flux J_W, reverse salt flux J_S, specific reverse salt flux J_S/J_W, and the ratio of theoretical concentration and analysed concentration (T/M-value) were determined.

Permeate flux was calculated with DS volume change ΔV_{DS}, membrane surface area A_M, and the corresponding time difference Δt according to equation 2. DS volume change was calculated by dividing the recorded weight change by the DS density, which was assumed to be 1 kg/L because only water molecules are supposed to pass through the membrane causing DS weight increase.

$$J_W = \frac{\Delta V_{DS}}{A_M \cdot \Delta t} \qquad (2)$$

Reverse salt flux was calculated using equation 3, where β_0 and β_t are the NaCl mass concentration in the beginning and the end of the time interval, and V_0 and V_t the corresponding FS volumes. To obtain the FS volume, FS weight was divided by the density, which was assumed to be 1 kg/L.

$$J_S = \frac{\beta_t \cdot V_t - \beta_0 \cdot V_0}{A_M \cdot \Delta t} \qquad (3)$$

NaCl concentration for reverse salt flux calculation was derived from an empirically obtained correlation between conductivity and a virtual NaCl concentration. This correlation is given in equation 4 with β being the virtual NaCl concentration in mg/L, and κ the electrical conductivity in µS/cm.

$$\beta = 5{,}703 \cdot 10^{-7} \cdot \kappa^2 + 4{,}915 \cdot 10^{-4} \cdot \kappa - 6 \cdot 10^{-4} \qquad (4)$$

3.2.4   Membrane Performance Deterioration, Cleaning and Fouling

To monitor the membrane performance before and in between test runs, membrane performance tests were conducted. These tests lasted 120 minutes. Deionized water and 1 mol/L sodium chloride solution were used as FS and DS, respectively. The flow velocity in both flow channels was 20 cm/s. Initial FS and DS volume was 1 L. The membrane orientation was maintained in accordance to the previous and subsequent test run. In between experiments, the membrane remained in the test cell and cleaning was applied by rinsing with deionised water on both FS and DS side. First, 2 L of deionised water were pumped through the test cell as FS and DS, respectively. Afterwards, 1.5 L of deionised water were circulated on both FS and DS side for at least 15 hours. The flow velocity was 20 cm/s, the same as in the experiments. By comparing the membrane performance tests of one test series, it was possible to see if fouling occurred that was not easily removable by rinsing with deionised water.

In order to investigate substance behaviour during the FO process, the T/M-value was introduced and used for analysis interpretation. It is the ratio of theoretical concentration (T) and analysed (measured) concentration (M). The theoretical concentration of a substance is calculated by the analysed concentration in the untreated effluent and the

dilution or concentration effect during FO process. In this case, it is assumed that the substance remains in the effluent unchanged. Calculation was done as shown in equation 5, where β_{start} and β_{end} are the concentration in the beginning and the end of the experiment, and m_{start} and m_{end} are the solution weight. The occurring density change was neglected.

$$T = \beta_{end} = \beta_{start} \cdot \frac{m_{start}}{m_{end}} \qquad (5)$$

If T/M equals 1, the theoretical and the measured concentration are the same and the substance remains unchanged in the solution. If T/M is larger than 1, the measured concentration is smaller than the theoretical concentration and the substance gets lost during FO operation. If T/M is smaller than 1, the measured concentration is larger than the theoretical concentration. This means, the substance increases during FO operation. One source for substance loss or increase may be a substance flow through the membrane. Another possibility is the accumulation or the detachment of substances on and of the membrane surface. By comparing the T/M-value of one substance for FS and DS, it is possible to find out if this substance causes fouling or reverse salt flux.

Within the regular FO experiments with industrial effluents, the membrane was only cleaned by rinsing with deionised water as mentioned above (flow velocity 20 cm/s). After test series A7 however, in which the membrane performance decreased dramatically, different cleaning-in-place methods were applied one after the other with a membrane performance test in between each time (table 3).

Table 3. Applied cleaning-in-place procedures after test series A7 (DI = deionised water)

FS	DS	duration [h]	flow velocity	Performance test afterwards
DI	DI	15.1	v = 20 cm/s	[A7]-P4
DI	DI	111.4	v = 20 cm/s	[A7]-CP1
DI	DI	20.6	$v_{(FS)}$ = 30 cm/s, $v_{(DS)}$ = 20 cm/s	[A7]-CP2
DI	DI	20.9	$v_{(FS)}$ = 30 cm/s, $v_{(DS)}$ = 20 cm/s, opposite flow direction	[A7]-CP3
NaCl (1 mol/L)	DI	2.3	Osmotic Backwash, v = 20 cm/s	[A7]-CP4
DI	DI	90.1	v = 20 cm/s	[A7]-CP5
HCl (0.001 mol/L)	-	1.3	pH=3.2 $v_{(FS)}$ = 20 cm/s, $v_{(DS)}$ = 0 cm/s	-
DI	DI	20.5	v = 20 cm/s	[A7]-CP6
HCl (0.01 mol/L)	-	1.2	pH=2,2	-
DI	DI	17.4	v = 20 cm/s	[A7]-CP7
NaOH (0.001 mol/L)	-	1.1	pH=11.1, $v_{(FS)}$ = 20 cm/s, $v_{(DS)}$ = 0 cm/s	-
DI	DI	21.6	v = 20 cm/s	[A7]-CP8
DI	DI	139.3	v = 20 cm/s	[A7]-CP9
NaOH (0.001 mol/L)	-	2.4	pH=11.1, $v_{(FS)}$ = 20 cm/s, $v_{(DS)}$ = 0 cm/s	-
DI	DI	16.4	v = 20 cm/s	[A7]-CP10
NaOH (0.001 mol/L)	-	3.8	pH=11.1, $v_{(FS)}$ = 20 cm/s, $v_{(DS)}$ = 0 cm/s	-
DI	DI	17.8	v = 20 cm/s	[A7]-CP11
NaOH (0.001 mol/L)	-	2.5	pH=11.1, $v_{(FS)}$ = 20 cm/s, $v_{(DS)}$ = 0 cm/s	-
DI	DI	65.8	v = 20 cm/s	[A7]-CP12
DI	DI	19.0	v = 20 cm/s	[A7]-CP13

All cleaning-in-place procedures were run in closed-loop mode. Since fouling was visible on the FS side only, cleaning procedures with chemicals were limited to this side of the membrane. Concentrated HCl and NaOH were used within the pH range that was given by the membrane manufacturer. Due to the limited availability of industrial effluents, cleaning experiments were only performed for one test series exemplarily.

3.3 Results & Discussion

3.3.1 Permeate Flux and Reverse Salt Flux

FO lab-scale experiments were carried out with four effluents from an automobile production plant and two effluents from a dairy. In this paper, the results of 9 test series are presented. The effluents were either used as FS (with 1 mol/L NaCl as DS), as DS (with deionized water as FS) or in combination with one effluent as FS and another effluent as DS. If not mentioned otherwise, deionized water was used as FS and 1 mol/L NaCl was used as DS. Figure 2 shows the obtained permeate fluxes and the occurred reverse salt fluxes. For each test series, the results from three subsequent experiments (T1, T2, T3) as well as the average value is shown.
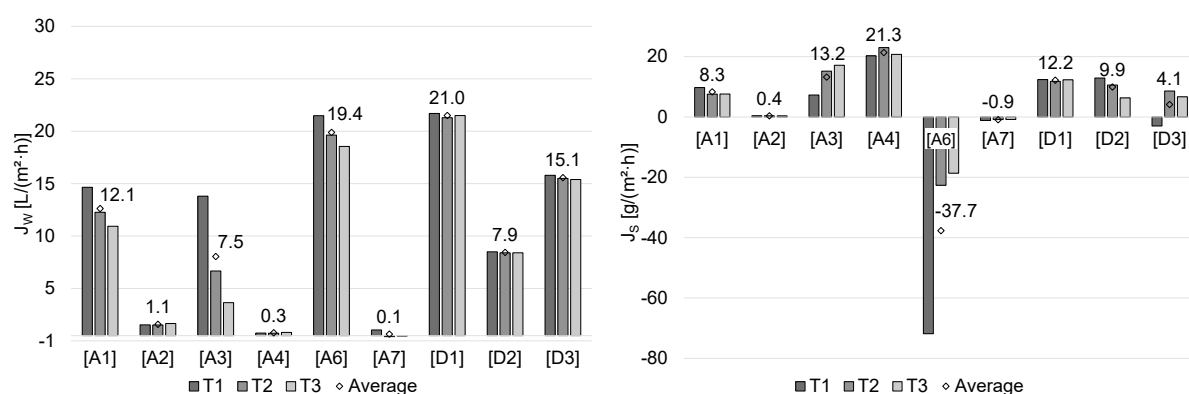
Figure 2. Permeate flux J_W and reverse salt flux J_S obtained in the lab-scale FO experiments with industrial effluents

Considering the automobile effluents (A1...A7), cathodic dip painting wastewater as FS (A6) reached the highest permeate flux, namely 19.4 L/(m²·h). Cathodic dip painting rinsing water (A1) and paint shop pre-treatment wastewater (A3) as FS produced moderate permeate fluxes of 12.1 and 7.5 L/(m²·h), respectively. Very low permeate fluxes were achieved when the DS was cooling tower circulation water (A2, A7) or cathodic dip painting wastewater (A4). Here, the permeate fluxes were between 0.1 and 0.3 L/(m²·h).

Regarding the dairy effluents (D1...D3), high permeate fluxes were obtained when cheese brine was used as the DS. Combined with deionized water as FS, the permeate flux was 21.0 L/(m²·h); with wastewater treatment RO concentrate as FS, the permeate flux

was 15.1 L/(m²·h). A moderate permeate flux of 7.9 L/(m²·h) was achieved when wastewater treatment RO concentrate was the FS and combined with 1 mol/L NaCl as DS.

In general, the occurring reverse salt flux was high when the permeate flux was high, and low when the permeate flux was low. The highest reverse salt flux occurred when cathodic dip painting wastewater was used as DS (A4), that is 21.3 g/(m²·h). Negative reverse salt fluxes took place when cathodic dip painting wastewater was the FS (A6). This means, that substances from the FS passed through the membrane into the DS. The reverse salt flux was calculated based on the conductivity change in the FS. However, there may also be other reasons for the conductivity change, e. g. remobilization of depositions from the membrane surface.

3.3.2 Membrane Performance Deterioration and Fouling

Comparing the permeate fluxes of the three experiments for each test series, it is obvious that in some cases a decrease in permeate flux happened. This decrease shows that the industrial effluent had a negative impact on the membrane. This influence can also be seen in figure 3a where the permeate flux for the performance tests is shown. Additionally, the ratio of permeate flux before the third experiment with industrial effluent (P3) and permeate flux before the first experiment (P1) is indicated. A high P3/P1-ratio means that the membrane performance did not deteriorate; a low P3/P1-ratio means that the membrane performance declined dramatically. Furthermore, the standard permeate flux given by the membrane manufacturer is visualized with a horizontal line in figure 3a.

During the dairy test series, only a small deterioration in membrane performance was noticeable although deposition on the membrane surface was visible. However, with some automobile effluents membrane performance decreased significantly. Standard permeate flux dropped to 39 % with cathodic dip painting rinsing water as FS (A1), and even worse to 19 and 28 % with paint shop pre-treatment wastewater as FS (A3, A7). Moderate influence was recorded when cathodic dip painting wastewater was used as DS (A4) and FS (A6). Here, standard permeate flux dropped to 60 and 57 %, respectively. Cooling tower circulation water had only little effect on membrane performance (A2).

Most probably, membrane performance deteriorated because substances from the industrial effluents deposited either on the membrane surface or accumulated inside the membrane structure. During the test series, the membrane surface could be visually observed because the membrane test cell consisted of acrylic glass. Depositions on the membrane surface were noted with paint shop pre-treatment wastewater as FS (A3, A7) and cathodic dip painting rinsing water as FS (A1) and all dairy effluents (D1...D3).
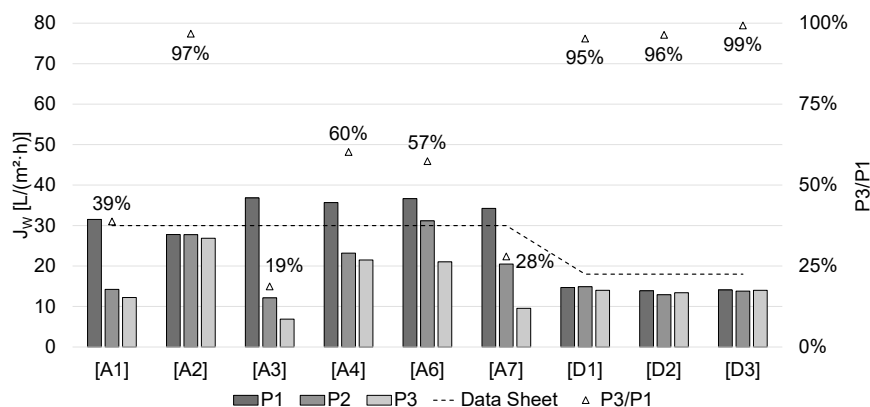
Figure 3. Permeate flux Jw obtained in standard membrane performance tests before each FO experiment with industrial effluents

Since the membrane performance declined the most when paint shop pre-treatment wastewater was used, further investigations were carried out. Figure 4 shows the calculated T/M-values of test series A7 when automobile paint shop pre-treatment wastewater was used as FS and cooling tower circulation water as DS. The T/M-value is given for both the FS and the DS side. It is obvious that TSS, iron, nickel, and silicon "disappear" from the paint shop pre-treatment wastewater (FS) because their T/M-values exceed 1.0 significantly. These substances are either lost due to deposition on the membrane or due to diffusion through the membrane into the DS. However, only nickel and silicon are increasing in the DS which can be seen by T/M-values below 1.0. The DS T/M-values show that on this side of the membrane TSS, iron, magnesium, and phosphate were reduced (T/M > 1). Only magnesium seems to be passing through the membrane into the FS where the magnesium T/M-value is below 1.0. The other substances probably deposited on the membrane surface or accumulated in the membrane structure.
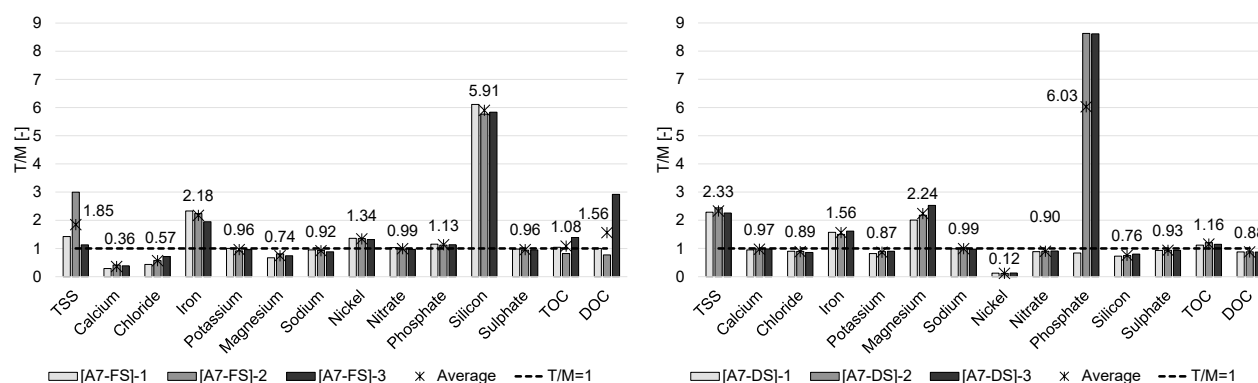
Figure 4. T/M-values of test series A7 with automobile paint shop pre-treatment wastewater as FS (left) and cooling tower circulation water as DS (right)

3.3.3   Cleaning and Membrane Performance Restoration after Test Series A7

Following test series A7, the membrane was kept in the test cell and different cleaning methods (physical and chemical cleaning, osmotic backwash) were investigated each followed by a membrane performance test (table 3). The resulting permeate fluxes are illustrated in figure 5. As a result, the standard permeate flux could be increased from 3.1 to 10.9 L/(m²·h) by rinsing with deionized water. Taking into consideration that this cleaning procedure lasted 7 days, it is ineffective. After applying osmotic backwashing, the permeate flux decreased to 9.8 L/(m²·h) showing that this cleaning procedure was also ineffective. Permeate flux increased further to 17.4 L/(m²·h) after rinsing with hydrochloric acid (pH = 3.2 and 2.2) showing a positive effect. The best improvement, however, was achieved after rinsing with deionized water and sodium hydroxide (pH = 11.1) several times. Eventually, the standard permeate flux reached 30.3 L/(m²·h) which equals the value given by the membrane manufacturer in the data sheet.
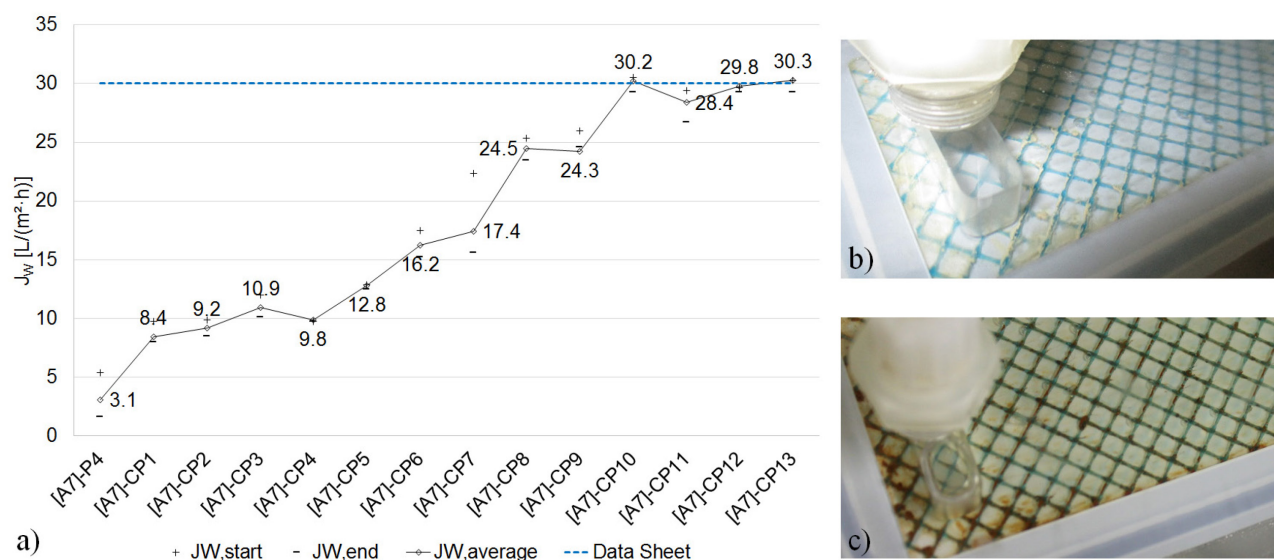
Figure 5. a) Permeate flux J$_W$ of membrane performance tests after different cleaning-in-place procedures; b) Yellow deposits on FS membrane surface after A7 before cleaning procedures; c) Brown deposits after A7 and cleaning procedures.

During the different cleaning processes, the visible deposition layer on the FS side of the membrane was not removed. However, the colour changed from yellow to brown when the membrane was rinsed with sodium hydroxide (see figure 5b and c). After the experiment, the deposits were removed from the spacer and analysed. The results showed that the deposits consisted mainly of iron. This fact and the observed colour change suggests that iron accumulated on the membrane surface as well as in the feed channel and was converted into iron hydroxide during the sodium hydroxide rinsing.

3.4   Conclusion

Lab-scale FO experiments were performed with four effluents from an automobile production site and two effluents from a dairy to investigate the priniciple applicability of FO. In general, cathodic dip painting rinsing and wastewater as well as paint shop pre-treatment wastewater from automobile industry appear suitable as FS for FO because the permeate fluxes were 12.1, 19.4 and 7.5 L/(m²·h) combined with 1 mol/L NaCl. Wastewater treatment RO concentrate from the dairy also produced good permeate fluxes of 7.9 (1 mol/L NaCl as DS) and 15.1 L/(m²·h) (cheese brine as DS) when used as FS. Regarding the permeate flux, these 4 effluents could be treated and concentrated by FO.

According to the permeate flux, only dairy cheese brine is a promising DS with permeate fluxes of 21.0 and 15.1 L/(m²·h) in combination with deionized water and dairy wastewater treatment RO concentrate as FS. Since dairy wastewater treatment RO concentrate also proved to be a suitable FS, a combination of both effluents in FO would be possible resulting in diluted cheese brine and further concentrated wastewater treatment RO concentrate. For the automobile production site, the investigated draw solutions had only a low osmotic pressure and could not produce a significant permeate flux. For this reason, both the cooling tower circulation water as well as the cathodic dip painting wastewater are unsuitable as DS. In order to apply FO in this automobile production site, other suitable DS need to be found. The following possibilities should be taken into consideration:

- Are there other liquids that are available, e. g. concentrated process chemicals that need to be diluted?
- May an additional DS be used that is circulated and reconcentrated in a separate treatment process? In this case, clean water is produced which is then applicable for diluting the cooling tower circulation water.
- Is there a way to raise the osmotic pressure of the cooling tower circulation water, e. g. with additives that do not influence cooling performance?
- Could pressure assisted osmosis increase the permeate flux when cooling tower circulation water is used as DS?

Fouling occurred in all of the lab-scale experiments. Different cleaning procedures were exemplarily investigated after one test series. Chemical cleaning with sodium hydroxide showed the best effect and permeate flux was restored. The different cleaning procedures should be applicable for automobile as well as dairy wastewater.

All in all, the results show that FO is a potential treatment technology for industrial effluents. Here, one of its main benefits is the combined, energy-efficient treatment of two effluents in the same treatment step. Surely, more applications in industry can be found helping to establish sustainable water usage.

References of Chapter 3

Ait-Kadi, M. 2016 Water for Development and Development for Water: Realizing the Sustainable Development Goals (SDGs) Vision. *Aquat. Procedia, At the Confluence 2015 – selection from the 2015 World Water Week in Stockholm* **6**, 106–110.

Cath, T.Y., Childress, A.E., Elimelech, M. 2006 Forward osmosis: Principles, applications, and recent developments. *J. Membr. Sci.* **281**, 70–87.

Chekli, L., Kim, Y., Phuntsho, S., Li, S., Ghaffour, N., Leiknes, T. & Shon, H.K. 2017 Evaluation of fertilizer-drawn forward osmosis for sustainable agriculture and water reuse in arid regions. *J. Environ. Manage.* **187**, 137–145.

Chekli, L., Phuntsho, S., Kim, J.E., Kim, J., Choi, J.Y., Choi, J.-S., Kim, S., Kim, J.H., Hong, S., Sohn, J. & Shon, H.K. 2016 A comprehensive review of hybrid forward osmosis systems: Performance, applications and future prospects. *J. Membr. Sci.* **497**, 430–449.

Coday, B.D., Hoppe-Jones, C., Wandera, D., Shethji, J., Herron, J., Lampi, K., Snyder, S.A. & Cath, T.Y. 2016 Evaluation of the transport parameters and physiochemical properties of forward osmosis membranes after treatment of produced water. *J. Membr. Sci.* **499**, 491–502.

Grattoni, A., Canavese, G., Montevecchi, F.M. & Ferrari, M. 2008 Fast Membrane Osmometer as Alternative to Freezing Point and Vapor Pressure Osmometry. *Anal. Chem.* **80**, 2617–2622.

Kim, J.E., Phuntsho, S., Chekli, L., Hong, S., Ghaffour, N., Leiknes, T., Choi, J.Y & Shon, H.K. 2017 Environmental and economic impacts of fertilizer drawn forward osmosis and nanofiltration hybrid system. *Desalination* **416**, 76–85.

Loo, S.-L., Fane, A.G., Krantz, W.B. & Lim, T.-T. 2012 Emergency water supply: A review of potential technologies and selection criteria. *Water Res.* **46**, 3125–3151.

Luo, H., Wang, Q., Zhang, T.C., Tao, T., Zhou, A., Chen, L. & Bie, X. 2014 A review on the recovery methods of draw solutes in forward osmosis. *J. Water Process Eng.* **4**, 212–223.

Mazlan, N. M., Peshev, D. & Livingston, A. G. 2016 Energy Consumption for Desalination — A Comparison of Forward Osmosis with Reverse Osmosis, and the Potential for Perfect Membranes. *Desalination* **377**, 138–51.

McGinnis, R.L. & Elimelech, M. 2008 Global Challenges in Energy and Water Supply: The Promise of Engineered Osmosis. *Environ. Sci. Technol.* **42**, 8625–8629.

Modern Water 2017 Modern Water secures sale of FO system to China's Hangzhou Water. *Membr. Technol.* **2017**, 5–6.

Phillip, W.A., Yong, J.S. & Elimelech, M. 2010 Reverse Draw Solute Permeation in Forward Osmosis: Modeling and Experiments. *Environ. Sci. Technol.* **44**, 5170–5176.

Thiruvenkatachari, R., Francis, M., Cunnington, M. & Su, S. 2016 Application of integrated forward and reverse osmosis for coal mine wastewater desalination. *Sep. Purif. Technol.* **163**, 181–188.

United Nations 2015 *Transforming our world: the 2030 agenda for sustainable development (A/RES/70/1).* United Nations, New York.

Wang, X., Chang, V.W.C. & Tang, C.Y. 2016 Osmotic membrane bioreactor (OMBR) technology for wastewater treatment and reclamation: Advances, challenges, and prospects for the future. *J. Membr. Sci.* **504**, 113–132.

WWAP 2017 *The United Nations World Water Development Report 2017: Wastewater, The Untapped Resource, WWAP (United Nations World Water Assessment Programme).* UNESCO, Paris.

Zhao, S., Minier-Matar, J., Chou, S., Wang, R., Fane, A.G. & Adham, S. 2017 Gas field produced/process water treatment using forward osmosis hollow fiber membrane: Membrane fouling and chemical cleaning. *Desalination* **402**, 143–151.

Zhao, S., Zou, L., Tang, C.Y. & Mulcahy, D. 2012 Recent developments in forward osmosis: Opportunities and challenges. *J. Membr. Sci.* **396**, 1–21.

4 Forward Osmosis Application for Semiconductor Wastewater

Anita Haupt, Felix Winkler and André Lerch, *Manuscript*.

Abstract

Forward osmosis (FO) is a membrane technology with potential for an energy-efficient, low-fouling water treatment. Due to its technical advantages, it has attracted growing interest not only in academic research but also in industrial development. The objective of our study was to investigate the applicability of FO in the semiconductor industry. In lab-scale experiments, different effluents from a semiconductor manufacturer were tested as FO feed solution (FS) and/or draw solution (DS). Four different effluents were applied in combination with either deionized water, 1 mol/L NaCl or another effluent. Membrane performance tests were used to monitor membrane fouling. Average permeate fluxes were between 10.5 and 33.4 L/(m²·h) and all industrial effluents were successfully treated by FO. Two effluent combinations were identified and found to be suitable for investigations in a larger scale. Besides technical aspects, economic aspects should then also be taken into consideration.

Keywords: forward osmosis; industrial wastewater; semiconductor industry; membrane filtration

4.1   Introduction

The driving force of conventional membrane filtration processes used in industrial water treatment is usually a transmembrane pressure difference, which is technically generated by pumping. Forward osmosis (FO) is another, innovative membrane process for water treatment [1–3]. FO uses the osmotic pressure difference as a natural driving force to overcome flow and membrane resistances. Water molecules pass through the membrane from a feed solution (FS) with low osmotic pressure into a draw solution (DS) with high osmotic pressure.

Due to the low demand of external energy, FO offers potential for energy-efficient water treatment [4,5]. Disadvantageous are the necessity of a second treatment step to obtain "pure" water out of the DS [6–8] and the so-called reverse solute flux, which describes that substances from the DS diffuse through the membrane and contaminate the FS [9]. Still, FO is a promising approach for further concentration of aqueous product and sewage streams, e. g. in industries [10, 11]. However, the economic viability of FO is a crucial point. An evaluation of pilot-scale studies showed that especially the energy needed for DS regeneration is critical [12]. Consequently, FO might be economically advantageous for FO application scenarios where no DS regeneration is needed, where evaporative technologies are used for desalination, and where desalination and wastewater treatment can be combined [12].

Since 2009 with the emergence of commercial FO membranes, research on FO has increased significantly focusing mainly on three fields: membrane development, fouling, and application [13]. Until now, regarding industries, research was conducted on FO application in food and beverage industry, chemical industry, pharmaceutical industry, coal processing, micro algae cultivation, textile industry, pulp and paper industry, electronic industry, and car manufacturing [14]. In order to further investigate FO application in industrial water and wastewater treatment, laboratory tests were carried out to examine FO applicability for the treatment of effluents from a semiconductor manufacturer. Similar applicability experiments were already performed for companies from dairy industry as well as automobile manufacturing [15].

4.2   Materials and Methods

A closed-loop lab-scale FO system was used for the experiments. The included flat-sheet test cell had an effective membrane area of 48 cm² with a channel dimension of 1200 mm in length, 40 mm in width, and 0.86 mm in depth. FS and DS were pumped through the cell in counter-current mode. The FS and DS tank were each placed on a scale. Weight change was measured to determine permeate flux. Conductivity meters in the DS and FS

tank were used to monitor the reverse salt flux. A more detailed description of the experimental set-up has been given elsewhere [15].

FO membranes from Toray Chemical Korea Inc. (Seoul, Korea) were used in the laboratory setup. The indicated standard permeate flux is 30±5 L/(m²·h), the indicated specific reverse NaCl flux is below 0.5 g/L. A new membrane sample was used for every test series. ALFS membrane orientation (FO mode) was used throughout all experiments. The flow velocity in both FS and DS flow channel was set to 20 cm/s. In order to evaluate membrane performance, standard membrane performance tests were conducted with deionized water as FS and 1 mol/L NaCl as DS. Initial volume for membrane performance tests was 1 L and test time was 2 h.

As a first step, data from a semiconductor production site (wastewater treatment as well as ultrapure water production) was evaluated. Possible FS and DS were determined considering the following criteria: electrical conductivity, pH, copper and hydrogen peroxide concentration, as well as semiconductor manufacturer's interest. Chosen FS were reverse osmosis concentrate from ultrapure water production (FS_1) and effluent from wastewater neutralization plant (FS_2). DS were filtrate from a chamber filter press dewatering copper precipitate (DS_1) and a wastewater with high copper concentration (DS_2). FS and DS characteristics are given in Table 1.

As a second step, FO process was evaluated applying the chosen FS and DS in the lab-scale experimental set-up as illustrated in Figure 1(a). Deionized water and 1 mol/L NaCl were used as standard FS and DS, respectively, to investigate the FO performance of one effluent alone. Furthermore, two combined test-runs were performed in which both FS and DS were semiconductor effluents. The test series were labelled S1, S2, S3, S4, S5, and S6. Experiments with industrial effluents used an initial volume of 1 L and ran for 5 h.
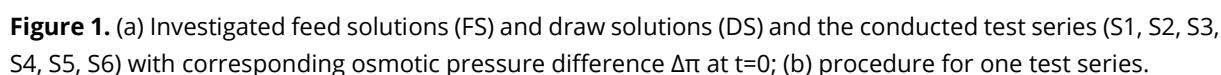
Figure 1. (a) Investigated feed solutions (FS) and draw solutions (DS) and the conducted test series (S1, S2, S3, S4, S5, S6) with corresponding osmotic pressure difference Δπ at t=0; (b) procedure for one test series.

Each test series consisted of three experiments with industrial effluents and four (membrane) performance tests. A new membrane sample was used for every test series and remained in the test cell for the whole test series. Before every experiment, a membrane performance test was conducted. After every experiment, the test cell was rinsed with deionized water as FS and DS for 15 h (DI rinsing). Here, 2 L of deionized water

were pumped once through the experimental set-up on both FS and DS side before 1.5 L of deionized water were circulated for 15 h on each side. The flow velocity during DI rinsing was 20 cm/s as in the experiments. After the third experiment and 15 h DI rinsing, a fourth membrane performance test was conducted. The procedure of one test series is illustrated in Figure 1(b).

Table 1. Parameters for industrial effluents from semiconductor industry (n.a. = not analyzed).

	FS_1 RO Concentrate UPW	DS_1 Cu Filtrate	FS_2 Neutralization Effluent	DS_2 Cu Concentrate
Conductivity, µS/cm	1.21	12'610	8'350	135'400
pH	5.55	8.82	7.8	0.55
Turbidity, FNU	0.14	0.51	1.29	0.00
H_2O_2, mg/L	<0,5	<0,5	<0,5	n.a.
Zinc, mg/L	<0,02 (0,01)	<0,02	0.02	0.13
Ammonium, mg/L	n.a.	35.6	45.7	n.a.
Lead, mg/L	<0,02 (0,00)	<0,02	<0,02	<0,02
Cadmium, mg/L	<0,02 (0,00)	<0,02	<0,02	<0,02
Calcium, mg/L	<2 (0,09)	1476	343	<2 (1,8)
Fluoride, mg/L	<0,01	7.3	<15	<0,5
Chloride, mg/L	<0,02	4532	2245	< 350
COD, mg/L	n.a.	<25	<25	n.a.
Iron, mg/L	<0,02 (0,00)	0.13	0.05	0.22
Potassium, mg/L	<0,02 (0,01)	33.8	29	0.35
Copper, mg/L	<0,02 (0,00)	0.88	<0,02	11'600
Magnesium, mg/L	<0,02 (0,00)	39.7	63.7	<0,02
Sodium, mg/L	<0,02 (0,00)	907	1'327	37.8
Nickel, mg/L	<0,02 (0,00)	0.03	<0,02	<0,02
Nitrate, mg/L	<0,02	30.7	34	26
Nitrite, mg/L	<0,02	<1	<1	<1
Phosphate, mg/L	<0,2	<10	<10	<200 (1:1000)
Sulfate, mg/L	<0,01	250	778	47'977
Osmolality, mOsmol/kg	2	190	133	1092
π (ρ=1000g/L), bar	0.05	4.63	3.24	26.60
π (ρ measured), bar	0.05	4.61	3.24	25.39
Density ρ, g/L	996.8	1004.7	1001.0	1047.6

A freezing-point microosmometer (Gonotec GmbH, Germany) was used to measure the osmolality of the effluents. The osmotic pressure was than calculated with the osmolarity c_{osm} (osmolality devided by density), the universal gas constant R, and the temperature T (equation 1).

$$\pi = c_{osm} \cdot R \cdot T \tag{1}$$

During the experiments, FS and DS weight were recorded as well as FS and DS conductivity. Permeate flux J_W was calculated with measured DS mass change Δm_{DS},

density ρ, membrane surface area A_M, and time interval Δt (equation 2). Density ρ was 1 kg/L.

$$J_W = \frac{\Delta m_{DS}}{\rho \cdot A_M \cdot \Delta t} \tag{2}$$

The NaCl mass concentration in the beginning and the end of a time interval (β_0 and β_t), and the corresponding FS volumes (V_0 and V_t) were used to calculate reverse solute flux J_S according to equation 3. FS volume was FS weight divided by density which was assumed to be 1 kg/L. An empirical correlation, which was determined in preceding experiments, using the conductivity κ in µS/cm delivered a virtual NaCl concentration β in mg/L (equation 4).

$$J_S = \frac{\beta_t \cdot V_t - \beta_0 \cdot V_0}{A_M \cdot \Delta t} \tag{3}$$

$$\beta_{NaCl} = 5.703 \cdot 10^{-9} \cdot \kappa^2 + 4.915 \cdot 10^{-4} \cdot \kappa - 6 \cdot 10^{-4} \tag{4}$$

In a previous publication, we introduced the so-called T/M-value for detailed investigation of solute flux through the membrane during the FO experiments [15]. Here, M is the measured concentration from analyzes. T is the theoretical concentration that is calculated according to equation 5. The calculation is based on the assumption that, during FO process, the total amount of a substance does not change in either FS or DS and only pure water passes the membrane. In equation 5, β_{start} is the analyzed concentration of a substance in the untreated effluent, T or β_{end} the calculated, theoretical concentration after FO; m_{start} and m_{end} are the weight of the effluent in the beginning and the end of the FO experiment, respectively. If T/M-values of one substance are compared for both FS and DS side, conclusions can be drawn about solute fluxes though the membrane and fouling caused by this substance.

$$T = \beta_{end} = \beta_{start} \cdot \frac{m_{start}}{m_{end}} \tag{5}$$

For the interpretation of the T/M-values three cases have to be considered:

- T/M = 1.0: Analyzed (M) and calculated (T) concentration are equal. This means that the total amount of the considered substance did not change. Hence, the substance did not diffuse through the membrane and did not attach to the membrane surface.

- T/M > 1.0: The analyzed concentration (M) is lower than the calculated concentration (T). Hence, the substance gets lost on this side of the membrane either via diffusion through the membrane or attachment on the membrane surface.

- T/M < 1.0: The analyzed concentration (M) is higher than the calculated concentration (T). Hence, the substance amount increases either via solute flux through the membrane from the other side or via detachment from the membrane surface.

4.3   Results

4.3.1   Permeate Flux

Six test series with four effluents from a semiconductor manufacturing site were performed as presented in Figure 1. Each test series consisted of three experiments with industrial effluents and four membrane performance tests. Figure 2 shows the obtained permeate fluxes in the experiments with industrial effluents. The osmotic pressure differences in the beginning of the experiments were between 4.6 and 46.3 bar. In all test series permeate fluxes above 10 L/(m²·h) were achieved.
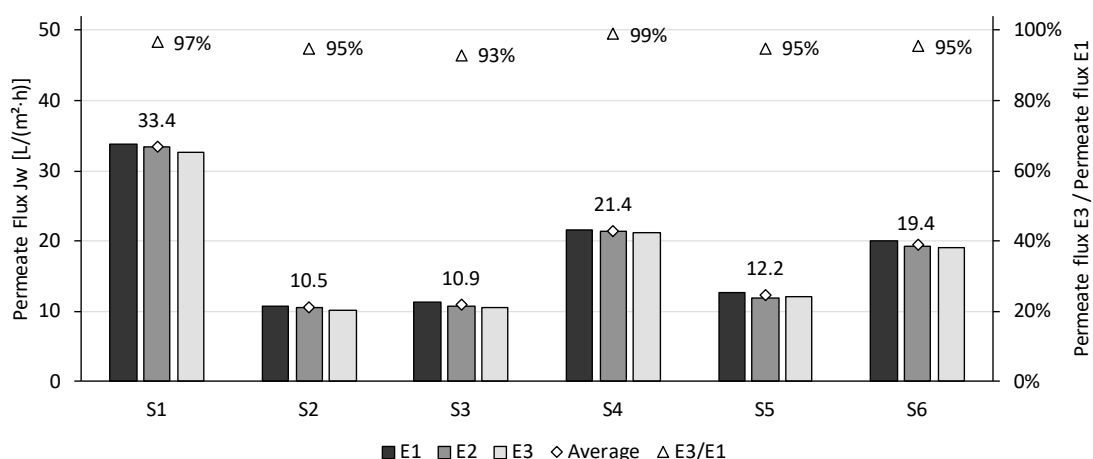
Figure 2. Permeate flux J_w obtained with semiconductor effluents in test series S1, S2, S3, S4, S5, and S6 in experiments E1, E2, and E3; average permeate flux from E1, E2, and E3; ratio of permeate flux from E3 and E1.

The highest average permeate flux of 33.4 L/(m²·h) occurred when RO concentrate from ultrapure water production was used as FS and 1 mol/L NaCl as DS (S1). RO concentrate combined with Cu filtrate as DS only delivered an average permeate flux of 10.5 L/(m²·h) (S2). A similar permeate flux of 10.9 L/(m²·h) was measured when Cu filtrate was used as DS in combination with deionized water as FS (S3). This can be explained by the fact that deionized water and semiconductor RO concentrate had almost the same quality and osmotic pressure difference in S2 and S3 were the same.

Moderate permeate fluxes of 21.4 and 19.4 L/(m²·h) were the results of neutralization effluent as FS combined with 1 mol/L NaCl as DS (S4) and deionized water as FS combined with Cu concentrate as DS (S6), respectively. When neutralization effluent as FS was combined with Cu concentrate as DS, the average permeate flux was 12.2 L/(m²·h) (S5).

In all test series, the permeate fluxes decreased slightly from the first experiment E1 to the last experiment E3. E3 permeate fluxes were 97%, 95%, 93%, 99%, 95%, and 95% of E1 permeate fluxes in test series S1, S2, S3, S4, S5, and S6, respectively. The decrease indicates that FO performance deteriorated moderately most probably due to membrane fouling and blocking, which could not be removed by the applied DI rinsing in between the experiments. Further evaluation of membrane performance and conclusions about long-term FO operation can be found in chapter 4.3.3.

4.3.2   Reverse Solute Flux

Figure 3 shows the reverse solute fluxes from DS to FS obtained in the experiments with semiconductor effluents via measurement of electrical conductivity in the FS and calculation of a virtual NaCl concentration.
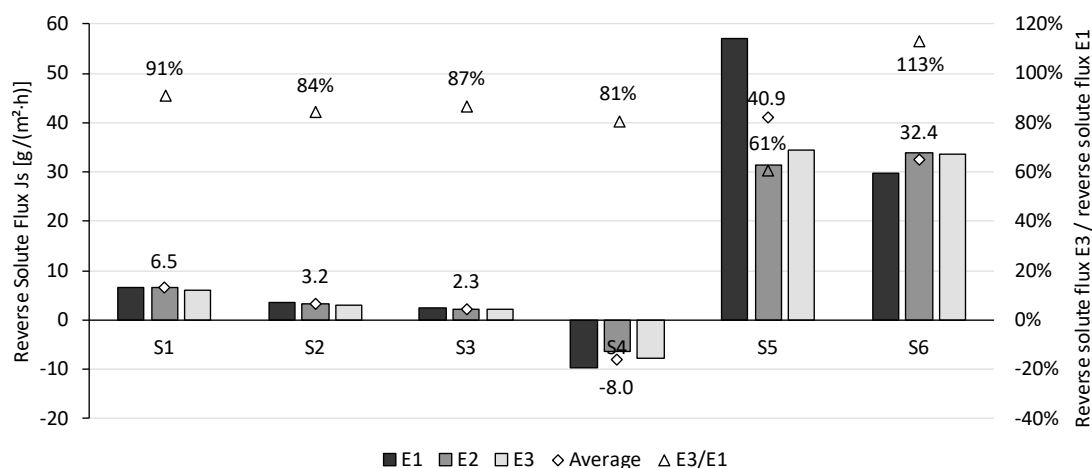
Figure 3. Reverse solute flux J_S obtained with semiconductor effluents in test series S1, S2, S3, S4, S5, and S6 in experiments E1, E2, and E3; average reverse solute flux from experiments E1, E2, and E3; ratio of reverse solute flux in E3 and E1.

In the first three test series (S1, S2, S3), reverse solute flux was between 6.5 and 2.3 g/(m²·h). In test series S4 with neutralization effluent as FS and 1 mol/L NaCl as DS, negative reverse solute fluxes were observed. This means that an unusual change in electrical conductivity was observed leading to the conclusion that substances left the FS and either deposited on the membrane surface or were transferred to the DS. This phenomenon is rather unusual in forward osmosis and has rarely been described in literature. Since no deposition layer was visible in test series S4, the substances probably diffused from FS into DS.

Very high reverse solute fluxes of 40.9 and 32.4 g/(m²·h) were measured when Cu concentrate was used as DS either with neutralization effluent as FS (S5) or deionized water as FS (S6).

In all test series except S6, reverse solute flux decreases significantly by 9 to 39% from experiment E1 to E3. This might be due to membrane fouling and blocking which not only hinders permeate flux but also impedes solute flux through the membrane. In test series S6, reverse solute flux increases by 13% from E1 to E3. An explanation of this affect is hard to find: Maybe, solute permeability of the membrane increased because of the low pH of Cu concentrate used as DS. However, this affect was not observed in test series S5 where Cu concentrate was also used as DS. However, the reverse solute flux of E1 in test series S5 was determined to be very high compared to the reverse solute fluxes of E2 and E3 of the same test series and compared to test series S6. So maybe, the reverse solute flux of E1 in S5 was subject to measurement inaccuracy. Since test series were only run once and not repeated, a definite explanation is not possible.

Solute flux is evaluated in more details by interpreting the analysis data. Those results can be found in chapter 4.3.4.

4.3.3   Membrane Performance Deterioration and Fouling

Permeate fluxes of all membrane performance tests are shown in Figure 4. Initial permeate flux of the six membrane samples (P1) was between 34.7 and 38.0 L/(m²·h); the average was 36.6 L/(m²·h) being slightly higher than the indicated standard permeate flux of 30±5 L/(m²·h) indicated by the membrane manufacturer. The discrepancy could be explained by manufacturer's test procedure which is not given in detail.

Figure 4. Permeate flux J_W of membrane performance tests P1, P2, P3, and P4 in test series S1, S2, S3, S4, S5, and S6; average permeate flux from P1, P2, P3, and P4; ratio of permeate flux in P4 and P1.

Permeate flux in membrane performance tests decreased by 7%, 3%, and 4% in test series S1, S2, and S3, respectively. In these tests, deionized water and RO concentrate from ultrapure water production were used as FS both having similar qualities with no impurities. 1 mol/L NaCl and Cu filtrate were the corresponding DS. The highest flux reduction of 7% was observed when NaCl was the DS. According to these values, Cu filtrate

apparently did have a low fouling propensity since flux decline was 3% and 4% only. Permeate fluxes in the experiments with industrial effluents decreased slightly by 3%, 5%, and 7% in S1, S2, and S3, respectively. According to these values, in contrast to the results of membrane performance test, Cu filtrate caused more fouling and flux decline than NaCl. This coincides with the observation of visible deposits on the DS side of the membrane when Cu filtrate was the DS in test series S2 and S3 (Figure 12, Figure 13).

In test series S4 permeate flux of membrane performance test did not decrease but stayed constant and even increased slightly by 1% over the course of the test series. Consequently, neutralization effluent, which was the FS, did not cause fouling. Permeate fluxes in the test series were also stable supporting the low fouling propensity of neutralization effluent. In test series S5 and S6 Cu concentrate was used as DS. In these test series, the permeate fluxes in the membrane performance tests decreased by 17% and 13% proving that Cu concentrate caused fouling and affecting FO performance negatively. Interestingly, deposits were observed in both test series on the FS side of the membrane, not on the DS side where Cu concentrate was in contact to the membrane. This leads to the assumption that reverse solute flux occurred and led to precipitation on the FS side. More information about the deposits are included in chapter 3.4.

Figure 5 illustrates the reverse solute fluxes measured in the membrane performance tests. Initial reverse solute flux of the six membrane samples was between 6.1 and 8.5 g/(m²·h); the average was 6.8 g/(m²·h). Reverse solute flux is desired to be low in forward osmosis. For this reason, an increase is not favorable. Interestingly enough, reverse solute flux decreased by 8 to 14%within the course of the first three test series, whereas is increased slightly by 2 to 6% within the course of the last three test series. Since the increase in our experiments was very low, the industrial effluents have no negative impact on reverse solute flux. The decrease in reverse solute flux in S1, S2, and S3 might be due to fouling layers that built up on the membrane surface hindering substance diffusion. In S1, S2, and S3, no visible deposits were observed on the membrane surface. Nevertheless, does the decreasing permeate flux in the experiments, which was discussed in chapter 3.1, as well as the decreasing permeate flux in the membrane performance tests indicate that fouling and blocking of the membrane occurred.

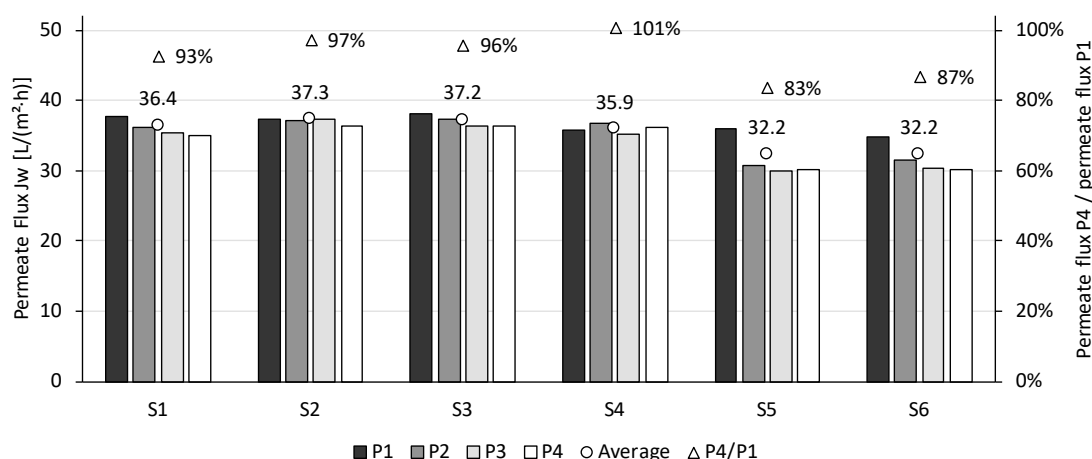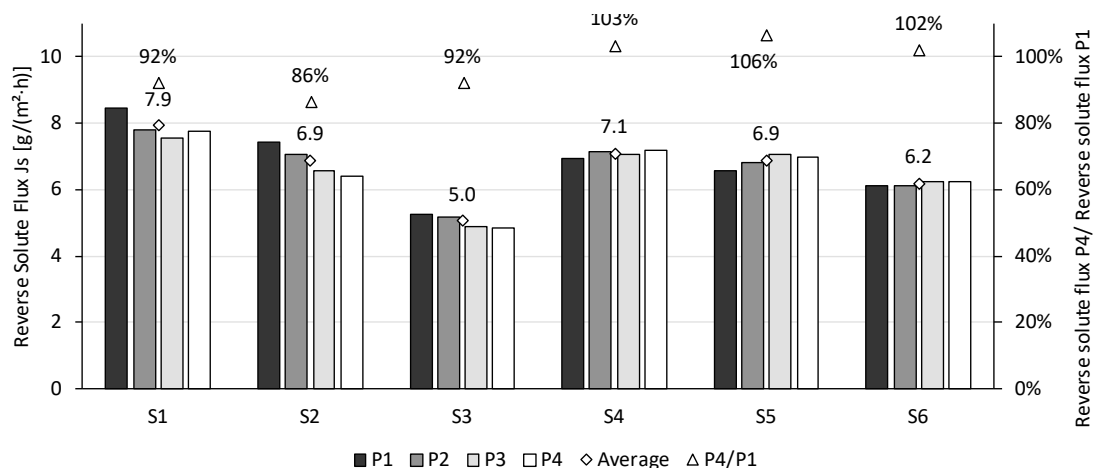**Figure 5.** Reverse salt flux Js in membrane performance tests P1, P2, P3, and P4 of test series S1, S2, S3, S4, S5, and S6; average reverse solute flux from P1, P2, P3, and P4; ratio of reverse solute flux in P4 and P1.

4.3.4   Solute Diffusion through the Membrane

As described above, samples of the treated effluents were analyzed after FO treatment and compared to the untreated effluents. Furthermore, deionized water was also analyzed before and after FO. Due to the high concentration of chloride, analysis of 1 mol/L NaCl before and after FO was not performed because samples would have had to be diluted strongly and results would have been prone to contain errors. All analytical results can be found in the Supplementary materials (S1-S5).

Since FS and DS are circulated in the experimental set-up, concentrations change due to dilution of DS and concentration of FS. To find out, whether concentration changes are further influenced by solute diffusion through the membrane, the T/M-value was introduced. If T/M equals 1, solute diffusion did not occur. If T/M is larger than 1, the substance gets lost during FO operation. If T/M is smaller than 1, the substance increases during FO operation. Besides solute diffusion through the membrane, a reason for substance loss or increase may be the accumulation or the detachment of substances on and of the membrane surface. The T/M-values for all test series as well as the mass data of all test series are included in the Supplementary materials. Here, test series S2 and S5 are evaluated in detail because in these test series both FS and DS were semiconductor effluents.

<u>Combined FO treatment of RO concentrate and Cu filtrate (S2)</u>

Figure 6, Figure 7 and Figure 8 contain excerpts of the analytical results and the calculated T/M-values for test series S2 where RO Concentrate and Cu Filtrate were FS and DS, respectively. For untreated RO concentrate, most concentrations were below detection limit (see Table 1). For this reason, they were assumed to be zero when calculating the corresponding T/M-value.
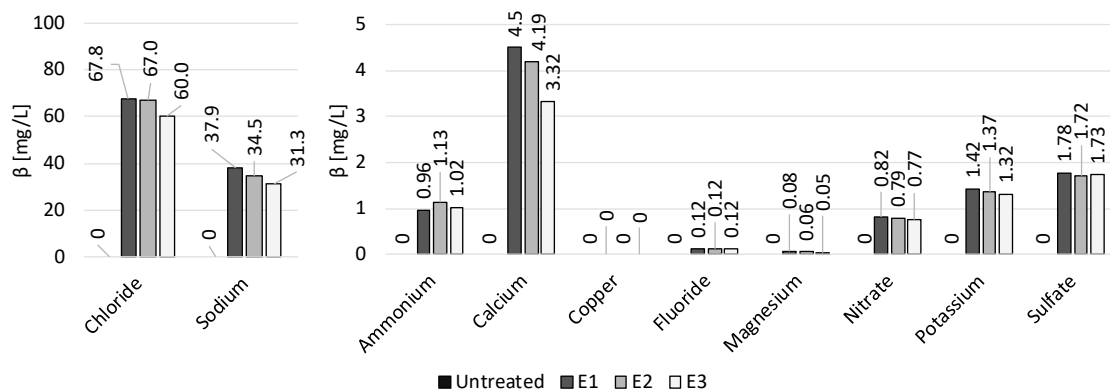
Figure 6. Analytical results of RO concentrate as FS in test series S2 with Cu filtrate as DS.

In Figure 6, it can be seen that the following substances increased in RO concentrate, here used as FS, during FO treatment: sodium and chloride above 30 and 60 mg/L, respectively; calcium above 3 mg/L; ammonium, potassium and sulfate above 1 mg/L; and nitrate up to 0.8 mg/L. Fluoride and magnesium were also found after FO treatment but only with very low concentrations of 0.1 mg/L. Since all of the described substances were basically not contained in RO concentrate before FO treatment, the T/M-values are below 1.0 and equal zero (see Figure 8 left). Thus it can be concluded, that the named substances diffused from the DS through the membrane into the FS.
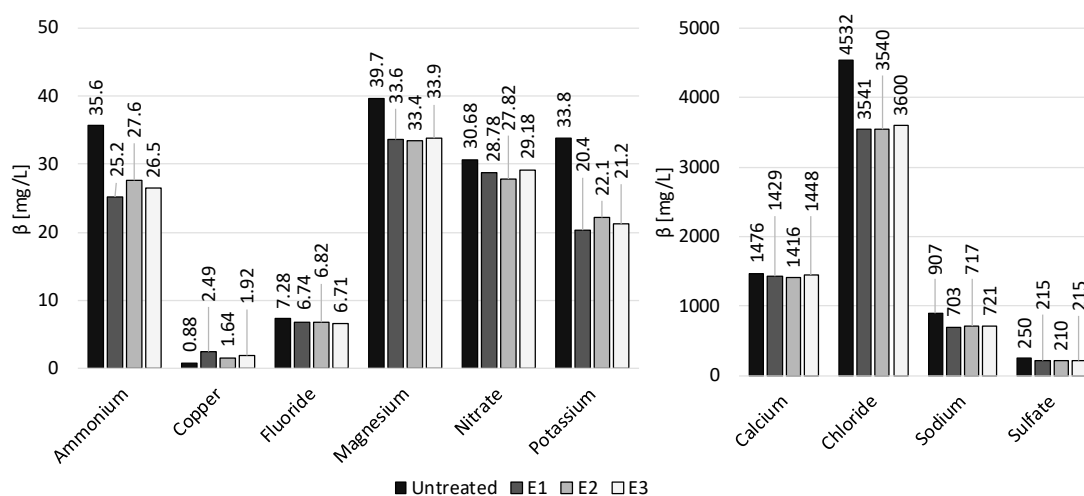
Figure 7. Analytical results of Cu filtrate as DS in test series S2 with RO concentrate as FS.

Analytical results and T/M-values for the DS of test series S2, Cu filtrate, can be found in Figure 7 and Figure 8 (right), respectively. It is interesting to see that for ammonium, chloride, potassium, and sodium the T/M-values are close to or above 1.0 showing that the amount of these substances was reduced during FO treatment or stayed nearly constant. The substances were found in the FS after FO treatment which leads to the conclusion that they diffused through the membrane. Calcium, copper, fluoride, magnesium, nitrate, and sulfate had T/M-values below 1.0 suggesting that the amount of these substances increased during FO treatment. As the RO concentrate as FS did not contain any substances, it is unclear how this phenomenon can be explained.
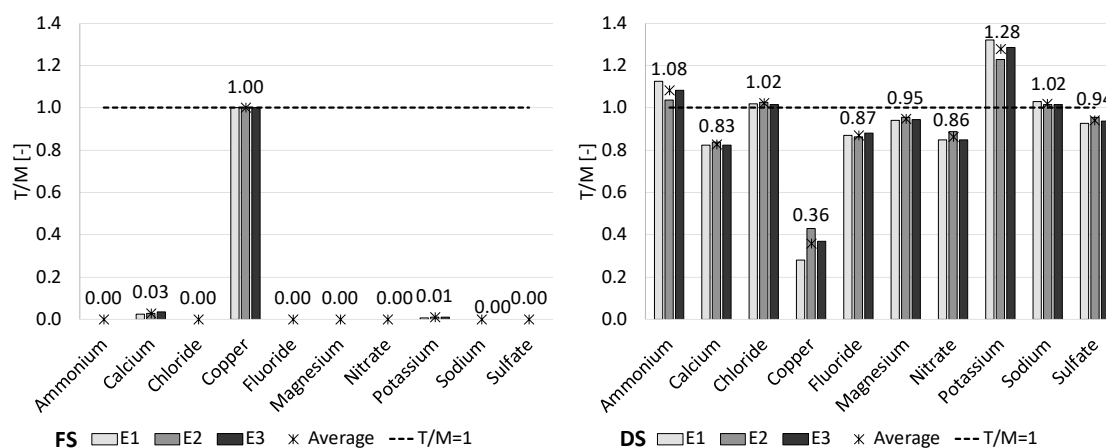
Figure 8. T/M-values for test series S2 with RO concentrate as FS (left) and Cu filtrate as DS (right).

Combined FO treatment of neutralization effluent and Cu concentrate (S5)

Analytical results and T/M-values for test series S5, where Neutralization effluent and Cu concentrate were FS and DS, respectively, are shown in Figure 9, Figure 10, and Figure 11.
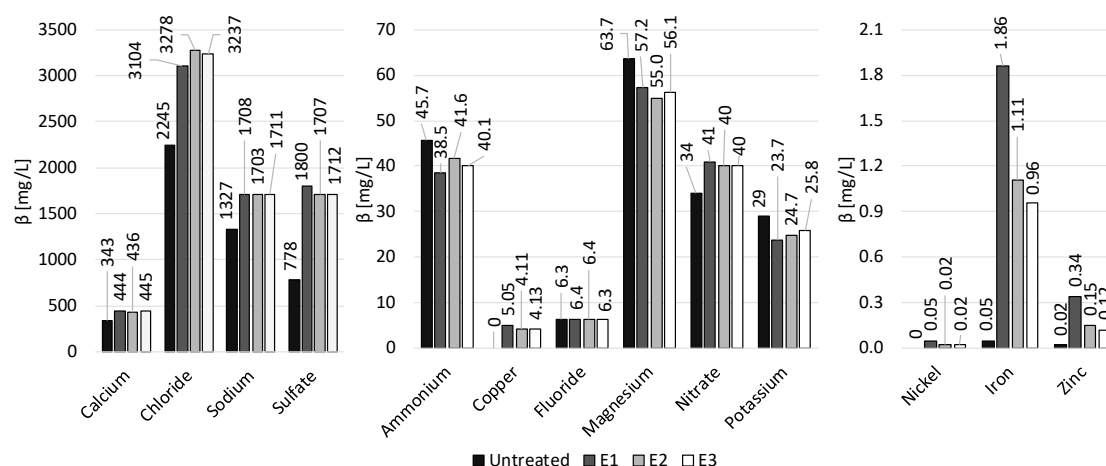
Figure 9. Analytical results of Neutralization effluent as FS in test series S5 with Cu concentrate as DS.

Due to the concentration during FO, substance concentration in the FS should increase. For the Neutralization effluent in test series S5 this was observed for calcium, chloride, sodium, sulfate, copper, nitrate, iron, and zinc (Figure 9). However, concentrations of ammonium, magnesium, and potassium decreased. Fluoride and nickel concentrations did not change significantly. T/M-values close to 1.0 show that the substance concentration changed according to permeate flux and water loss on the FS side. Only chloride had a T/M-value of 1.0 so apparently, no chloride passed through the membrane (Figure 11 left). T/M-values for ammonium, calcium, fluoride, potassium, magnesium, sodium, and nitrate were above 1.0 suggesting that these substances were removed from the FS either by deposition on the membrane or diffusion through the membrane into the DS. Zinc, iron, copper, nickel, and sulfate had T/M-values below 1.0 meaning that these substances got into the FS probably from the DS by diffusion through the membrane.
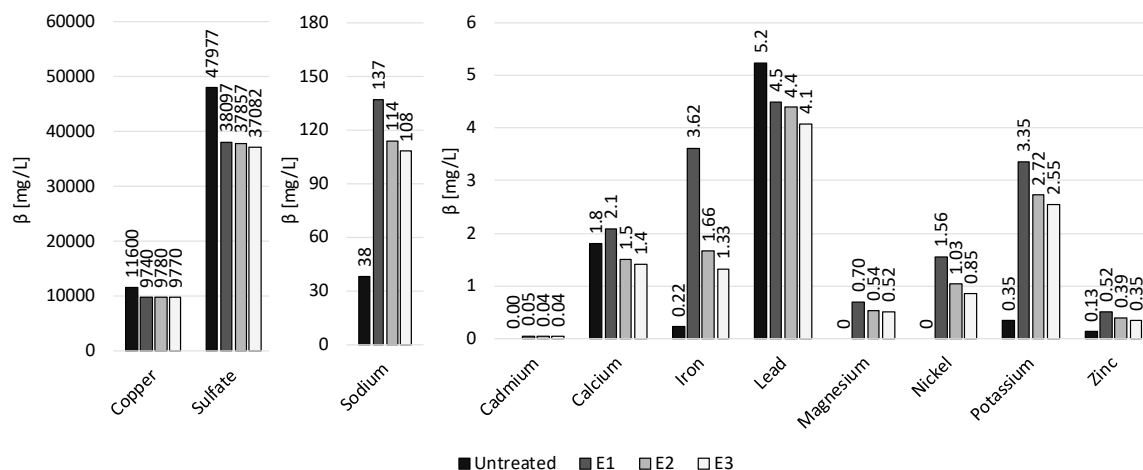
Figure 10. Analytical results of Cu concentrate as DS in test series S5 with Neutralization effluent as DS.

Substance concentration in the DS should decrease during FO process due to dilution. In test series S5, this was observed for copper, sulfate, calcium (partially), and lead (Figure 10). Contrary to that, concentrations of sodium, potassium, magnesium, zinc, and iron increased. Despite sulfate, all named substances had T/M-values blow 1.0 suggesting that they got into the FS (Figure 11 right). One reason might be substance diffusion through the membrane. Another reason in this case might also be that substances were dissolved from components of the experimental set-up because of the extreme low pH of the DS.
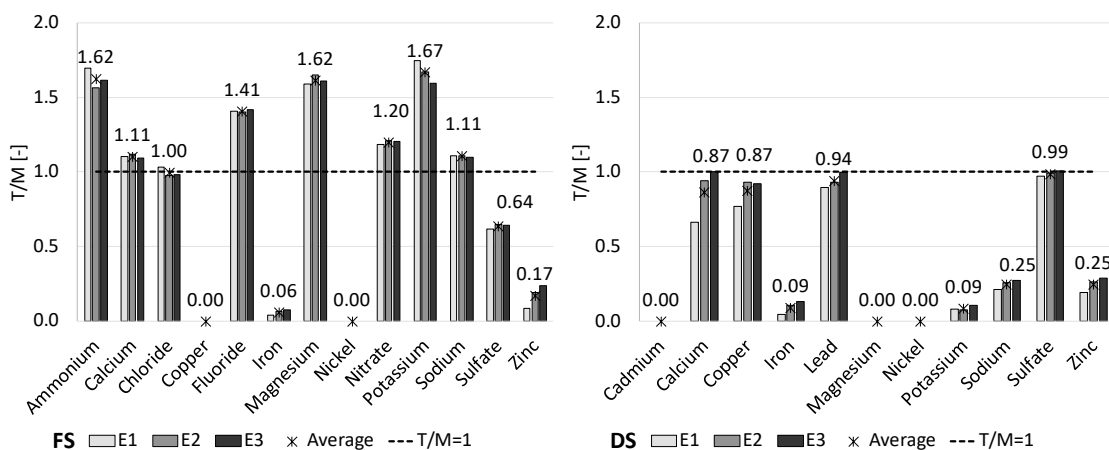
Figure 11. T/M-values for test series S5 with Neutralization effluent as FS (left) and Cu concentrate as DS (right).

In test series S5 and S6, when Cu filtrate was used as DS, an interesting phenomenon was observed: black deposits formed on the FS side of the membrane. With neutralization effluent as FS in test series S5, more deposits were seen (Figure 12) than with deionized water as FS in test series S6 (Figure 13). In both cases, the structure of the spacer material can clearly be recognized on the membrane material.
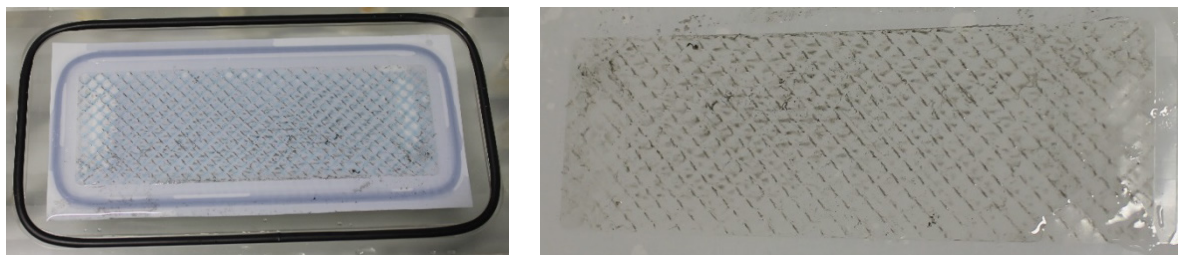
Figure 12. Black deposits on the FS side of the membrane after test series S5 (membrane test cell was opened and FS spacer removed for better visibility).

After removing the membrane from the test cell, the membrane surface was rinsed with deionized water from a wash bottle. By doing so, most of the deposits could be removed from the membrane surface. By applying soft mechanical impact (rubbing with finger), the remaining deposits were removed. Analytical results showed that the deposits from test series S5 consisted of iron, zinc, chromium, nickel, copper, and lead with iron being the main substance (Figure 14).
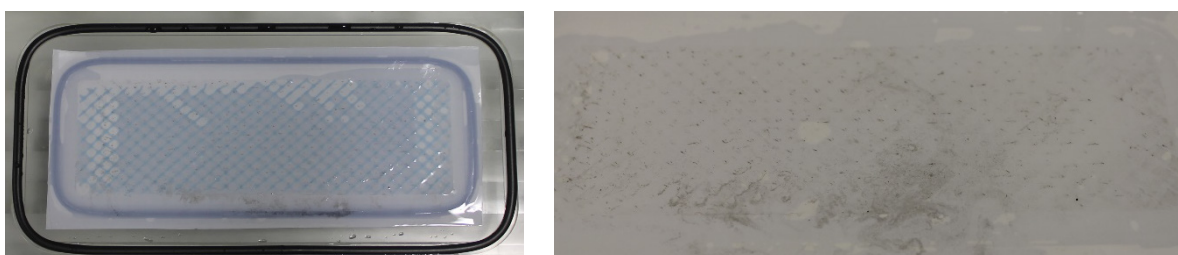
Figure 13. Black deposits on the FS side of the membrane after test series S6 (membrane test cell was opened and FS spacer removed for better visibility).

As described before, although the performance test showed deterioration of permeate fluxes by 17 and 13% within test series S5 and S6, permeate fluxes in the experiments only declined by 5%. Thus, the deposits obviously did not have a strong negative effect on the FO process. That is why, within this study, no investigations were performed on possible cleaning strategies to remove the deposits.

Figure 14. Composition of black deposits on the FS side of the membrane during test series S5.

4.4   Conclusions

Laboratory-scale forward osmosis experiments were performed with effluents from a semiconductor manufacturer. Four different effluents were used and examined for their suitability as feed solution or draw solution. FS were either combined with 1 mol/L NaCl

as DS or another industrial effluent. DS were either combined with deionized water as FS or another industrial effluent.

Considering the average permeate fluxes between 10.5 and 33.4 L/(m²·h), all industrial effluents were successfully treated by FO. Suitable feed solutions were reverse osmosis concentrate from ultrapure water production (RO concentrate) and effluent from wastewater neutralization plant (neutralization effluent). Suitable draw solutions were filtrate from a chamber filter press dewatering copper precipitate (Cu filtrate) and a wastewater with high copper concentration (Cu concentrate). However, the use of the latter is difficult due to the low pH value and high reverse solute flux which caused visible deposits on the FS side of the membrane.

Declining permeate fluxes within the test series down to 93% showed that membrane fouling occurred to some extent. Furthermore, deposits on the membrane and in the flow channel were observed in the experiments with Cu concentrate. Moderate permeate flux decline was also measured in the membrane performance tests. Here, the highest flux declines were 17% and 13% and occurred when Cu concentrate was used as DS. In general, flux decline was low compared to former experiments with wastewater from automobile and dairy industry [15].

No cleaning procedures were applied apart from rinsing with deionized water for 15 hours after the experiments of one test series. When the membrane was removed from the test cell at the end of the test series with Cu concentrate, the deposits could easily be removed by rinsing the membrane and the spacer with deionized water from a wash bottle. It was also observed that the deposits were attached to the spacer rather than to the membrane surface. This leads to the conclusion that deposits could be easily removed or prevented by enhanced mechanical cleaning or improved flow channel and spacer design.

Since all four investigated effluents proved to be technically suitable for FO treatment, further aspects are to be considered. Above all, the question of meaningfulness and cost-effectiveness must be considered more closely. As mentioned before, FO treatment might be economically advantageous if no artificial DS is necessary and no DS regeneration step is required [12]. Thus, FO application scenarios are of interest where both FS and DS are semiconductor effluents. Furthermore, in those scenarios the concentration of FS and the dilution of DS should lead to positive effects in the further processing of these effluents.

RO concentrate as FS and Cu filtrate as DS were successfully treated simultaneously in FO. However, RO concentrate from ultrapure water production is an effluent of high quality and is currently used for further applications. Economically, concentration of RO concentrate itself is not necessary. If, however, it would be economically reasonable, to dilute an appropriate DS such as Cu filtrate, RO concentrate would be a suitable FS.

Currently, Cu filtrate is further treated and disposed to the local sewer system without major problems. For this reason, FO treatment is not essential.

Combined FO treatment would also be possible with Cu concentrate as DS and neutralization effluent as FS. Currently, the further usage, treatment, and disposal of Cu concentrate is difficult and dilution with FO treatment would have a positive effect. Neutralization effluent is disposed to the local sewer network. Since Cu concentrate amounts are much smaller than neutralization effluent, an adapted process scheme would be possible and advantageous: Cu concentrate as DS could be circulated until the desired dilution is achieved but ensuring that the osmotic pressure is high enough. Neutralization effluent as FS would pass the FO module just once without recirculation. This way, the influence of the occurring reverse solute flux, which for example leads to a decreasing pH value, would be neglectable. The extreme low pH of Cu concentrate represents a problem though that must not be ignored.

For both combinations, further investigations in a larger scale and over a longer period of time would make sense to optimize FO operation. Besides technical aspects, economic aspects should then also be taken into consideration.

Supplementary Materials: Table S1: Analytical results of FS1 (RO concentrate UPW) before FO and after FO (S1: 1 mol/L NaCl as DS; S2: Cu filtrate as DS), Table S2: Analytical results of DS1 (Cu filtrate) before FO and after FO (S2: RO concentrate as FS; S3: deionized water as FS), Table S3: Analytical results of FS2 (Neutralization effluent) before FO and after FO (S4: 1 mol/L NaCl as DS; S5: Cu concentrate as DS), Table S4: Analytical results of DS2 (Cu concentrate) before FO and after FO (S5: Neutralization effluent as FS; S6: deionized water as FS), Table S5: Analytical results of deionized water used as FS before FO and after FO (S3: Cu filtrate as DS; S6: Cu concentrate as DS), Table S6: Mass data for all test series, Table S7: T/M-values of test series,

References of Chapter 4

1. Cath, T.Y.; Childress, A.E.; Elimelech, M. Forward osmosis: Principles, applications, and recent developments. *J. Membr. Sci.* **2006**, *281*, 70–87.
2. Shaffer, D.L.; Werber, J.R.; Jaramillo, H.; Lin, S.; Elimelech, M. Forward osmosis: Where are we now? *Desalination* **2015**, *356*, 271–284.
3. McCutcheon, J.R. Forward osmosis: A technology platform here to stay. *Desalination* **2017**, *421*, 1–2.
4. Mazlan, N.M.; Peshev, D.; Livingston, A.G. Energy consumption for desalination — A comparison of forward osmosis with reverse osmosis, and the potential for perfect membranes. *Desalination* **2016**, *377*, 138–151.
5. Roy, S.; Ragunath, S. Emerging Membrane Technologies for Water and Energy Sustainability: Future Prospects, Constraints and Challenges. *Energies* **2018**, *11*, 2997.
6. Chekli, L.; Phuntsho, S.; Shon, H.K.; Vigneswaran, S.; Kandasamy, J.; Chanan, A. A review of draw solutes in forward osmosis process and their use in modern applications. *Desalination Water Treat.* **2012**, *43*, 167–184.
7. Luo, H.; Wang, Q.; Zhang, T.C.; Tao, T.; Zhou, A.; Chen, L.; Bie, X. A review on the recovery methods of draw solutes in forward osmosis. *J. Water Process Eng.* **2014**, *4*, 212–223.

8.   Johnson, D.J.; Suwaileh, W.A.; Mohammed, A.W.; Hilal, N. Osmotic's potential: An overview of draw solutes for forward osmosis. *Desalination* **2018**, *434*, 100–120.

9.   Zou, S.; Qin, M.; He, Z. Tackle reverse solute flux in forward osmosis towards sustainable water recovery: reduction and perspectives. *Water Res.* **2019**, *149*, 362–374.

10. Lutchmiah, K.; Verliefde, A.R.D.; Roest, K.; Rietveld, L.C.; Cornelissen, E.R. Forward osmosis for application in wastewater treatment: A review. *Water Res.* **2014**, *58*, 179–197.

11. Chekli, L.; Phuntsho, S.; Kim, J.E.; Kim, J.; Choi, J.Y.; Choi, J.-S.; Kim, S.; Kim, J.H.; Hong, S.; Sohn, J.; et al. A comprehensive review of hybrid forward osmosis systems: Performance, applications and future prospects. *J. Membr. Sci.* **2016**, *497*, 430–449.

12. Awad, A.M.; Jalab, R.; Minier-Matar, J.; Adham, S.; Nasser, M.S.; Judd, S.J. The status of forward osmosis technology implementation. *Desalination* **2019**, *461*, 10–21.

13. Ang, W.L.; Wahab Mohammad, A.; Johnson, D.; Hilal, N. Forward osmosis research trends in desalination and wastewater treatment: A review of research trends over the past decade. *J. Water Process Eng.* **2019**, *31*, 100886.

14. Haupt, A.; Lerch, A. Forward Osmosis Application in Manufacturing Industries: A Short Review. *Membranes* **2018**, *8*, 47.

15. Haupt, A.; Lerch, A. Forward osmosis treatment of effluents from dairy and automobile industry – results from short-term experiments to show general applicability. *Water Sci. Technol.* **2018**, *78*, 467–475.

5 Modelling Forward Osmosis Treatment of Automobile Wastewaters

Abstract

Forward osmosis (FO) has rarely been investigated as a treatment technology for industrial wastewaters. Within this study, common FO model equations were applied to simulate forward osmosis treatment of industrial wastewaters from the automobile industry. Three different models from literature were used and compared. Permeate and reverse solute flux modelling was implemented using MS Excel with a Generalized Reduced Gradient (GRG) Nonlinear Solver. For the industrial effluents, the unknown diffusion coefficients were calibrated and the influences of the membrane parameters were investigated. Experimental data was used to evaluate the models. It could be proven that common model equations can describe FO treatment of industrial effluents from the automobile industry. Even with few known solution properties, it was possible to determine permeate fluxes and draw conclusions about mass transport. However, the membrane parameters, which are apparently not solution independent and seem to differ for each industrial effluent, are critical values. Fouling was not included in the model equations although it is a crucial point in FO treatment of industrial wastewaters. But precisely for this reason, modelling is a good complement to laboratory experiments since the difference between the results allows conclusions to be drawn about fouling.

Keywords: automobile industry; forward osmosis; modelling; wastewater treatment

5.1   Introduction

In industries, increasing water scarcity combined with a high water demand as well as stricter laws for environmental protection has led to a growing awareness about efficient water usage [1]. Different technologies are used for wastewater treatment and water recycling, e.g., membrane filtration processes. Here, forward osmosis (FO) is a technology that has been investigated more and more within the last years [2–6].

In FO, the osmotic pressure difference between the feed solution (FS) and the draw solution (DS) is the driving force, that makes water diffuse through a semipermeable membrane from FS into DS. This permeate flux dilutes the DS; the FS is concentrated (Figure 1). No physical pressure needs to be applied. In order to obtain pure water, the DS has to be regenerated in a separate treatment step. In many possible applications, an artificial DS needs to be used, such as salt solutions [7]. Here, the necessity of the DS regeneration steps is a main impact factor on economic efficiency [8, 9].
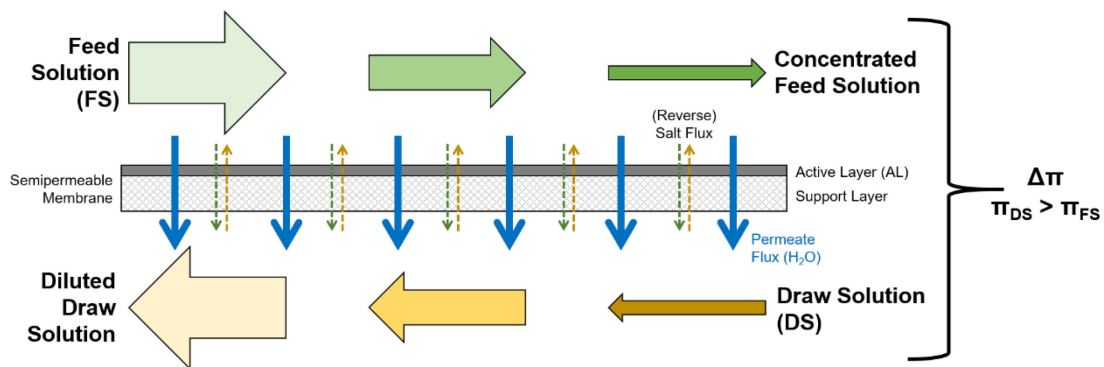
Figure 1. Forward osmosis (FO) process with membrane active layer facing towards the feed solution (FS) (active layer feed solution (ALFS) or FO-mode) [6].

The advantages of FO are low energy consumption, easy removable fouling layers, and treatable high salt concentrations [2, 10–12]. The reverse solute flux through the membrane as well as concentration polarization are disadvantages [13, 14] and are to be met by high performance FO membranes. FO membranes usually consist of a dense active layer (AL) and a porous support layer (SL). In the FO process, membranes can either be used with the AL facing the FS (ALFS orientation or FO mode) or with the AL facing the DS (ALDS orientation or PRO mode). An ALDS orientation enables higher permeate fluxes due to reduced concentration polarization within the SL [2]. However, due to the fact that the SL is more prone to fouling, the ALFS orientation is used more often [15]. FO membranes are characterized by three parameters: Water permeability A and solute permeability B, which relate to the active layer, and the structural parameter S, which relates to the support layer. These intrinsic parameters used to be determined by a combination of pressurized reverse osmosis tests and non-pressurized FO tests (RO–FO test) [16]. Lately, a methodology was suggested that utilizes only non-pressurized FO tests (FO-only test) [17]. If spacers are used in the FS and DS channels, their geometry also

influences permeate flux and might be taken into consideration. The impact of spacers especially in spiral wound membrane modules has been studied for membrane filtration processes [18–22].

So far, FO has been applied for desalination and various water treatment processes [23–27]. However, few full-scale FO plants have been realized so far [8]. The application in industries has also been studied [6, 28–31]. In these studies, mostly lab-scale experiments, which are time- and cost-consuming, were conducted to investigate FO performance. In order to get a rough estimation of FO performance for different application scenarios, it would be useful to simulate the FO process with a suitable model.

Several theoretical transport models have been proposed in the literature [16, 32–47]. In 1981, Lee et al. introduced a model for pressure-retarded osmosis that described transport processes through an asymmetric membrane taking internal concentration polarisation (ICP) into account [32]. In 2006, McCutcheon et al. included not only ICP but also external concentration polarisation (ECP) on the selective membrane layer within their model [16]. In 2010, Philipp et al. reported about their model that described reverse solute flux (RSF) [37]. Shortly afterwards, Yip et al. and Tiraferri et al. published articles presenting FO models including RSF, ICP, and ECP on the selective membrane layer [44, 46]. Here, Yip et al. considered an ALDS membrane orientation whereas Tiraferri et al. considered an ALFS membrane orientation. In 2015, Bui et al. then proposed a model that regarded RSF, ICP, and ECP on the selective layer as well as on the porous support layer [47].

However, so far these models have mostly been evaluated with experiments using NaCl or other salt solutions and deionized water only.

Within our research, three FO models from literature were partially adapted and integrated in MS Excel with a Generalized Reduced Gradient (GRG) Nonlinear Solver. FO performance was calculated for the treatment of different automobile wastewaters. The results from the FO experiments with these real wastewaters were used to evaluate the models.

5.2 Materials and Methods

5.2.1 Lab-Scale Experiments

Lab-scale experiments were conducted with four different wastewaters from an automobile manufacturing site as well as deionized water and 1 mol/L NaCl. The experimental set-up consisted of a flat-sheet membrane test cell with an active membrane area of 48 cm². Flow channel dimensions in the test-cell were 1200 mm in length, 40 mm in width, and 0.86 mm in height on both sides of the membrane. During

the experiment, FS and DS were circulated leading to a decreasing osmotic pressure difference overtime due to permeate flux. Thus, the observed permeate flux also decreased within the course of the experiment. Further decrease in permeate flux might be caused by membrane fouling. The detailed set-up has been described elsewhere [48].

CSM FO membranes from Toray Chemical Korea Inc. (Seoul, Korea) were used for all experiments. The manufacturers indicated that the standard permeate flux was 30 ± 5 L/(m²·h). A new membrane sample was used for every test series.

The four different automobile wastewaters were cathodic dip painting rinsing water, cathodic dip painting wastewater, paint shop pre-treatment wastewater, and cooling tower circulation water. These waters were either used as FS or DS and combined with deionized water as FS, 1 mol/L NaCl as DS, or another effluent. FS and DS, osmotic pressure difference $\Delta\pi$, and membrane orientation of the six experimental test series (A1–A6) and the performance tests (P) are given in Table 1. Further information can be found elsewhere [48].

Table 1. FS and DS, osmotic pressure difference $\Delta\pi$, and membrane orientation of the six experimental test series (A1–A6) and the performance tests (P).

Test Series	Feed Solution (FS)	Draw Solution (DS)	$\Delta\pi$ [bar]	Membrane orientation ALFS	ALDS
A1	Cathodic dip painting rinsing water	1 mol/L NaCl	44.8	✓	-
A2	Deionized Water (DI)	Cooling tower circulation water	1.1	✓	-
A3	Paint shop pre-treatment wastewater	1 mol/L NaCl	44.5	✓	-
A4	Deionized Water (DI)	Cathodic dip painting wastewater	2.1	✓	-
A5	Deionized Water (DI)	Cooling tower circulation water	1.1	-	✓
A6	Cathodic dip painting wastewater	1 mol/L NaCl	43.5	✓	-
P	Deionized Water (DI)	1 mol/L NaCl	44.5	✓	-

Six test series with industrial wastewater were conducted using an ALFS membrane orientation, and one using an ALDS membrane orientation. The experimental procedure and the results of these test series are described in detail in another publication [48]. Within the experiments with industrial wastewaters, each test series consisted of three subsequent wastewater tests interrupted by a cleaning procedure and a membrane performance test. However, for the model evaluation, only the first wastewater test of each test series was used. One wastewater test lasted five hours.

Besides the wastewater tests, standard performance tests were conducted with deionized water as FS and 1 mol/L NaCl as DS. These tests lasted two hours and were, among others,

performed before every test series when a new membrane sample was used. Thus, the experimental results of six performance tests were used for model evaluation.

5.2.2 Model Setup

In order to predict permeate flux J_W and reverse solute flux J_S, three different FO models were used for ALFS and ALDS membrane orientation (Table 2 and Table 3). These models were chosen because they are commonly used in FO modelling.

Table 2. Model equations for permeate and reverse solute flux using an ALFS membrane orientation.

Model	Permeate flux	Reverse solute flux	Ref.
I	$J_w = \dfrac{D_{DS}}{S} \, ln\left(\dfrac{B + A\,\pi_{DS}}{B + A\left[\pi_{FS}\exp\left(\frac{J_w}{k_{FS}}\right)\right] + J_w}\right)$	$J_s = B\,\dfrac{c_{DS}\exp\left(-\frac{J_w S}{D_{DS}}\right) - c_{FS}\exp\left(\frac{J_w}{k_{FS}}\right)}{1 + \frac{B}{J_w}\left[exp\left(\frac{J_w}{k_F}\right) - \exp\left(-\frac{J_w S}{D_{DS}}\right)\right]}$	[16] mod., [46]
II$_{ALFS}$	$J_w = A\,\dfrac{\pi_{DS}\exp\left(-\frac{J_w S}{D_{DS}}\right) - \pi_{FS}\exp\left(\frac{J_w}{k_{FS}}\right)}{1 + \frac{B}{J_w}\left[exp\left(\frac{J_w}{k_{FS}}\right) - \exp\left(-\frac{J_w S}{D_{DS}}\right)\right]}$		
III	$J_w = A\,\dfrac{\pi_{DS}\exp\left[-J_w\left(\frac{1}{k_{DS}}+\frac{S}{D_{DS}}\right)\right] - \pi_{FS}\exp\left(\frac{J_w}{k_{FS}}\right)}{1 + \frac{B}{J_w}\left[exp\left(\frac{J_w}{k_{FS}}\right) - J_w\left(\frac{1}{k_{DS}}+\frac{S}{D_{DS}}\right)\right]}$	$J_s = B\,\dfrac{c_{DS}\exp\left[-J_w\left(\frac{1}{k_{DS}}+\frac{S}{D_{DS}}\right)\right] - c_{FS}\exp\left(\frac{J_w}{k_{FS}}\right)}{1 + \frac{B}{J_w}\left[exp\left(\frac{J_w}{k_{FS}}\right) - \exp\left[-J_w\left(\frac{1}{k_{DS}}+\frac{S}{D_{DS}}\right)\right]\right]}$	[47]

water permeability A, solute permeability B, structural parameter S, osmotic pressure π, concentration c, diffusion coefficient D, mass transfer coefficient k, feed solution indexed FS, draw solution indexed DS

Table 3. Model equations for permeate and reverse solute flux using an ALDS membrane orientation.

Model	Permeate flux	Reverse solute flux	Ref.
I	$J_w = \dfrac{D_{FS}}{S} \, ln\left(\dfrac{B + A\,\pi_{DS}\,exp\left[-\frac{J_w}{k}\right] - J_w}{B + A\,\pi_{FS}}\right)$	$J_s = B\,\dfrac{c_{DS}\,exp\left(-\frac{J_w}{k_{DS}}\right) - \pi_{FS}\exp\left(\frac{J_w S}{D_{FS}}\right)}{1 + \frac{B}{J_w}\left[\exp\left(\frac{J_w S}{D_{DS}}\right) - exp\left(-\frac{J_w}{k_{DS}}\right)\right]}$	[16] mod., [44]
II$_{ALDS}$	$J_w = A\,\dfrac{\pi_{DS}\,exp\left(-\frac{J_w}{k_{DS}}\right) - \pi_{FS}\exp\left(\frac{J_w S}{D_{FS}}\right)}{1 + \frac{B}{J_w}\left[\exp\left(\frac{J_w S}{D}\right) - exp\left(-\frac{J_w}{k_{DS}}\right)\right]}$		
III	$J_w = A\,\dfrac{\pi_{DS}\exp\left(-\frac{J_w}{k_{DS}}\right) - \pi_{FS}\exp\left[J_w\left(\frac{1}{k_{FS}}+\frac{S}{D_{FS}}\right)\right]}{1 + \frac{B}{J_w}\left[\exp\left[J_w\left(\frac{1}{k_{FS}}+\frac{S}{D_{FS}}\right)\right] - exp\left(-\frac{J_w}{k_{DS}}\right)\right]}$	$J_s = B\,\dfrac{c_{DS}\exp\left(-\frac{J_w}{k_{DS}}\right) - c_{FS}exp\left[J_w\left(\frac{1}{k_{FS}}+\frac{S}{D_{FS}}\right)\right]}{1 + \frac{B}{J_w}\left[\exp\left[J_w\left(\frac{1}{k_{FS}}+\frac{S}{D_{FS}}\right)\right] - exp\left(-\frac{J_w}{k_{DS}}\right)\right]}$	[47]

water permeability A, solute permeability B, structural parameter S, osmotic pressure π, concentration c, diffusion coefficient D, mass transfer coefficient k, feed solution indexed FS, draw solution indexed DS

Parameters A, B, and S are the water permeability in L/(m²·h·bar), the solute permeability in L/(m²·h) and the structural parameter of the membrane in m; π is the osmotic pressure in bar, c the molar concentration of NaCl in mol/L, and D the diffusion coefficient of the solution in m²/s; k in m/s describes the mass transfer coefficient from bulk solution to the membrane surface. Indexes FS and DS mean feed solution and draw solution, respectively.

Models I, II, and III all include internal concentration polarization but differ in the extent of external concentration polarization considered. Model I and Model II only consider external concentration polarization on the active layer side of the membrane. Model III combines internal concentration polarization and external concentration polarization on the active as well as the support layer of the membrane. The original Model I did not include the reverse solute flux and B was assumed to be zero [16]. Therefore, we used these results and added the concentrative ECP-term on the feed side, by keeping B ≠ 0. Furthermore, no equation for the RSF is offered, therefore the equation for the RSF of Model II was applied [46].

Membrane parameters A, B, and S were taken from literature as indicated in Table 4. Two different parameter sets, Par1 and Par2, were used: One that was determined by RO–FO tests and one that was determined by FO-only tests (see Table 4).

Table 4. Membrane parameters used for modelling.

Membrane parameter set	Water permeability A [L/(m² h bar)]	Solute permeability B [L/(m² h)]	Structural parameter S [10^{-6} m]	Method	Lit.
Par1	5.36	0.95	266	FO-only	[49]
Par2	8.9 ± 0.14	5.68 ± 0.14	466	RO–FO	[50]

For modelling FO, it is necessary to consider the diffusion coefficient D of FS and DS. If the components and concentrations of FS and DS are known, the diffusion coefficient can be calculated [35,42]. However, industrial wastewaters like the automobile wastewaters are multi-component mixtures and analyzing all components would be very complex. Furthermore, the diffusion coefficient is prone to change during the FO experiment due to the concentration of FS and the dilution of DS, respectively, because of FS and DS circulation. For these reasons, it was decided to calibrate the diffusion coefficient ranging from 1.10^{-11} and 5.10^{-9} m²/s within the modelling procedure. This offers two advantages: Firstly, mixing of the solution within the support layer is covered by the calibrated diffusion coefficient; secondly, due to the unsure structural parameter S, the uncertainty and maybe errors can be compensated. Within the modelling procedure, flux calculation for one test run was repeated with a new diffusion coefficient several times. The diffusion coefficient was varied linearly by beginning at the lower boundary of the range and stepping upwards to the upper boundary of the calibration range.

The osmotic pressure π was determined from the osmolality, which was measured with a freezing-point microosmometer (Hermann Roebling Messtechnik, Germany), by applying Equation (1) [51]. Here, c_{osm} is the osmolality, T the temperature and R the universal gas constant.

$$\pi = c_{osm} \cdot R \cdot T \qquad (1)$$

A virtual NaCl concentration β was determined by empirical Equations (2) and (3) using the measured electrical conductivity κ [48]. The molar concentration c was then calculated by multiplying with NaCl molecular weight. When pure NaCl solution or deionized water were the DS and FS, respectively, the exact concentration was used as input parameter for modelling. When automobile wastewaters were the DS and FS, only osmolality and electrical conductivity were used as input parameters in order to minimize analytical expense.

Low electrical conductivity κ < 1.0 mS/cm (β in g/L; κ in μS/cm)

$$\beta = 5.703 \cdot 10^{-9} \cdot \kappa^2 + 4.9515 \cdot 10^{-4} \cdot \kappa - 6 \cdot 10^{-4} \tag{2}$$

High electrical conductivity κ > 1.0 mS/cm (β in g/L; κ in mS/cm)

$$\beta = 1.4363 \cdot 10^{-3} \cdot \kappa^2 + 0.5419 \cdot \kappa + 0.152 \tag{3}$$

The mass transfer coefficient k was calculated using Equation (4) with diffusion coefficient D, Sherwood number Sh, and hydraulic diameter dh [16]. The Sherwood number Sh was calculated according to Equations (5) and (6) with Reynolds number Re, Schmidt number Sc, hydraulic diameter dh,, and channel length L [16].

$$k = \frac{Sh \cdot D}{d_h} \tag{4}$$

$$Sh = 1.85 \left(Re \cdot Sc \cdot \frac{d_h}{L} \right)^{0.33} \text{ laminar flow} \tag{5}$$

$$h = 0.04 \cdot Re^{0.75} \cdot Sc^{0.33} \text{ turbulent flow} \tag{6}$$

The hydraulic diameter dh for our rectangular flow channel was calculated through the cross-section area A_{cs} (width multiplied by height) and the wetted perimeter l_u (doubled sum of width and height), as illustrated in Equation (7).

$$d_h = \frac{4 \cdot A_{cs}}{l_u} \tag{7}$$

The Schmidt number Sc is a dimensionless number, describing the relationship between the viscous diffusion (described by the dynamic viscosity η) and the mass diffusion, described by the diffusion coefficient D and the density ρ [52]. It was calculated by Equation (8).

$$Sc = \frac{\eta}{D \cdot \varrho} \tag{8}$$

Equation (9) was used to calculate the Reynolds number with dynamic viscosity η, the density ρ, the fluid velocity v, and the cross-section area A_{cs} [53]. Fluid velocity v was determined by dividing the known flowrate by cross-section area A_{cs}. The density ρ in

kg/m³ and the dynamic viscosity η in Pa.s were calculated by Equations (10) and (11), respectively, using the measured temperature ϑ in °C. These equations are empirically determined based on data published in literature and are valid for temperatures ranging from 0 to 30 °C [54, 55].

$$Re = \frac{\varrho \cdot \text{v} \cdot d_h}{\eta \cdot A_{cs}} \tag{9}$$

$$\varrho = 0.0000482484 \cdot \vartheta^3 - 0.00819257 \cdot \vartheta^2 + 0.0624602 \cdot \vartheta + 999.846 \tag{10}$$

$$\eta = 0.0001 \cdot (17.9098 - 0.6003 \cdot \vartheta + 0.01299 \cdot \vartheta^2 - 0.000134 \cdot \vartheta^3) \tag{11}$$

Permeate and reverse solute flux modelling was implemented using MS Excel from Microsoft Corporation (Redmond, WA, USA). The MS Excel workbook consisted of four worksheets: an introduction sheet as user-manual, an input data-sheet, a calibration-sheet, and a calculation sheet. All equations used are self-depending making it possible to solve the iteration with a Generalized Reduced Gradient (GRG) Nonlinear Solver from Frontline Systems Inc. (Incline Village, NV, USA) included in MS Excel. Precision for solving the iteration was set to 0.001. The temporal discretization for the model was chosen to be 1 min.

Furthermore, the following assumptions were made for the model:

- FS and DS behave like ideal solutions.
- The temperature is constant during the experiments.
- The permeate flux is directed from FS to DS.
- The reverse solute flux is directed from DS to FS.
- Membrane parameters A, B, and S are the same for all membrane samples.
- Membrane parameters A, B, and S are constant during the experiment.
- The diffusion coefficient D is constant during the experiment.
- Fouling does not occur.
- Chemical reactions do not occur.
- Spacers are not considered although they were used in the experiments.
- The fluxes axial across the membrane are constant; no local dependencies are assumed.
- The system is a steady-state system.

5.2.3 Model Evaluation

The introduced models were evaluated by comparing the simulated results with those from the experiments with real automobile wastewaters. Two evaluation parameters were used: The mean square error (MSE) and the Nash–Sutcliffe efficiency (NSE).

The MSE is a common way to describe model performance and is calculated according to Equation (12) with J_{mod} and J_{exp} being the modeled and the experimental flux at a certain time t. MSE values are strictly positive and the smaller they are, the better are the modeled results [56].

$$MSE = \sum_{n=1}^{N} \left(J_{mod}^{t} - J_{exp}^{t}\right)^2 \tag{12}$$

The Nash–Sutcliffe efficiency is used for evaluating the prediction of a hydraulic discharge and is commonly used for hydrological models [57]. The NSE is the normalized version of the MSE and calculated according to Equation (13). The NSE can range from -∞ to 1, whereby an efficiency of 1.0 indicates a perfect fit of modeled and experimental data. If the NSE is close to 0, the calculated model is as accurate as the mean value of the experimental data; whereby NSE values less than zero suggest that the experimental data is better than the calculated one. Good performing models should have an NSE between 0 and 1 [57].

$$NSE = 1 - \frac{\sum_{n=1}^{N} \left(J_{mod}^{t} - J_{exp}^{t}\right)^2}{\sum_{n=1}^{N} \left(J_{exp}^{t} - \overline{J_{exp}}\right)^2} = 1 - \frac{MSE}{\sum_{n=1}^{N} \left(J_{exp}^{t} - \overline{J_{exp}}\right)^2} \tag{13}$$

5.3 Results and Discussion

5.3.1 Modelling the Permeate Flux for Standard Performance Tests with Deionized Water and 1 mol/L NaCl

As described in the previous chapter, standard membrane performance tests were performed with deionized water as FS and 1 mol/L NaCl as DS for 2 hours using ALFS mode. In the beginning of each test series, before the experiments with industrial effluents began, a performance test was conducted with a new membrane sample. Using the three models and two membrane parameter sets, the performance tests were modelled using diffusion coefficients ranging from 1.2×10^{-9} to 1.5×10^{-9} m²/s, which is typical for 1 mol/L NaCl and temperatures between 17 and 25 °C [58]. The first performance tests of six test series were used to validate the modelled results. The detailed evaluation of the experiments was published in a previous paper [48].

Figure 2 shows the experimental and modelled permeate fluxes for the three models (I, II, III) and two membrane parameter sets (Par1, Par2). Experimental results are illustrated by boxplots showing the 25% and the 75% quantile as well as the median of six tests. Modelled results are illustrated as broad strips, the width of which is caused by the variation of the diffusion coefficient. The mean value is shown as a dashed line. The more the modelled results overlap with the experimental results, the better suitable is the applied model and the used membrane parameter set.
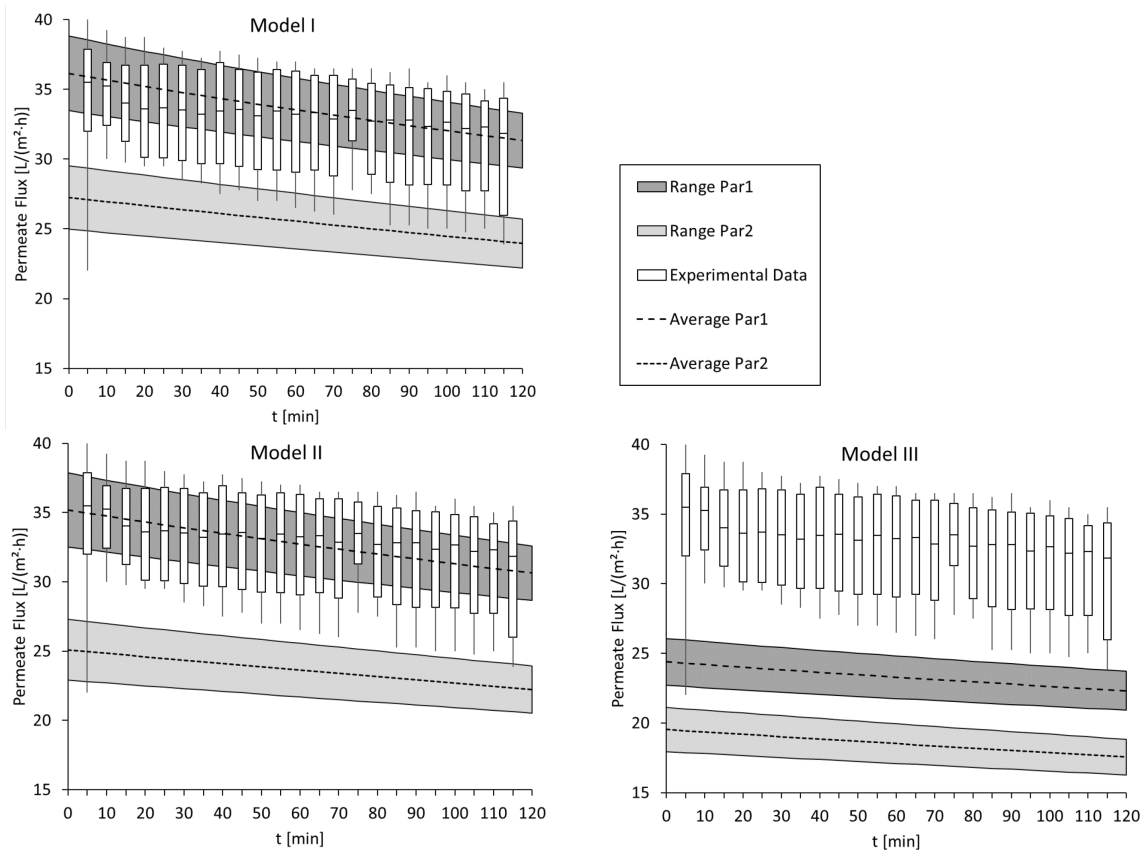
Figure 2. Modelled and experimental permeate fluxes of membrane performance tests. Experimental results are illustrated by boxplots showing the 25% and the 75% quantile as well as the median of six tests. Modelled results are illustrated as broad strips, the width of which is caused by the variation of the diffusion coefficient. The mean value is shown as a dashed line.

It can be seen that Model I and Model II successfully simulated the experiments when Par1 was used since modelled and experimental results overlap almost completely. Model III did not match the experimental permeate fluxes with either membrane parameter set.

In general, the overlap of experimental and modelled data was higher for Model I and Model II, showing that the performance of Model I and Model II was better than Model III. For the same reason, membrane parameter set Par1, which was determined by FO-only method, is more suitable than Par2, which was determined by RO-FO method. The decrease in permeate flux due to FS and DS recirculation is also well simulated. Membrane fouling is not considered in the modelling but might happen in the

experiments. Apparently, no membrane fouling occurred in the performance tests since the decrease of experimental and modelled permeate fluxes are the same.

Applied model equations assume that the membrane has a porous active layer. The used FO membrane, however, is equipped with a dense active layer. Still, the model equations deliver mostly matching results, proving that the chosen model equations can be applied successfully.

Furthermore, by modelling the membrane performance tests, it was shown that the calibration for assuming the diffusion coefficient is applicable.

5.3.2   Modelling of Permeate Flux in ALFS Mode for Wastewater Experiments

FO laboratory experiments were conducted with four different automobile wastewaters, deionized water, and 1 mol/L NaCl. In five test series, an ALFS membrane orientation was used. One test lasted 300 min. Previously, the detailed evaluation of the experiments was published elsewhere [48]. In Figure 3, modelled and experimental permeate fluxes are illustrated for the ALFS experiments with automobile wastewater. Permeate fluxes are given exemplarily for 10, 150, and 300 min test time. Experimental values are illustrated with columns. Modelled results for Model I, II, and III are shown as dashed line with crosses when membrane parameter set Par1 was used, and with circles when Par2 was used. Modelling runs were performed with different diffusion coefficients. In Figure 3, only the best fitting modelling run is illustrated and the corresponding diffusion coefficient is indicated next to the dashed line.

Permeate fluxes differed strongly depending on the utilized FS and DS. For this reason, the axis for the permeate flux was adjusted accordingly. In test series A2 and A4, the experimental permeate fluxes in the experiments were between 0.1 and 1.1 L/(m²·h). These low fluxes are due to the low osmotic pressure difference between FS and DS. In test series A1, A3, and A6, the experimental permeate fluxes were between 8.0 and 25.0 L/(m²·h). The higher permeate fluxes can be explained by the higher osmotic pressure differences between FS and DS (see Table 1). A detailed evaluation of the experimental results is included in another publication [48].
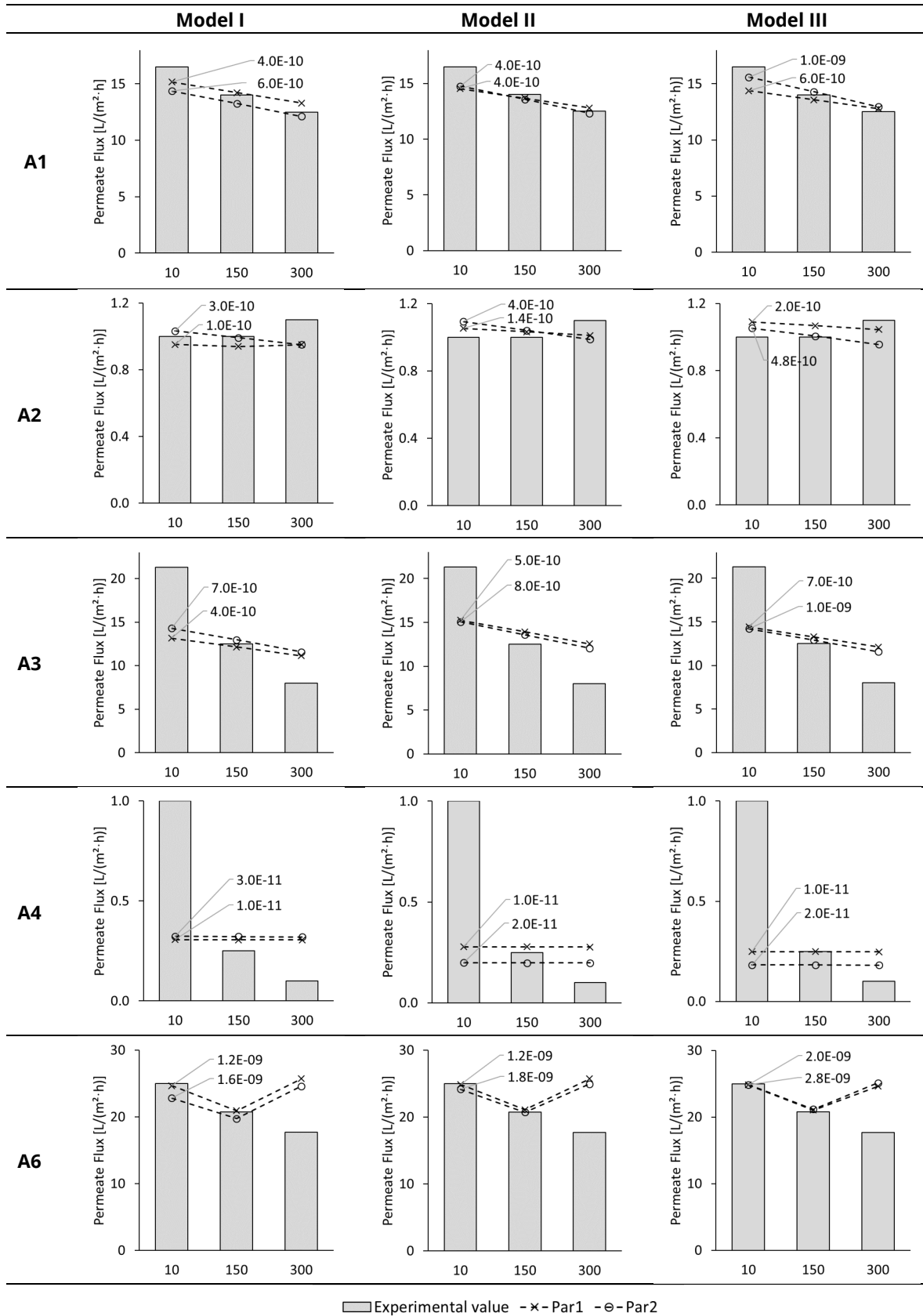
Figure 3. ALFS permeate fluxes of test series A1, A2, A3, A4, and A6 for 10, 150, and 300 min test time from experiments (columns) and Model I, Model II, and Model III with membrane parameter set Par1 (dashed line with crosses) and Par2 (dashed line with circles). Modelled results are shown for best best-fitting diffusion coefficient which is indicated next to the corresponding line.

Due to FS and DS recirculation and permeate flux through the membrane, FS and DS are concentrated and diluted, respectively, during the experiment. For this reason, the osmotic pressure difference between FS and DS also decreases leading to a decreasing permeate flux. This fact is included in the model equations. However, permeate flux in the experiments might additionally decrease because of membrane fouling or temperature changes affecting viscosity as well as diffusion coefficients and mass transfer coefficients. These effects are not considered in the model equations. The slope of the permeate fluxes in Figure 3 illustrates the decreasing permeate flux in the course of FO treatment.

With every model, five test series were modelled with two different parameter sets. Thus, 30 data points are illustrated for each model. The modelled results are described as "good" if the deviation from the experimentally determined value is a maximum of 15% and as "very good" if the deviation is a maximum of 5%.

With Model I, 10 data points were modelled very well, 7 well, and 13 poorly. Model I showed "good" and "very good" results simulating complete test series A1 and test series A2 with Par 2. Furthermore, "very good" results were obtained for the 10-min-flux in test series A2 with Par1, the 150-min-flux in A3 with both Par1 and Par2, the 10- and 150-min-flux in A6 with Par1, and the 150-min-flux in A6 with Par2. "Good" matches were obtained for the 150-min-flux in A2 with Par1 and for the 10-min-flux in A6 with Par2.

With Modell II, 11 data points were modelled very well, 8 were modelled well, and 11 were modelled poorly. Model II delivered "good" and "very good" results for the complete test series A1 and A2. Further "very good" matches were the 10- and 150-min-flux in A6; further "good" matches were the 150-flux in A3 and the 150-min-flux in A4 with Par1.

With Model III, 13 data points were modelled very well, 5 well, and 12 poorly. Modell III simulated test series A1 and A2 well and very well. Further, "very good" matches were obtained for the 150-min-flux in A3 with Par2 as well as the 10- and 150-min-flux in A6. Another "good" match was found for the 150-min-flux in A3.

Considering the 30 data points, which were analyzed, Model III delivered the most results labeled as "very good". However, it delivered one poor result more than Model II. Therefore, Model II and Model III both seem more suitable for modelling the permeate flux because they achieved 19 and 18 good and very good results, respectively.

Test series A1 had permeate fluxes decreasing from 16.5 to 12.5 L/(m²·h) and was simulated well by all models. The decreasing permeate flux was well reflected by the models. Since the slope of modelled and experimental values is the same, apparently no fouling occurred during the 300-min-test. Test series A3 had permeate fluxes starting at 21.3 and decreasing to 8.0 L/(m²·h). Here, the 150-min-value was well predicted by all models. However, the 10-min-value was underestimated by the models; the 300-min-value overestimated. The slope of the experimental values was steeper than the modelled

values. So it is probable that membrane fouling occurred during the experiments. The reason for the high experimental permeate flux in the beginning of the test compared to the modelled results is not clearly identifiable. One reason might be that membrane samples from one manufacturer still differ to some extent and might have different membrane parameters leading to different initial permeate fluxes.

Test series A2 and A4 had low permeate fluxes below 1.1 L/(m²·h). A decreasing permeate flux was modelled for A2 but not measured in the experiment. The constant or even increasing permeate flux that was measured in the experiment might be due to the regular measurement inaccuracy in the experimental set-up, especially, when only low mass changes occurred. Mathematically a higher permeate flux only occurs due to two reasons: A higher osmotic pressure difference or an increasing diffusion coefficient. Reasons for these effects may be rising temperatures or a dilutive ICP in the support layer of the membrane. In regard to A4, a constant permeate flux was modelled but not measured. Again, the 10-min-value was underestimated by the models; the 300-min-value overestimated. Apparently, membrane fouling occurred in A4 and could not be simulated by the models. Due to the very low permeate fluxes, test series A2 and A4 are not ideal for model validation.

Within the experimental test series, A6 is special because a negative reverse solute flux occurred during the experiments. This means that substances from the FS diffused to the DS. Usually, reverse solute flux occurs from draw to feed side in the opposite direction than the permeate flux. None of the applied models was able to consider this effect. Therefore, in order to simulate a permeate flux, the measured reverse solute flux was used as input data instead of calculated reverse solute flux. With this adaption, it was possible to get very good fits between experimental and modelled results for 10 and 150 min test time. The high deviation for the 300-min-value can be explained by the extremely negative experimental reverse solute flux used as input data. Here, problems within the experimental procedure, especially difficulties to measure only small differences in conductivity and changing FS and DS composition, might be the reason for incorrectly measured reverse solute fluxes. Because of the mentioned problems, model validation with test series A6, especially the 300-min-value, should be treated with caution.

In general, it is interesting to see that in most cases the 150-min-value for the permeate flux was well predicted. Regarding the membrane parameters, no parameter set delivered better results than the other. With Par1, 17 "very good" and 11 "good" matches were obtained; with Par2, 17 "very good" and 10 "good" matches were found.

Figure 4 shows the NSE-values that were obtained with Model I, Model II, and Model III. For Model I, the NSE ranges from –0.31 up to 0.24. NSE-values close to zero and between zero and 1.0 are considered good results. NSE-values between 0 and 1.0 were achieved

for test series A1 and A3. NSE-values close to zero were further calculated for A2. Thus, 6 out of 10 NSE-values are good.

Figure 4. NSE for permeate fluxes of test series A1, A2, A3, A4, and A6 simulated with Model I, Model II, and Model III using membrane parameter set Par1 and Par2.

For Model II, the NSE ranges from –0.16 up to 0.30. Good NSE-values between 0 and 1.0 were achieved for test series A1 and A3. NSE-values close to zero were further calculated for A2 as well as A4 with Par2 and A6 with Par1. Altogether, 8 out of 10 NSE-values are good.

For Model III, good NSE-values between 0 and 1.0 were achieved for test series A1 and A3. NSE-values close to zero were further calculated for A2 as well as A4. So 8 out of 10 NSE-values are good.

Since Model II and Model III each delivered 8 good NSE-values, they appear more suitable than Model I, which only delivered 6 good NSE-values.

5.3.3 Modelling of Reverse Solute Flux in ALFS Mode for Wastewater Experiments

In Figure 5, the experimental and modelled reverse solute fluxes (RSF) are illustrated for the test series with automobile wastewaters for 10, 150, and 300 min when the membrane was used in ALFS mode. Modelled results are shown for test series A1, A2, A3, and A4. Here, reverse solute fluxes were between 8.2 and 11.3, between 0.28 and 0.34, between 2.4 and 9.0, and between 37.8 and 9.5 g/(m²·h), respectively. No reverse solute flux could be modelled for test series A6 because a negative reverse solute flux occurred here. This means, that substances passed from the FS into the DS, not the other way around as usually expected. All three models were unable to include this phenomenon.

The driving force for RSF is the concentration gradient which exists between FS and DS. Ideally, a solute flux through the membrane should be prevented by the membrane itself. However, solute flux still occurs with present FO membranes. Due to permeate flux, the concentration gradient decreases in the course of FO treatment and RSF should therefore also decrease.

Figure 5. ALFS reverse solute fluxes of test series A1, A2, A3, and A4 for 10, 150, and 300 min test time from experiments (columns) and Model I, Model II, and Model III with membrane parameter set Par1 (dashed line with crosses) and Par2 (dashed line with circles). Modelled results are shown for best-fitting diffusion coefficient which is indicated next to the corresponding line.

In Figure 5, 24 modelled data points are illustrated for each model. As in the previous chapter, when modelled and experimental data points are compared, they are labelled as "very good fit" when the modelled result is within 5% of the experimental result and as "good fit" when both values are in a range of 15%.

Model I only showed two "very good" results in regard to the reverse solute flux. In test series A3, the 10-min-value matched very well when Par1 was used. Furthermore, the 150-min-value in the same test series with Par2 was a "very good" fit. All other 22 data points fitted poorly.

Model II was able to reach two "very good" fits and two "good" fits. The 10-min-value of A1 with Par2 and the 300-min-value in A3 with Par2 fitted "very good". The 150- and 300-min-value in A1 with Par2 fitted well. 20 data points fitted poorly.

Model III resulted in two "very good" fits and one "good" fit. The 10-min-value in A1 with Par2 as well as the 300-min-value in A3 with Par2 were the "very good" fits. The 150-min-value in A1 with Par2 was the "good" fit. 23 data points were modelled with poor results.

In general, the used modelling approaches were unable to simulate reverse solute flux with satisfying results. However, Model II and Model III delivered slightly better results than Model I.

The NSE- and MSE-values for Model, I, Model II, and Model III are given in Figure 6. NSE-values for Model I are all below zero ranging from –0.01 down to –4.68. That indicates that modelled and experimental reverse solute fluxes did not fit well at all. Only for test series A1, the NSE-values are close to zero with –0.03 and –0.01, which shows that here the modelling was not too bad.
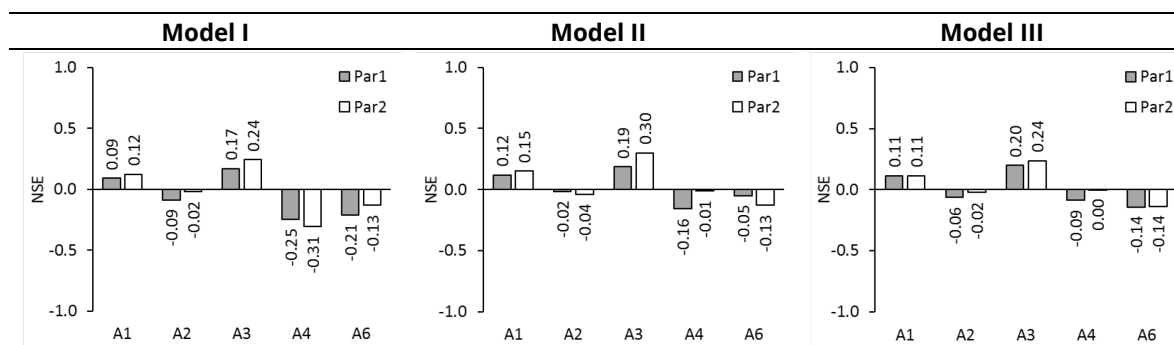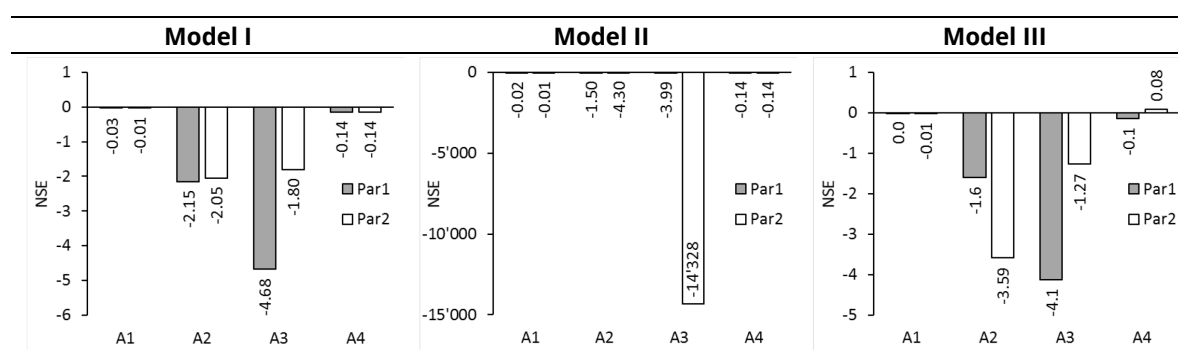

Figure 6. NSE for reverse solute fluxes of test series A1, A2, A3, and A4 simulated with Model I, Model II, and Model III using membrane parameter sets Par1 and Par2.

For Model II the NSE-values are also below zero ranging from –0.01 down to –14'328. Again, only test series A1 was modelled fairly well according to an NSE-value of –0.01 and –0.02. The NSE-value for test series A3 and Par2 was -14'328 and thus extremely low. The negative NSE-values show that modelled and experimental reverse solute fluxes did not fit well for Model II.

The NSE-values for Model III are between –4.1 and 0.08. NSE-values between 0 and 1.0 were achieved for A1-Par1 and A4-Par2: They were 0.0 and 0.08, respectively. Furthermore, NSE-values just below zero were found for A1-Par2 and A4-Par1: They were

–0.01 both times. Out of the three modelling approaches, Model III delivered the best reverse solute fluxes when the NSE-values are taken as evaluation criterion.

RSF was not successfully modelled. For modelling, the electrical conductivity was taken as sole input parameter to minimize analysis effort. It was assumed that the electrical conductivity was caused by NaCl only. In reality, however, RSF strongly depends on the composition of FS and DS because each substance behaves differently in regard to membrane diffusion. This so-called selective diffusion was not considered in the models and might be the reason for discrepancy between modelled and experimental RSF.

5.3.4   Modelling of Permeate Flux and Reverse Solute Flux in ALDS Mode for Wastewater Experiments

In addition to the five test series that used the ALFS membrane orientation, one test series was performed in ALDS mode. This test series was also modelled using the three modelling approaches described in Section 2.2 and two membrane parameter sets. Permeate fluxes and reverse solute fluxes were determined.

Figure 7 shows the modelled and experimental permeate fluxes for 10, 150, and 300 min test duration. The experimental permeate fluxes were 2.5, 2.3, and 2.4 L/(m²·h), respectively. Altogether 6 data points were obtained for each model. Modelled results are labelled as "very good" if the deviation is 5% or less and as "good" if it is 15% or less.
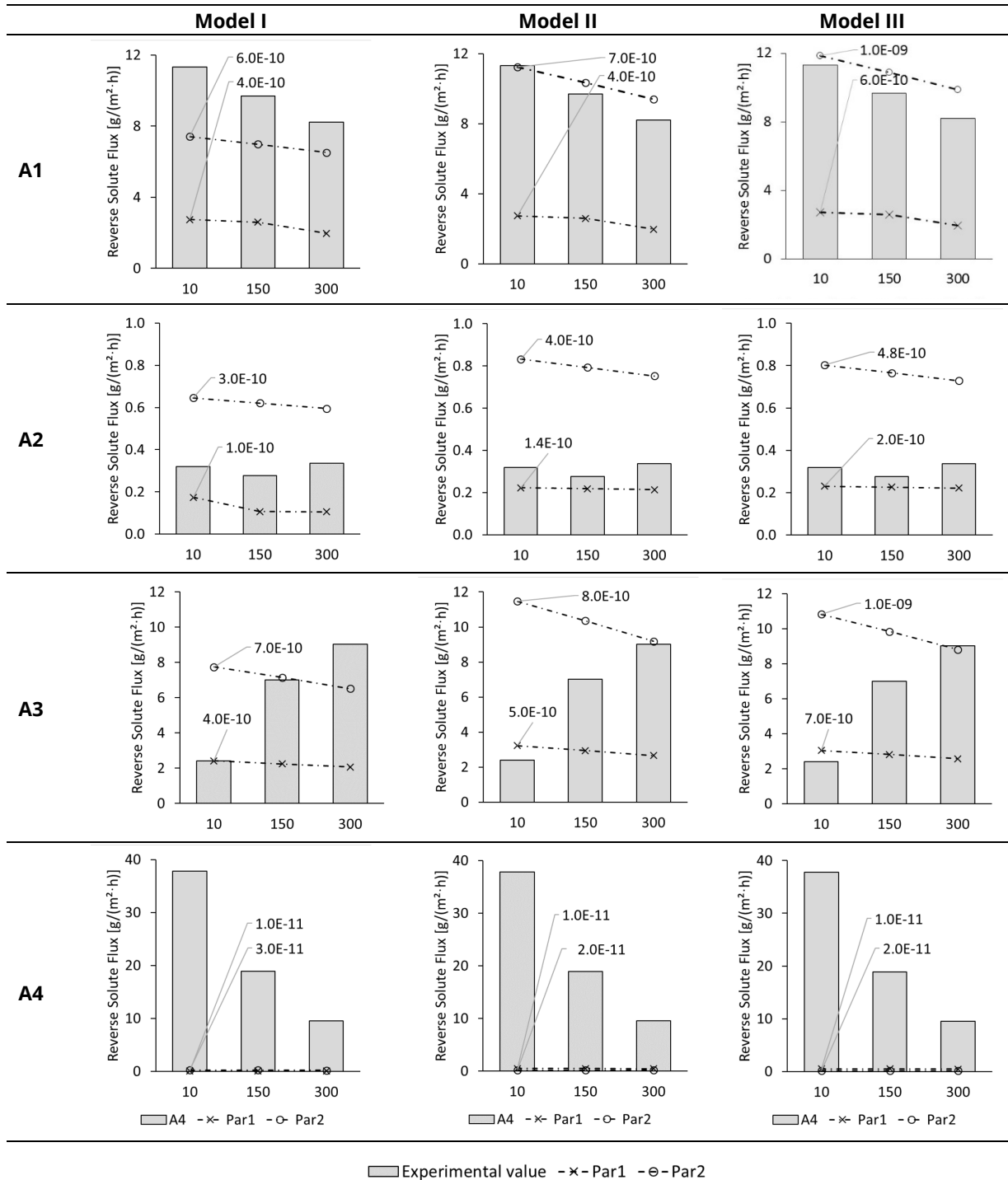

Figure 7. ALDS permeate flux of test series A5 for 10. 150, and 300 min test time from experiments (columns) and Model I, Model II, and Model III with membrane parameter set Par1 (dashed line with crosses) and Par2 (dashed line with circles). Modelled results are shown for best-fitting diffusion coefficient which is indicated next to the corresponding line.

Model I delivered three "very good", two "good" and only one "poor" result. The "very good" matches were the 10-minute-values as well as the 150-min-value with Par1. The "good" matches were the 150-min-value with Par2 and the 300-min-value with Par1.

Model II resulted in three "very good" and two "good" fits. No "poor" matches occurred with this model. The 10-min-value with Par 2 as well as the 150-min-values were the "very good" fits. The 10-min-value with Par1 and the 300-min-values were the "good" fits.

With Model III four "very good", two "good", and one "poor" result was obtained. Here, the 10- and 150-min-values were modelled very well and the 300-min-value with Par1 was modelled well.

If the number of poor matches between experimental and modelled data points are taken as evaluation criterion, all three models showed good permeate flux results with Model II being the best modelling approach.

NSE-values for the permeate fluxes are illustrated in Figure 8. NSE-values were all below zero ranging from –0.72 up to –0.09. No optimal NSE-values between 0 and 1.0 were achieved. However, NSE-values close to zero were achieved with Model II and Par1 as well as with Model III and Par1: They were –0.08 and –0.09. Taking the NSE-value as evaluation criterion, Model II and Model III combined with Par1 are the most suitable modelling approaches.

Figure 8. NSE for permeate fluxes of test series A5 (ALDS mode) simulated with Models I, II, and III using membrane parameter sets Par1 and Par2.

In Figure 9, experimental and modelled reverse solute fluxes are illustrated for 10, 150, and 300 min. The experimental reverse solute fluxes were between 0.4 and 0.6 g/(m²·h). Six data points were obtained for each model. Modelled results are labelled as "very good" if the deviation is 5% or less and as "good" if it is 15% or less.

With Model I only one good result was obtained: The 300-min-value with Pa1. All other 5 data points resulted in poor matches, whereby the results with Par1 were closer to the experimental results than with Par2.

One "very good" and one "good" match was found with Model II. Here, again the values with Par1 were better than with Par2. The 10-min-value was the "very good" fit and the 300-min-value was the "good" fit.

Model III showed similar results as Model II. Again the 10-min-value and the 300-min-value with Par1 were "very good" and "good" matches. All other modelled results matched poorly. The modelled results with Par1 were again closer than with Par2.
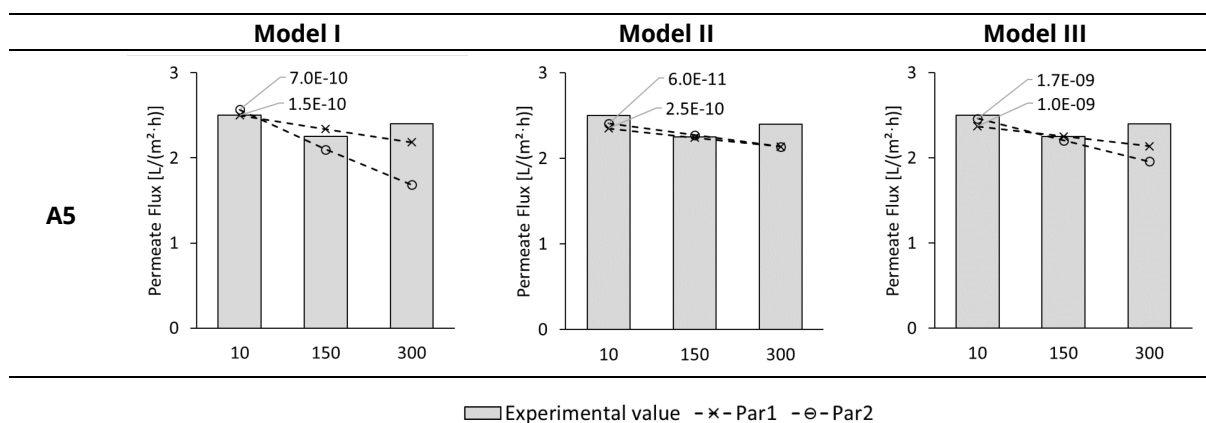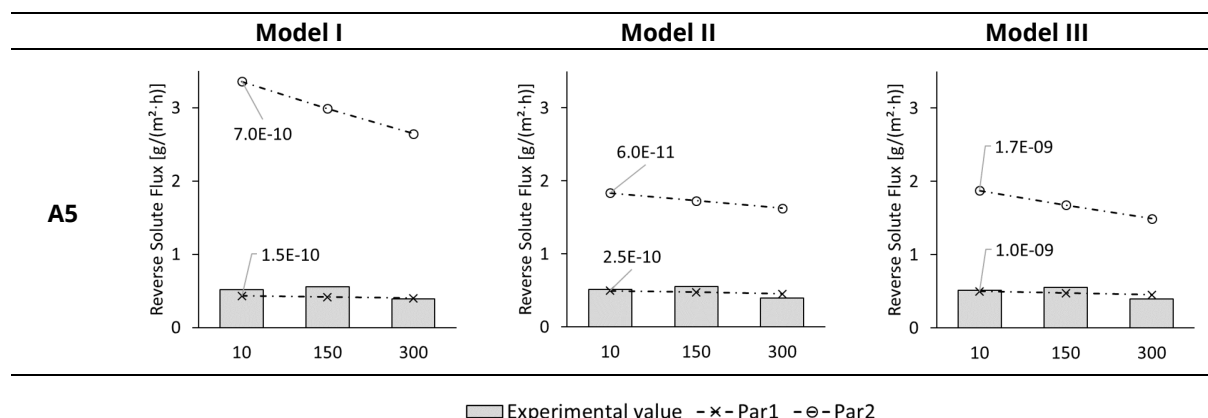

Figure 9. ALDS reverse solute flux of test series A5 for 10. 150, and 300 min test time from experiments (columns) and Model I, Model II, and Model III with membrane parameter set Par1 (dashed line with crosses) and Par2 (dashed line with circles). Modelled results are shown for best-fitting diffusion coefficient which is indicated next to the corresponding line.

With a maximum of two "very good" and "good" matches out of six, reverse solute flux was modelled rather poorly in ALDS-mode. Altogether, reverse solute flux was modelled better with Par1 than with Par2. With Par1 at least 1, 2, and 2 "very good" and "good" matches were achieved for Model I, Model II, and Model III, respectively.

The NSE-values for the modelled reverse solute flux with an ALDS membrane orientation are shown in Figure 10. NSE-values were between –245 and –0.01. No optimal NSE-value between 0 and 1.0 occurred. However, NSE-values just below zero resulted from Model I with Par1 and Model III with Par1: They were –0.05 and –0.01, respectively. NSE-values were between –245 and –24 when Par2 was used. Thus, Par2 appears to be unsuitable for reverse solute flux modelling. Par1 appears more suitable because NSE-values were between –0.31 and –0.0.1.

The choice of FS and DS used in test series A6 generated a very low permeate flux. Changes in permeate flux and reverse solute flux were hard to measure within the experiments. For this reason, modelling this one test series in ALDS mode was also error-prone. In order to further validate the ALDS model equations, experiments with FS and DS conditions similar to test series A1, A3, and A6 should have been performed. However, since the experiments were performed separately from the modelling, no further experiment could be conducted. For this reason, a good comparison between ALFS and ALDS modelling was not possible within this study.
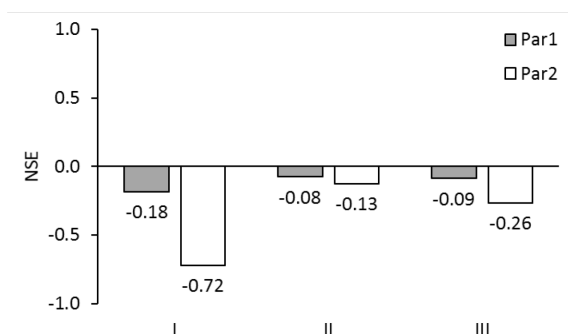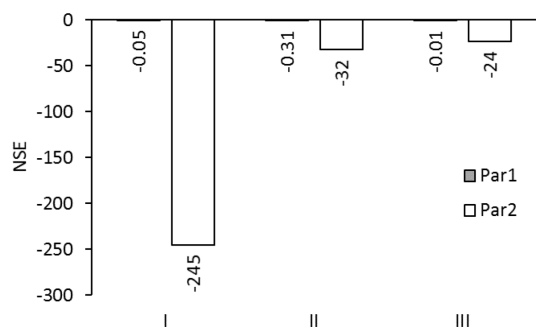
Figure 10. NSE for reverse solute fluxes of test series A5 simulated with Models I, II, and III using membrane parameter sets Par1 and Par2.

5.4 Conclusion

Three different models were implemented in MS Excel to simulate FO lab-scale experiments that were performed with different wastewaters from the automobile industry. The models differed mainly in the extent in which concentration polarization was considered. Permeate flux and reverse solute flux were calculated and compared with the experimental values. Two different membrane parameter sets (water permeability A, solute permeability B, structural parameter S) were used: One that was determined by FO-only test method (Par1) and one that was determined by RO–FO test method (Par2). Five experimental test series used an ALFS membrane orientation, and one used an ALDS membrane orientation.

Within modelling, the automobile experiments, as presented previously by Haupt and Lerch, [48] were simulated. Partly, the permeate fluxes could be well represented others were over- or under-estimated. Here, Model II and Model III showed better results than Model I. There are two possible reasons for the differences between modelled and experimental permeate fluxes: Firstly, fouling effects occurred in the experiments that influenced permeate flux negatively. However, fouling was not considered in the models but could be observed in the experiments. Second, the amount of model input parameters was low. This enabled easy and fast modelling with few analytical expenses. Still, the complex structure and composition of the industrial wastewaters might influence the FO process differently.

The calculation of the reverse solute fluxes showed mostly large deviations compared to the actual measurements. Thus, modifications need to be made to better predict reverse solute flux. One possibility might be the use of more input parameters than just the electrical conductivity and the performance of long-term experiments.

An important parameter of the model equations is the diffusion coefficient. In our study, several modelling runs were performed with different diffusion coefficients. By comparing the results with experimental data, the best fitting diffusion coefficient was chosen for

further validation. This approach has produced satisfactory results in our case. However, it is not optimal since the modelling is time-consuming. Moreover, the diffusion coefficient probably changes during FO due to concentration polarization as well as dilution and concentration of DS and FS, respectively. A diffusion coefficient that is concentration-dependent might be implemented for more precise modelling, as studied in depth by D'Haese et al. [59]. Regarding the two membrane parameter sets, neither proved to be better than the other.

In FO treatment of industrial waters, membrane fouling is a crucial point to be considered. The effect of fouling on permeate fluxes was not part of the model equations. However, the gap between experimental and modelled permeate fluxes allows conclusions to be drawn about the extent of fouling. Thus, the proposed models are a suitable supplement to experiments to predict fouling.

Nomenclature

A	Water permeability [L/(m² h bar)]
A_{CS}	Cross-section area [m²]
B	Solute permeability [L/(m² h)]
c	Concentration [mol/L]
c_{osm}	Osmolality [osmol/kg]
d_h	Hydraulic diameter [m]
D	Diffusion coefficient of solution [m²/s]
J	Flux
J_s	Reverse solute flux [g/(m²·h)]
J_w	Permeate flux [L/(m²·h)]
k	Mass transfer coefficient from bulk solution to membrane interface [m/s]
L	Flow channel length [m]
l_u	Wetted perimeter [m]
MSE	Mean square error
NSE	Nash-Sutcliffe efficiency [-]
R	Universal gas constant [J/(K·mol)]
Re	Reynolds number [-]
S	Structural parameter [m]
Sc	Schmidt number [-]
Sh	Sherwood number [-]
T	Temperature [K]
v	Fluid velocity [m/s]

Greeks

β	Concentration [g/L]
ρ	Density [kg/m³]
Δ	Difference
κ	Electrical conductivity [μS/cm or mS/cm]
η	Dynamic viscosity [Pa·s]
π	Osmotic pressure [bar]
ϑ	Temperature [°C]

Subscripts

DS	Draw solution
exp	Experimental value
FS	Feed solution
mod	Modelled value
N	Number of values
t	Time

References of Chapter 5

1. Sachidananda, M.; Webb, D.P.; Rahimifard, S. A Concept of Water Usage Efficiency to Support Water Reduction in Manufacturing Industry. *Sustainavility* **2016**, *8*, 1222.

2. Cath, T.; Childress, A.; Elimelech, M. Forward osmosis: Principles, applications, and recent developments. *J. Membr. Sci.* **2006**, *281*, 70–87.

3. Lutchmiah, K.; Verliefde, A.; Roest, K.; Rietveld, L.; Cornelissen, E. Forward osmosis for application in wastewater treatment: A review. *Water Res.* **2014**, *58*, 179–197.

4. Shaffer, D.L.; Werber, J.R.; Jaramillo, H.; Lin, S.; Elimelech, M. Forward osmosis: Where are we now? *Desalination* **2015**, *356*, 271–284.

5. McCutcheon, J.R. Forward osmosis: A technology platform here to stay. *Desalination* **2017**, *421*, 1–2.

6. Haupt, A.; Lerch, A. Forward Osmosis Application in Manufacturing Industries: A Short Review. *Membranes* **2018**, *8*, 47.

7. Johnson, D.J.; Suwaileh, W.A.; Mohammed, A.W.; Hilal, N. Osmotic's potential: An overview of draw solutes for forward osmosis. *Desalination* **2018**, *434*, 100–120.

8. Awad, A.M.; Jalab, R.; Minier-Matar, J.; Adham, S.; Nasser, M.S.; Judd, S. The status of forward osmosis technology implementation. *Desalination* **2019**, *461*, 10–21.

9. Jalab, R.; Awad, A.M.; Nasser, M.S.; Minier-Matar, J.; Adham, S.; Judd, S.J. An empirical determination of the whole-life cost of FO-based open-loop wastewater reclamation technologies. *Water Res.* **2019**, *163*, 114879.

10. Zhao, S.; Zou, L.; Tang, C.Y.; Mulcahy, D. Recent developments in forward osmosis: Opportunities and challenges. *J. Membr. Sci.* **2012**, *396*, 1–21.

11. Li, L.; Liu, X.P.; Li, H.Q. A review of forward osmosis membrane fouling: Types, research methods and future prospects. *Environ. Technol. Rev.* **2017**, *6*, 26–46.

12. Qin, D.; Liu, Z.; Liu, Z.; Bai, H.; Sun, D.D. Superior Antifouling Capability of Hydrogel Forward Osmosis Membrane for Treating Wastewaters with High Concentration of Organic Foulants. *Environ. Sci. Technol.* **2018**, *52*, 1421–1428.

13. Zou, S.; Qin, M.; He, Z. Tackle reverse solute flux in forward osmosis towards sustainable water recovery: Reduction and perspectives. *Water Res.* **2019**, *149*, 362–374.

14. Qin, J.J.; Lay, W.C.L.; Kekre, K.A. Recent developments and future challenges of forward osmosis for desalination: A review. *Desalin. Water Treat.* **2012**, *39*, 123–136.

15. Ibrar, I.; Naji, O.; Sharif, A.; Malekizadeh, A.; Alhawari, A.; AlAnezi, A.A.; Altaee, A. A Review of Fouling Mechanisms, Control Strategies and Real-Time Fouling Monitoring Techniques in Forward Osmosis. *Water* **2019**, *11*, 695.

16. McCutcheon, J.R.; Elimelech, M. Influence of concentrative and dilutive internal concentration polarization on flux behavior in forward osmosis. *J. Membr. Sci.* **2006**, *284*, 237–247.

17. Kim, B.; Gwak, G.; Hong, S. Review on methodology for determining forward osmosis (FO) membrane characteristics: Water permeability (A), solute permeability (B), and structural parameter (S). *Desalination* **2017**, *422*, 5–16.

18. Tielen, S. Enhancing reverse osmosis with feed spacer technology. *Filtr. Sep.* **2016**, *53*, 24–27.

19. Haidari, A.; Heijman, S.; Van Der Meer, W. Optimal design of spacers in reverse osmosis. *Sep. Purif. Technol.* **2018**, *192*, 441–456.

20. Kavianipour, O.; Ingram, G.D.; Vuthaluru, H.B. Feed spacers in reverse osmosis. *Filtr. Sep.* **2015**, *52*, 20–21.

21. Koutsou, C.; Yiantsios, S.; Karabelas, A.; Karabelas, A. A numerical and experimental study of mass transfer in spacer-filled channels: Effects of spacer geometrical characteristics and Schmidt number. *J. Membr. Sci.* **2009**, *326*, 234–251.

22. Karabelas, A.J.; Koutsou, C.P.; Sioutopoulos, D.C. Comprehensive performance assessment of spacers in spiral-wound membrane modules accounting for compressibility effects. *J. Membr. Sci.* **2018**, *549*, 602–615.

23. Islam, M.S.; Sultana, S.; McCutcheon, J.R.; Rahaman, M.S. Treatment of fracking wastewaters via forward osmosis: Evaluation of suitable organic draw solutions. *Desalination* **2019**, *452*, 149–158.

24. Zhou, Y.; Huang, M.; Deng, Q.; Cai, T. Combination and performance of forward osmosis and membrane distillation (FO-MD) for treatment of high salinity landfill leachate. *Desalination* **2017**, *420*, 99–105.

25. Qasim, M.; Mohammed, F.; Aidan, A.; Darwish, N.A. Forward osmosis desalination using ferric sulfate draw solute. *Desalination* **2017**, *423*, 12–20.

26. Wang, X.; Chang, V.W.; Tang, C.Y.; Chang, V.W.C. Osmotic membrane bioreactor (OMBR) technology for wastewater treatment and reclamation: Advances, challenges, and prospects for the future. *J. Membr. Sci.* **2016**, *504*, 113–132.

27. Chekli, L.; Kim, Y.; Phuntsho, S.; Li, S.; Ghaffour, N.; Leiknes, T.; Shon, H.K. Evaluation of fertilizer-drawn forward osmosis for sustainable agriculture and water reuse in arid regions. *J. Environ. Manag.* **2017**, *187*, 137–145.

28. Gwak, G.; Kim, D.I.; Hong, S. New industrial application of forward osmosis (FO): Precious metal recovery from printed circuit board (PCB) plant wastewater. *J. Membr. Sci.* **2018**, *552*, 234–242.

29. Law, J.Y.; Mohammad, A.W.; Tee, Z.K.; Zaman, N.K.; Jahim, J.M.; Santanaraj, J.; Sajab, M.S. Recovery of succinic acid from fermentation broth by forward osmosis-assisted crystallization process. *J. Membr. Sci.* **2019**, *583*, 139–151.

30. Dou, P.; Zhao, S.; Song, J.; He, H.; She, Q.; Li, X.M.; Zhang, Y.; He, T. Forward osmosis concentration of a vanadium leaching solution. *J. Membr. Sci.* **2019**, *582*, 164–171.

31. Li, M.; Wang, X.; Porter, C.J.; Cheng, W.; Zhang, X.; Wang, L.; Elimelech, M. Concentration and Recovery of Dyes from Textile Wastewater Using a Self-Standing, Support-Free Forward Osmosis Membrane. *Environ. Sci. Technol.* **2019**, *53*, 3078–3086.

32. Lee, K.; Baker, R.; Lonsdale, H. Membranes for power generation by pressure-retarded osmosis. *J. Membr. Sci.* **1981**, *8*, 141–171.

33. Loeb, S. Effect of porous support fabric on osmosis through a Loeb-Sourirajan type asymmetric membrane. *J. Membr. Sci.* **1997**, *129*, 243–249.

34. McCutcheon, J.R.; Elimelech, M. Modeling water flux in forward osmosis: Implications for improved membrane design. *AIChE J.* **2007**, *53*, 1736–1744.

35. Tan, C.H.; Ng, H.Y. Modified models to predict flux behavior in forward osmosis in consideration of external and internal concentration polarizations. *J. Membr. Sci.* **2008**, *324*, 209–219.

36. Shakaib, M.; Hasani, S.; Mahmood, M. CFD modeling for flow and mass transfer in spacer-obstructed membrane feed channels. *J. Membr. Sci.* **2009**, *326*, 270–284.

37. Phillip, W.A.; Yong, J.S.; Elimelech, M. Reverse Draw Solute Permeation in Forward Osmosis: Modeling and Experiments. *Environ. Sci. Technol.* **2010**, *44*, 5170–5176.

38. Yaroshchuk, A. Influence of osmosis on the diffusion from concentrated solutions through composite/asymmetric membranes: Theoretical analysis. *J. Membr. Sci.* **2010**, *355*, 98–103.

39. Gruber, M.; Johnson, C.; Tang, C.; Jensen, M.; Yde, L.; Hélix-Nielsen, C. Computational fluid dynamics simulations of flow and concentration polarization in forward osmosis membrane systems. *J. Membr. Sci.* **2011**, *379*, 488–495.

40. Jung, D.H.; Lee, J.; Kim, D.Y.; Lee, Y.G.; Park, M.; Lee, S.; Yang, D.R.; Kim, J.H. Simulation of forward osmosis membrane process: Effect of membrane orientation and flow direction of feed and draw solutions. *Desalination* **2011**, *277*, 83–91.

41. Li, W.; Gao, Y.; Tang, C.Y. Network modeling for studying the effect of support structure on internal concentration polarization during forward osmosis: Model development and theoretical analysis with FEM. *J. Membr. Sci.* **2011**, *379*, 307–321.

42. Park, M.; Lee, J.J.; Lee, S.; Kim, J.H. Determination of a constant membrane structure parameter in forward osmosis processes. *J. Membr. Sci.* **2011**, *375*, 241–248.

43. Tiraferri, A.; Yip, N.Y.; Phillip, W.A.; Schiffman, J.D.; Elimelech, M. Relating performance of thin-film composite forward osmosis membranes to support layer formation and structure. *J. Membr. Sci.* **2011**, *367*, 340–352.

44. Yip, N.Y.; Tiraferri, A.; Phillip, W.A.; Schiffman, J.D.; Hoover, L.A.; Kim, Y.C.; Elimelech, M. Thin-Film Composite Pressure Retarded Osmosis Membranes for Sustainable Power Generation from Salinity Gradients. *Environ. Sci. Technol.* **2011**, *45*, 4360–4369.

45. Tan, C.H.; Ng, H.Y. Revised external and internal concentration polarization models to improve flux prediction in forward osmosis process. *Desalination* **2013**, *309*, 125–140.

46. Tiraferri, A.; Yip, N.Y.; Straub, A.P.; Castrillón, S.R.V.; Elimelech, M. A method for the simultaneous determination of transport and structural parameters of forward osmosis membranes. *J. Membr. Sci.* **2013**, *444*, 523–538.

47. Bui, N.N.; Arena, J.T.; McCutcheon, J.R. Proper accounting of mass transfer resistances in forward osmosis: Improving the accuracy of model predictions of structural parameter. *J. Membr. Sci.* **2015**, *492*, 289–302.

48. Haupt, A.; Lerch, A. Forward osmosis treatment of effluents from dairy and automobile industry—Results from short-term experiments to show general applicability. *Water Sci. Technol.* **2018**, *78*, 467–475.

49. Chun, Y.; Qing, L.; Sun, G.; Bilad, M.R.; Fane, A.G.; Chong, T.H. Prototype aquaporin-based forward osmosis membrane: Filtration properties and fouling resistance. *Desalination* **2018**, *445*, 75–84.

50. Kim, J.; Blandin, G.; Phuntsho, S.; Verliefde, A.; Le-Clech, P.; Shon, H. Practical considerations for operability of an 8" spiral wound forward osmosis module: Hydrodynamics, fouling behaviour and cleaning strategy. *Desalination* **2017**, *404*, 249–258.

51. Grattoni, A.; Canavese, G.; Montevecchi, F.M.; Ferrari, M. Fast Membrane Osmometer as Alternative to Freezing Point and Vapor Pressure Osmometry. *Anal. Chem.* **2008**, *80*, 2617–2622.

52. Kune, J. *Dimensionless Physical Quantities in Science and Engineering*; Elsevier Insights; Elsevier: Amsterdam, The Netherlands; Heidelberg, Germany, 2012; ISBN 978-0-12-416013-2.

53. Bollrich, G. *Technische Hydromechanik 1*; Verlag Für Bauwesen: Berlin, Germany, 1996; ISBN 978-3-345-00608-1.

54. Verein Deutscher Ingenieure. VDI-Wärmeatlas: Berechnungsblätter für den Wärmeübergang. In *Gesellschaft Verfahrenstechnik und Chemieingenieurwesen*, 5th Ed.; VDI-Verlag: Düsseldorf, Germany, 1988; ISBN 978-3-18-400850-5.

55. Perry, R.H.; Green, D.W.; Maloney, J.O. *Perry's Chemical Engineers' Handbook*; 6th ed.; McGraw-Hill Companies, Inc.: New York, NY, USA, 1984; ISBN 0-07-049479-7.

56. Gupta, H.V.; Kling, H. On typical range, sensitivity, and normalization of Mean Squared Error and Nash-Sutcliffe Efficiency type metrics. *Water Resour. Res.* **2011**, *47*, 47.

57. Moriasi, D.N.; Arnold, J.G.; Van Liew, M.W.; Bingner, R.L.; Harmel, R.D.; Veith, T.L. Model Evaluation Guidelines for Systematic Quantification of Accuracy in Watershed Simulations. *Trans. ASABE* **2007**, *50*, 885–900.

58. Lobo, V.M.M. Mutual diffusion coefficients in aqueous electrolyte solutions (Technical Report). *Pure Appl. Chem.* **1993**, *65*, 2613–2640.

    D'Haese, A.K.; Motsa, M.M.; Van Der Meeren, P.; Verliefde, A.R. A refined draw solute flux model in forward osmosis: Theoretical considerations and experimental validation. *J. Membr. Sci.* **2017**, *522*, 316–331.

6   Summary

6.1   Summary & Conclusions

In recent years, the topic of sustainability and environmental protection has received more and more attention. The efficient use of resources, especially in industrial production processes, is of great interest in this context. Especially the efficient usage and recycling of water is important. Different technologies, e.g. membrane filtrations technologies, are used to purify industrial wastewater before recycling or discharge. Unlike conventional membrane filtration technologies, forward osmosis uses the natural osmotic pressure as a driving force for water treatment. Therefore, in addition to other possible advantages this technology requires less energy. In this study the possible application of forward osmosis in industrial water management was investigated. This way a contribution towards a more ecologically and economically favorable water treatment was made.

State of the Art

In chapter 2 of this thesis, the basic principle of forward osmosis is described and the results of an in-depth literature review about the state of art about forward osmosis application, especially in manufacturing industries, is presented. Application of forward osmosis has been studied for some industries (food and beverage, chemical, pharmaceutical, textile, pulp and paper, electronic, coal processing, micro algae cultivation) as well as industry-related topics such as heavy metal elimination and cooling water treatment. However, so far only lab-scale investigations were performed. The problem with lab-scale investigations is that the procedures are not standardized. Therefore, the results are difficult to compare. Furthermore, in many publications the specification of test parameters is incomplete which impedes comparison even more. Information should always be given about feed and draw solution (type and initial volume), the membrane (type, supplier, active surface area, orientation) and the operation (circulation type, flow velocities, duration of experiment, cleaning procedures).

Another finding in the literature review is that more and more companies are emerging selling forward osmosis technology, either membranes, modules or whole plants. Still, publications about forward osmosis application beyond laboratory tests are rare. Pilot-scale investigations were done or are planned for desalination, fertigation and mining wastewater treatment as well as chemical, semiconductor and dairy industry. Full-scale forward osmosis application is – according to company's information – realized for seawater desalination and treatment of power plant wastewater to achieve zero liquid discharge.

Proof-of-Principle Studies

Chapters 3 and 4 of this thesis describe the proof-of-principle studies that were conducted exemplarily for automobile, dairy, and semiconductor industry. Possible feed and draw solutions were identified and used in lab-scale forward osmosis experiments. The effluents were tested either as FS or DS and combined with 1 mol/L NaCl as DS, deionized water as FS, or another effluent as FS or DS. A closed-loop experimental set-up was used containing a membrane test cell for flat-sheet membrane samples. Similar set-ups are used in other lab-scale investigations elsewhere. The experimental procedure of one test series was a sequence of standardized membrane performance tests, experiments with industrial wastewater and mechanical cleaning with deionized water. Experiments with industrial wastewater were repeated three times. For automobile as well as semiconductor industry, four effluents were investigated in six test series. For dairy industry, two effluents were evaluated in three test series.

The average permeate fluxes achieved in the laboratory tests with real industrial wastewater are shown in Figure 1. The permeate fluxes were between 0.1 and 19.4 L/(m²·h) for the automobile industry, between 7.9 and 21.0 L/(m²·h) for the dairy industry and between 10.5 and 33.4 L/(m²·h) for the semiconductor industry.
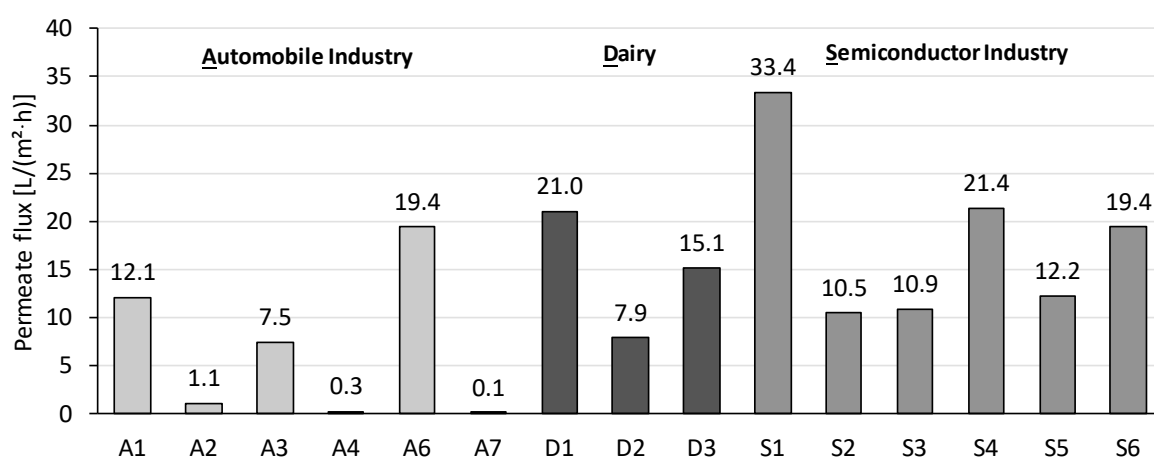
Figure 1. Average permeate fluxes during FO experiments with wastewaters from different industries

Figure 2 shows the correlation between the achieved average permeate fluxes and the osmotic pressure differences in the beginning of the experiments. It can be seen that there is no clear correlation. Since the osmotic pressure difference is the driving force for permeate flux in forward osmosis, a high pressure difference should lead to a high permeate flux. However, there are five test series that had almost the same pressure difference between 43 and 46 bar. Still, the achieved permeate flux ranged from 7 up to 33 L/(m²·h). Furthermore, two dairy test series had a very high osmotic pressure difference of 151 and 158 bar but permeate fluxes were 15 and 21 L/(m²·h) only. Thus, it can be concluded that the permeate flux depends strongly on the osmotic pressure

difference between feed and draw solution but is also influenced by other factors. These other factors are probably mainly the wastewater composition and constituents that lead to deposit formation.
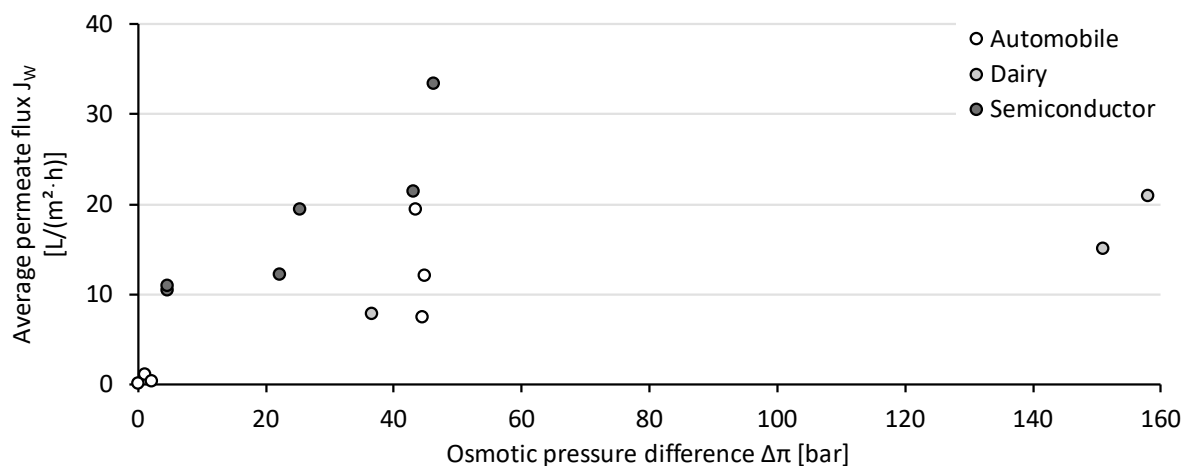
Figure 2. Correlation between average permeate fluxes from lab-scale experiments and osmotic pressure difference in the beginning of the experiments with wastewater from automobile, dairy, and semiconductor industry

Within the experiments, reverse solute flux was determined via conductivity measurements. The results of which are presented in Figure 3. The reverse solute fluxes were between 37.7 and 21.3 g/(m²h), between 4.1 and 12.2 g/(m²h) and between 8.0 and 40.9 g/(m²h), respectively.
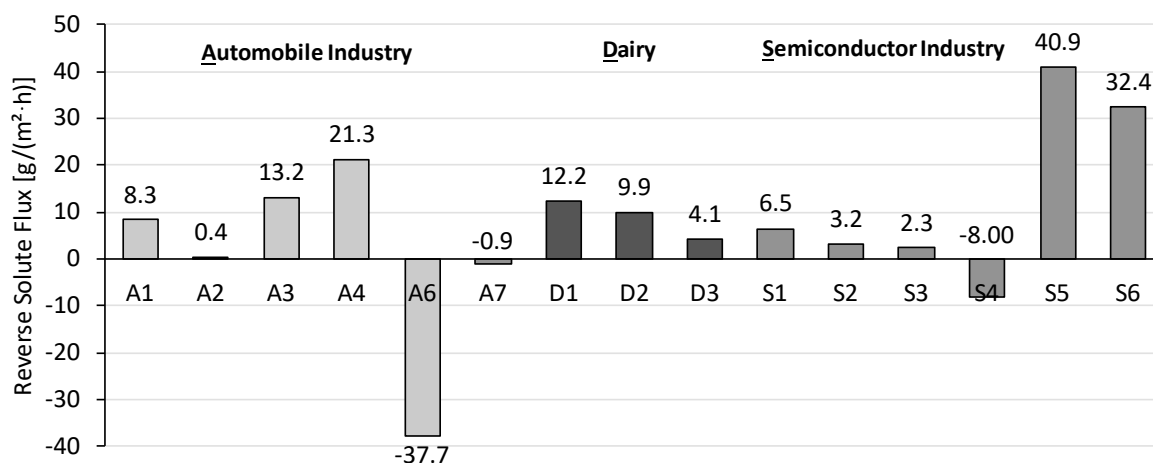
Figure 3. Average reverse solute fluxes during FO experiments with wastewaters from different industries

It becomes obvious that solute flux is an important issue to be taken into consideration. Solute flux appeared in all test series. Reverse solute flux means that substances diffuse through the membrane in the opposite direction as water from DS side with high osmotic pressure to FS side with low osmotic pressure. In two test series, a negative reverse solute flux was measured meaning that substances diffused from the FS side to the DS side. For

this reason, a change in the composition of FS but also DS cannot be excluded during FO operation.

Standardized membrane performance tests before and after experiments were used to monitor fouling. In the test series with dairy wastewater moderate performance deterioration was measured although deposits were visible on the membrane surface. The same happened in the experiments with semiconductor effluents: Performance decreased only moderately even in test series were visible deposits formed. In both cases, no cleaning procedures were tested but it can be assumed that deposit removal should be feasible. When automobile effluents were used in FO, performance deteriorated strongly in almost all test series. Here, deposits on the membrane were observed as well. Since fouling influenced performance so strongly, different cleaning methods including physical cleaning, osmotic backwash and chemical cleaning were applied. Eventually, the original permeate flux was successfully restored.

Conclusions from Proof-of-Principle Studies

Within the experiments with automobile wastewater, three effluents were used as FS and two effluents were used as DS. Rinsing water and wastewater from cathodic dip painting as well as, paint shop pre-treatment wastewater was used successfully as FS. However, none of the tested effluents was suitable as DS (cooling tower circulation water and cathodic dip painting wastewater). Thus, FO could only be applied if an artificial DS was used which would then require an additional treatment step for its regeneration. Furthermore, strong fouling occurred and caused permeate flux deterioration, especially when paint shop pre-treatment wastewater was used. Different cleaning procedures were applied and the original permeate flux could be successfully restored.

For the dairy industry, wastewater treatment reverse osmosis concentrate was evaluated as FS and cheese brine as DS. In the tests, both effluents had good results and also the combined treatment resulted in high permeate fluxes of 15.1 L/(m²·h) showing that, in this case, forward osmosis application would be possible without an artificial draw solution and without another treatment technology. The result would be dewatered reverse osmosis concentrate and diluted cheese brine.

Semiconductor wastewaters used as FS were RO concentrate from ultrapure water production and neutralization effluent from wastewater treatment. Investigated DS were Cu filtrate and Cu concentrate also from wastewater treatment. All wastewaters delivered permeate fluxes above 10 L/(m²·h). With Cu concentrate treatment the extreme low pH value and deposit formation on the membrane surface are critical issues. Still, a combined treatment of Cu concentrate as DS and neutralization effluent as FS might be feasible and economically reasonable, if Cu concentrate is circulated and neutralization effluent is pumped through only once. Since the volume of Cu concentrate, which requires dilution,

is much lower than the volume of neutralization effluent, this semi-batch operation might be an appropriate solution.

Modelling

Chapter 5 contains the description of forward osmosis modelling and its evaluation. Three different models from literature were utilized and partly modified to calculate permeate flux and reverse solute flux with only few input parameters. Model equations were implemented using Microsoft Excel with a Generalized Reduced Gradient (GRG) Nonlinear Solver. Within modelling, the experiments with water from the automobile industry were simulated. Comparison of modelled and experimental results was used to evaluate the models.

The permeate fluxes could be well represented in some cases. The calculation of the reverse solute fluxes showed sometimes large deviations compared to the actual measurements. Models II and III generally shows better results than Model I. The large number of deviations may be due to the low number of input parameters. However, since only few input parameters are required, easy and fast modelling is possible. Fouling was also not included in the model equations. For these reasons, modelling can only deliver a rough estimation of permeate fluxes to be expected in real experiments. Still, in addition to real experiments, modelling can help to show the degree of fouling that influences forward osmosis. In order to calculate more accurate reverse solute fluxes, model equations should be modified and more input parameters should be included.

Application Scenarios and Critical Issues

As a result, application scenarios were developed for the use of forward osmosis in the investigated industrial plants (Figure 4).
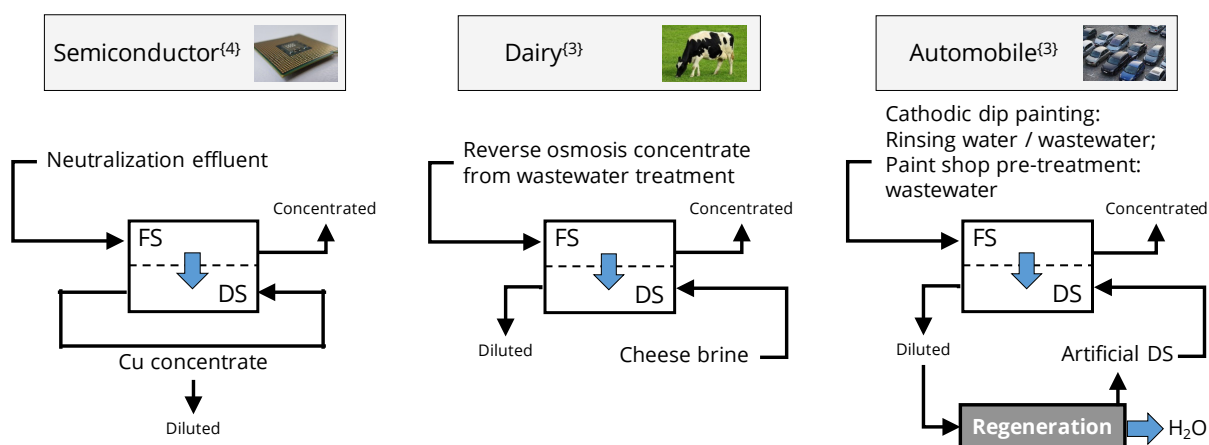
Figure 4. Possible forward osmosis application scenarios for semiconductor, dairy, and automobile industry based on the proof-of-principle studies

For economic reasons, those scenarios in which both the feed and the draw solution are industrial waters and two liquids are treated simultaneously in one step are of particular interest here. The use of an artificial draw solution and its treatment is unnecessary in this case. Combined application is possible in semiconductor and dairy industry. In automobile industry, FO can only be applied with an artificial DS that is regenerated in a separate treatment step.

Critical points when using forward osmosis are the reverse solute flux through the membrane, the deterioration of membrane performance due to fouling as well as economic efficiency of the process. More in-depth investigations are required here.

6.2   Outlook

Within this study, lab-scale investigations on forward osmosis application were carried out for the water management of three industrial branches. Since the production processes differ from branch to branch and even from company to company within one branch, the results of those proof-of-principle can be transferred to other applications to a limited extent only. It is recommended to examine and evaluate each potential application scenario individually. For this purpose, the developed combination of lab-scale experiments and modelling is well suited and can be employed easily. The experimental sequence of membrane performance tests, tests with industrial wastewater and physical cleaning is an appropriate procedure to get information about permeate fluxes, reverse solute fluxes, and fouling effects. Modelling can be done with few input parameters only and therefore delivers an easy and fast estimation of permeate fluxes to be expected. In combination with experimental results, modelling provides further knowledge about fouling effects.

From a technical point of view, the critical points in forward osmosis application are membrane fouling and solute flux through the membrane. In order to keep both issues under control, long-term investigations beyond lab-scale should be conducted. This way, an optimal operation mode could be developed. As mentioned earlier in this thesis, more and more companies enter the market and different forward osmosis membranes as well as different module types are commercially available. The starting point for large-scale experiments could be a recently published review article in which 15 laboratory-scale studies from various fields of forward osmosis application are evaluated and compared [1].

The critical points of fouling and solute flux are closely linked to the used forward osmosis membranes and have been studied in depth elsewhere [2-7]. A review about the state-of-the-art concerning forward osmosis membranes has been published recently and summarizes manufacturing techniques, membrane properties for active and support

layer as well as membrane characterization [8, 9]. As can be seen from the number of publications, a lot of research is being conducted on the field of forward osmosis membranes. Optimized membranes may on the one hand help to improve the technical aspects of forward osmosis application; on the other hand, it may also help to improve economic efficiency of forward osmosis application since the membrane material is one large cost factor apart from energy demand.

From an entrepreneurial point of view, economic efficiency of forward osmosis application is crucial. Here, the lack of information is closely linked with only limited investigations beyond lab- and pilot-scale. There are few publications dealing with economic aspects of forward osmosis often they relate to energy consumption of the forward osmosis process and required draw solution recovery. Mostly, those publications are about forward osmosis for desalination purposes [10-14]. Therefore, in addition to long-term investigations on larger scale, economic aspects of forward osmosis application should be analyzed for application fields beyond desalination.

References of Chapter 6

1. Awad, A.M.; Jalab, R.; Minier-Matar, J.; Adham, S.; Nasser, M.S.; Judd, S.J. The status of forward osmosis technology implementation. *Desalination* **2019**, *461*, 10–21.
2. Ly, Q.V.; Hu, Y.; Li, J.; Cho, J.; Hur, J. Characteristics and influencing factors of organic fouling in forward osmosis operation for wastewater applications: A comprehensive review. *Environ. Int.* **2019**, *129*, 164–184.
3. Chollom, M.N.; Rathilal, S. Fouling and Cleaning in Osmotically Driven Membranes. *Osmotically Driven Membr. Process. - Approach Dev. Curr. Status* **2018**.
4. Abdelrasoul, A.; Doan, H.; Lohi, A.; Cheng, C.-H. Fouling in Forward Osmosis Membranes: Mechanisms, Control, and Challenges. *Osmotically Driven Membr. Process. - Approach Dev. Curr. Status* **2018**.
5. Siddiqui, F.A.; She, Q.; Fane, A.G.; Field, R.W. Exploring the differences between forward osmosis and reverse osmosis fouling. *J. Membr. Sci.* **2018**, *565*, 241–253.
6. Zou, S.; Qin, M.; He, Z. Tackle reverse solute flux in forward osmosis towards sustainable water recovery: reduction and perspectives. *Water Res.* **2019**, *149*, 362–374.
7. Chekli, L.; Pathak, N.; Kim, Y.; Phuntsho, S.; Li, S.; Ghaffour, N.; Leiknes, T.; Shon, H.K. Combining high performance fertiliser with surfactants to reduce the reverse solute flux in the fertiliser drawn forward osmosis process. *J. Environ. Manage.* **2018**, *226*, 217–225.
8. Eyvaz, M.; Arslan, S.; İmer, D.; Yüksel, E.; Koyuncu, İ. Forward Osmosis Membranes – A Review: Part I. *Osmotically Driven Membr. Process. - Approach Dev. Curr. Status* **2018**.
9. Eyvaz, M.; Arslan, S.; İmer, D.; Yüksel, E.; Koyuncu, İ. Forward Osmosis Membranes – A Review: Part II. *Osmotically Driven Membr. Process. - Approach Dev. Curr. Status* **2018**.
10. Chung, H.W.; Banchik, L.D.; Swaminathan, J.; Lienhard V, J.H. On the present and future economic viability of stand-alone pressure-retarded osmosis. *Desalination* **2017**, *408*, 133–144.
11. Mazlan, N.M.; Peshev, D.; Livingston, A.G. Energy consumption for desalination — A comparison of forward osmosis with reverse osmosis, and the potential for perfect membranes. *Desalination* **2016**, *377*, 138–151.
12. Valladares Linares, R.; Li, Z.; Yangali-Quintanilla, V.; Ghaffour, N.; Amy, G.; Leiknes, T.; Vrouwenvelder, J.S. Life cycle cost of a hybrid forward osmosis – low pressure reverse osmosis system for seawater desalination and wastewater recovery. *Water Res.* **2016**, *88*, 225–234.

13. Coday, B.D.; Miller-Robbie, L.; Beaudry, E.G.; Munakata-Marr, J.; Cath, T.Y. Life cycle and economic assessments of engineered osmosis and osmotic dilution for desalination of Haynesville shale pit water. *Desalination* **2015**, *369*, 188–200.

14. Choi, Y.; Cho, H.; Shin, Y.; Jang, Y.; Lee, S. Economic Evaluation of a Hybrid Desalination System Combining Forward and Reverse Osmosis. *Membranes* **2015**, *6*.

Annex

Annex 1: Supplementary Material to Chapter 2

Table S1. Lab-scale set-ups used for investigation of forward osmosis application in manufacturing industries

Annex 2: Supplementary Material to Chapter 4

Table S1: Analytical results of FS1 (RO concentrate UPW) before FO and after FO (S1: 1 mol/L NaCl as DS; S2: Cu filtrate as DS)

Table S2: Analytical results of DS1 (Cu filtrate) before FO and after FO (S2: RO concentrate as FS; S3: deionized water as FS)

Table S3: Analytical results of FS2 (Neutralization effluent) before FO and after FO (S4: 1 mol/L NaCl as DS; S5: Cu concentrate as DS)

Table S4: Analytical results of DS2 (Cu concentrate) before FO and after FO (S5: Neutralization effluent as FS; S6: deionized water as FS)

Table S5: Analytical results of deionized water used as FS before FO and after FO (S3: Cu filtrate as DS; S6: Cu concentrate as DS)

Table S6: Mass data for all test series

Table S7: T/M-values of test series

Annex 1: Supplementary Material to Chapter 2

Table S1. Lab-scale set-ups used for investigation of forward osmosis application in manufacturing industries

Branche of Industry	FS (type + volume)	DS (type + volume)	Membrane Area; Flow channel	Membrane type	Membrane Orientation	Flow Features	Temp.	Duration	Permeate Flux/Concentration factor/Yield	Hybrid technology	Lit.
3.2 Food & Beverage Industry											
Dairy (whey)	Whey protein powder + DI water (6%) 3 L	NaCl (0.3/0.5M/1.0); 8 L	106 cm² (15 fibers)	hollow fiber FO; self-manufactured; TFC	ALFS	circulation; counter-current; DS 22 cm/s; FS 55 or 15 cm/s	22.5±1.5°C (room temperature)	8 h 22 h	start permeate flux 10.3 and 11.7 L/(m²·h); 10 % decrease	-	[112]
Dairy (whey)	Whey 3 L	NH$_4$HCO$_3$ (2 M); 3 L	140 cm²	3 RO-membranes (Hydronautics); CTA (HTI)	ALFS ALDS	circulation; concurrent; 50 cm/s	30±0.5°C	4 h	start permeate flux 12 L/(m²·h) end permeate flux 5 L/(m²·h)	-	[110, 111]
Dairy (whey)	Acid cheese whey; 3.5 L	2 M NaCl (constant concentration); 3,5 L	140 cm²	flat sheet FO; CTA, HTI (USA)	ALFS	circulation; concurrent; 50 cm/s	25±0.5°C (constant)	21 h (fresh FS 4 times)	Water recovery 66...68 %	MD	[107]
Dairy (whey)	Acid cheese whey; 3.5 L	2 M NaCl and 2 M NH$_4$HCO$_3$ (constant concentration); 3,5 L	140 cm²	flat sheet FO; CTA (HTI)	ALFS	circulation; concurrent; 50 cm/s	25±0.5°C 30±0.5°C (constant)	14 h (fresh FS 3 times)	permeate volume 2.7 L and 1.6 L; start permeate flux 28.5 and 8,5 L/(m²·h)	RO; thermolytic RO	[108]
Dairy (whey)	Acid cheese whey; 3 L	3 M NaCl; 3 L	140 cm²	flat sheet FO; CTA (HTI)	ALFS	circulation; concurrent; 25/50/75/ 100 cm/s (150/300/450/ 600 L/h)	20/25/30/ 35/ 40±0.5°C (constant)	6 h	permeate volume 1.6 L, dry matter increased from 6.8 to 14.3 %	MF	[109]
Dairy (whey) Acetic acid production	1) whey (protein separation) 2) acetic acid	1 M MgSO$_4$	-	flat sheet, polyamide, NF-membrane	-	circulation; counter-current	-	-	permeate flux ca. 19 and 25 L/(m²·h)	MF, UF, NF, fermentation	[113]
Dairy (wastewater)	Dairy wastewater (after 24 h precipitation); 2 L	1 M NaCl; 2 L	-	flat sheet; CTA-ES (HTI), AQP (Sterlitech)	ALFS	circulation; concurrent; 0.5 L/min	20±21 °C (room temperature)	3x6 h		MD	[114]
Dairy (wastewater)	I) RO concentrate from dairy wastewater treatment plant; II) DI water; 1 L	III) 1 M NaCl; IV) cheese brine; 1 L	48 cm²; 1200x40x0.86 mm	flat-sheet; CTA (HTI)	ALFS	circulation; counter-current; 20 cm/s	room temperature	3x5 h	average permeate flux = 15.1 L/(m²·h) (I)+(IV) = 21.0 L/(m²·h) (II)+(IV) = 7.9 L/(m²·h) (II)+(III)	-	[115]

Branche of Industry	FS (type + volume)	DS (type + volume)	Membrane Area; Flow channel	Membrane type	Membrane Orientation	Flow Features	Temp.	Duration	Permeate Flux/Concentration factor/Yield	Hybrid technology	Lit.
Food & Beverage (Tea extract)	tea extract; 2 L	5 M $CaCl_2$; 8 L	540 cm²	hollow-fiber membrane contactor (1.7 55 MiniModule, 3M Deutschland GmbH, Wuppertal, Germany)	tea extract shell side	circulation; counter-current	23±2°C	5 h	tea concentration of 40 %	-	[116]
Food & Beverage (Distillery)	sugarcane molasses distillery wastewater	3/4 M $MgCl_2.6H_2O$	43 cm²	flat-sheet FO; TFC (Aquaporin A/S)	ALFS	circulation; counter-current; 1 L/min	-	5x24 h	J_W = 2.8 L/(m²·h); water recovery (24 h) = 70%; melanoidin rejection 85-90%	-	[118]
Food & Beverage (Olive mill)	a) Olive mill wastewater (filtered); b) UF permeate of FO-concentrated olive mill wastewater; 3 L	$MgCl_2·6H_2O$; 3.7 M (1,8-7,5 M); 4 L	200 cm²; 200x50x6 mm	flat sheet FO; CTA (HTI)	ALFS	circulation; concurrent; 6 cm/s (2.0-8.6 cm/s)	-	24 h (10 d)	a) J_W = 7.1-9.8 L/(m²·h); volume reduction 71%; b) J_W = 5 L/(m²·h); volume reduction 64%	filtration, MF, UF, NF	[117]
Food & Beverage (Grain processing); CO_2 sequestration	wastewater from grain processing	a) brine from CO_2 sequestration site; b) 20 % $MgSO_4$	42 cm²; Sterlitech CF042-FO	flat-sheet FO; (Aquaporin A/S)	ALDS	circulation; counter-current; 1 L/min	-	1-100 h	a) J_W = 5-15 L/(m²·h); b) J_W = 3-4.5 L/(m²·h)	MD; **direct FO application**	[119]

3.3 Chemical Industry

Branche of Industry	FS (type + volume)	DS (type + volume)	Membrane Area; Flow channel	Membrane type	Membrane Orientation	Flow Features	Temp.	Duration	Permeate Flux/Concentration factor/Yield	Hybrid technology	Lit.
Chemical Industry	secondary effluent from industrial wastewater treatment plant (probably chemical industry), preconcentrated by UF or RO, -	NaCl, Na_2SO_4, $MgCl_2$ (1 M); *reference to other literature (Zhao et al. 2016): constant concentration*	*reference to other literature (Zhao et al. 2016): 33.15 cm²; 8.5x3.9x 0.2cm*	flat sheet FO; (Toray Chemical Korea Inc.)	ALFS	circulation; counter-current; - (450 mL/min) *reference to other literature (Zhao et al. 2016): 12,9 cm/s*	25°C (constant)	*reference to other literature (Zhao et al. 2016): 11 h*	for 67% recovery: DS = $MgCl_2$: J_W = 13.0 L/(m²·h) DS = Na_2SO_4: J_W = 8.08 L/(m²·h) DS = NaCl: J_W = 9.63 L/(m²·h)	FS pretreatment (concentrate further treated with FO): UF+RO+softening,	[57]
Chemical Industry	pretreated esterification wastewater		-	-					J_W declined within first 5 h from 9.56 to 6.0 L/(m²·h)		[120]
Chemical Industry	PVC latex; 273 g	NaCl (0.3-1.8 M) = synthetic seawater; 1500 g	32 cm²	flat-sheet FO; 2 CTA (HTI)	ALFS	circulation of DS only, FS stirred in tank above membrane; DS 1 L/min	20±2°C (room temperature)	24 h	start J_W = 8 and 4.5 L/(m²·h); after 24 h PVC latex 75wt%	**direct FO application**	[48]

Branche of Industry	FS (type + volume)	DS (type + volume)	Membrane Area; Flow channel	Membrane type	Membrane Orientation	Flow Features	Temp.	Duration	Permeate Flux/Concentration factor/Yield	Hybrid technology	Lit.
Chemical Industry (Ammonia absorption)	anaerobically digested sludge centrate from municipal WWTP	wastewater from ammonia absorption	42 cm²; Sterlitech CF042-FO	flat-sheet FO; CTA-NW (HTI) + AIM (Aquaporin)	ALFS	circulation; counter-current; - (0.5 L/min)	-	72 h	end J_W = 3.56 and 3.13 L/(m²·h) (AIM and CTA-NW)	**direct FO application**	[121]
Chemical Industry (Ammonia absorption)	activated sludge	wastewater from ammonia absorption	42 cm²; Sterlitech CF042-FO	flat-sheet FO; CTA-NW (HTI)	ALFS	circulation; counter-current; - (0.5 L/min)	-	35 d	J_W = 1-3 L/(m²·h)	FS pretreatment (bioreactor) = OMBR	[87]
Chemical Industry (Fermentation)	succinic acid (10/20/30/40 g/L); 1.0 L	NaCl (1/3/5 M), real seawater; 0.6/1.0 L	42 cm²; Sterlitech CF042-FO	flat-sheet FO; CTA-ES (HTI)	ALFS	circulation; counter-current; -	25±1°C (room temperature)	2.5 h	J_W = 0-4.8 L/(m²·h)	fermentation; **direct FO application**	[122]
Chemical Industry	acetic, butyric, valeric, and lactic acid (carboxylic acids, 10 mM); 1 L	NH4Cl (1 M); 0.5 L	42 cm²; 9.207x4.572x 0.23cm	flat-sheet FO; TFC-ES (HTI)	ALFS	circulation; counter-current; 25 cm/s	28±0.5°C (air conditioning)	30 h	J_W = 4.8 L/(m²·h)	-	[129]
Chemical Industry	lactic acid (8%); a) 2 L (2 kg) b) 3 L (3 kg)	glucose (60%); a) 0.7 L (1 kg) b) 2.8 L (4 kg)	a) 42 cm²; Sterlitech CF042P-FO; a) 140 cm²; Sterlitech SEPA CF-FO	flat-sheet FO; I) TFC (Aquaporin) II) TFC (Toray)	ALFS	circulation; concurrent; - (1-1.2 L/min)	20/40/ 60°C (constant)	a) 2h b) ca. 980 h	a) J_W = 2.1-10.0 L/(m²·h) (Aquaporin); J_W = 3.7-10.0 L/(m²·h) (Toray); b) J_W = 12 L/(m²·h) (Toray)	fermentation; **direct FO application**	[125]
Chemical Industry (Fermentation)	butyric acid (2 g/L); 1 L	MgCl₂ (5 M); 20 L	40 cm²; 4x10x0.5cm	flat-sheet FO CTA (HTI); flat-sheet RO TFC (XLE)	-	circulation; concurrent; 12.5 cm/s (1.5 L/min)	25°C	50% water recovery	J_W = 16-18 L/(m²·h)	fermentation; NF; RO	[124]
Chemical Industry (Fermentation)	a) crude glycerol (1/2/5%) b) pretreated and enzymatically hydrolysed wheat straw (PHWS) (5/20%)	a) crude glycerol (100%) b) pretreated and enzymatically hydrolysed wheat straw (PHWS) (100%)	33.15 cm²; 8.5x3.9x2.3cm; Sterlitech Acrylic CF042A-FO	flat-sheet FO; Aquaporin	ALFS	circulation; counter-current; a) 0.1 cm/s (50 mL/min); b) 1.7 cm/s (173 mL/min)	37°C (constant)	15 h	a) J_W = 8.4, 9.0, 10.5 L/(m²·h) (5/2/1%); b) J_W = 1.3, 5.4, 6.2 L/(m²·h) (20/5/0%)	fermentation; **direct FO application**	[126]

Branche of Industry	FS (type + volume)	DS (type + volume)	Membrane Area; Flow channel	Membrane type	Membrane Orientation	Flow Features	Temp.	Duration	Permeate Flux/Concentration factor/Yield	Hybrid technology	Lit.
Chemical Industry (Fermentation)	a) model sugar solution (20 g/L xylose + 0.45 g/L acetic acid) b) liquid fraction from rice straw pretreated with hot water	I) 2.5 M NaCl; switchable polarity solvents (SPS): II) 3.6 M Triethylamine-carbon dioxide (TEA-CO_2) ; III) 4.3 M Trimethyl-amine-carbon dioxide (TMA-CO_2) (constant concentration)	-	flat-sheet FO; TFC-ES (HTI)	ALFS	circulation; counter-current; - (FS 0.4 L/min; DS 0.75 L/min)	-	a) 48 h; b) 72 h	a) start J_W = 8.8, 5.7, 2.9 L/(m²·h) (I/II/III); after 48 h J_W < 0.8 L/(m²·h); b) start J_W = 4 L/(m²·h) (II); after 48 h J_W = 1.8 L/(m²·h)	fermentation; **direct FO application**	[127]
Chemical Industry (Fermentation)	liquid fraction from rice straw pretreated with hot water	switchable polarity solvent (SPS): 3.6 M Triethylamine-carbon dioxide (TEA-CO_2)	43 cm²	flat-sheet FO; TFC-ES (HTI)	ALFS	circulation; counter-current; - (FS 0.4 L/min; DS 0.75 L/min)	-	72 h	start J_W = 3.9 L/(m²·h); after 48 h J_W = 1.8 L/(m²·h); total sugar content produced 107 g/L;	fermentation; NF; enzymatic hydrolysis; **direct FO application**	[128]

3.5 Pharmaceutical Industry

Branche of Industry	FS (type + volume)	DS (type + volume)	Membrane Area; Flow channel	Membrane type	Membrane Orientation	Flow Features	Temp.	Duration	Permeate Flux/Concentration factor/Yield	Hybrid technology	Lit.
Pharmaceutical Industry	I) tetracycline (0, 1000, 2000, 5000, 10000 ppm) dissolved in ethanol II) tetracycline (0, 2000 ppm) in isopropanol (IPA) III) triglycerides (0, 20 wt%) dissolved in hexane	IV) LiCl (2 M) V) 50 wt% methyl palmitate VI) citric acid (2 M) VII) polyethylene glycol (100 G/L PEG1000) VIII) diethanolamine (2 M)	4 cm²	flat-sheet FO; TFC; self-manufactured	ALFS ALDS	circulation; counter-current; - (0.2 L/min)		2 h	average permeate flux ALDS & ALFS (no tetracycline/triglycerides) (I+IV) = 3.82±0.37 & 2.52±0.14 L/(m²·h) (II+IV) = 0.51±0.11 & 0.34±0.06 L/(m²·h) (III+V)= 2.04±0.34 & 1.87±0.13 L/(m²·h) (I+VI) = 2.85±0.72 & 2.05±0.30 L/(m²·h) (I+VII) = 1.23±0.19 & 0.89±0.24 L/(m²·h) (II+VIII) = 0.52±0.05 & 0.32±0.07 L/(m²·h)	-	[130]
Pharmaceuticak Industry	protein solution (bovine serum albumin = BSA solution); 0.5 L	NaCl; 0.5 L	-	hollow-fiber NF	ALFS	circulation; concurrent; 6 cm/s	22.5°C	2 h	Initial water flux (0.5/1/1.5/2 M NaCl) = 2.7/3.6/5.1/5.3 L/(m²·h)	MD	[161]

Branche of Industry	FS (type + volume)	DS (type + volume)	Membrane Area; Flow channel	Membrane type	Membrane Orientation	Flow Features	Temp.	Duration	Permeate Flux/Concentration factor/Yield	Hybrid technology	Lit.
3.5 Coal Processing											
Coal processing	Coke-oven wastewater; 15 L	NaCl, MgSO$_4$, and CaCl$_2$·H$_2$O; 15 L	150 cm²	flat sheet NF/MF; TFC (Sepro Membranes, USA)	ALFS	circulation; counter-current; 21-42 cm/s	constant	12 h/d for 7 days	42-46 L/(m²·h)	NF	[131]
Coal processing	3 Artificial coal gasification wastewaters (100 mg/L three different phenolic compounds); 2 L	NaCl (1.75-10.5%, concentration adjusted hourly); 2 L	60 cm²; 100x60x2 mm	flat sheet FO; TFC (HTI)	ALFS	circulation; concurrent; 14 cm/s (1 L/min)	FS 20°C, DS 30°C (constant)	4 h	8.5-10.5 L/(m²·h).	-	[133]
Coal processing	phenol solution; -	NaCl (0.5-4 M)	24 cm²; 80x30x2 mm	flat sheet FO; CTA & TFC (FTS) + self-manufactured	ALFS ALDS	circulation; concurrent; 25 cm/s	25±1°C (constant)	100 mL permeate	3-34 L/(m²·h)	-	[74]
3.6 Micro Algae Cultivation											
Microalgae Cultivation	0.2 g/L algal suspension (3 different species); 1 L	sea salt solution (70 g/L); MgCl2 (86.5 g/L); CaCl2 (114.3 g/L); 6 L	200 cm²	flat-sheet FO; CTA (HTI)	ALFS	circulation; counter-current; 9.6 cm/s	25±1°C (constant)	until 75% permeate	start J$_W$ = 7.0 L/(m²·h); final ΔJ$_W$ = 5.3-70.9%; algae dewatering efficiency = 59-80%	microalgae cultivation	[139]
Microalgae Cultivation	0.2 g/L algal suspension (1 species); 1 L	sea salt solution (70 g/L); MgCl2 (86.55 g/L); CaCl2 (68.96 g/L); NaCl (68.96 g/L); 6 L	200 cm²	flat-sheet FO; CTA + TFC (HTI)	ALFS ALDS	circulation; counter-current; 9.6 cm/s	25±1°C (constant)	until 75% permeate	start J$_W$ = 6.7-8.2 L/(m²·h); final JW = 1.5-5.9 L/(m²·h); final ΔJ$_W$ = 10-59%;	microalgae cultivation	[140]
Microalgae (Cultivation)	0.1 g/L algal suspension (in 10 mM NaCl or 7 mM NaCl + 1 mM MgCl$_2$)	0.2-5 M NaCl; 0.15-1.5 M MgCl$_2$ (concentration raised stepwise every 30 min)	29.2 cm²	flat-sheet FO; CTA (HTI)	ALFS ALDS	circulation; concurrent	-	2-3 h		-	[141]
Microalgae (Cultivation)	0.1 g/L algal suspension (in 10 mM NaCl); 4 L	a) 0.3-5 M NaCl; b) 0.5/2.0 M MgCl$_2$; 5 L	60 cm²	flat-sheet FO; CTA (HTI)	ALFS ALDS	circulation; concurrent; 22.5 cm/s	22±1°C	4 h	a) J$_W$ = 7-30 and 10-50 L/(m²·h) (ALFS and ALDS); b) J$_W$ = 14-55 (ALDS);	-	[142]
Microalgae Cultivation	algae (0.5-2 g/L) in artificial medium or municipal wastewater	artificial or natural seawater	900 cm²	modified X-Pack Hydration Bags (HTI)	ALFS	batch; no circulation; membrane bag in water bath or ocean	-	4 h - 52 d	J$_W$ = 2 L/(m²·h)	microalgae cultivation	[143]

Branche of Industry	FS (type + volume)	DS (type + volume)	Membrane Area; Flow channel	Membrane type	Membrane Orientation	Flow Features	Temp.	Duration	Permeate Flux/Concentration factor/Yield	Hybrid technology	Lit.
3.7 Textile Industry											
Textile Industry	artificial dye-containing wastewater; 0.5 L	NaCl (1-2 M, constant)	10 cm²	flat-sheet FO; TFC, self-manufactured	ALFS ALDS	circulation; counter-current; 1.7 cm/s	22±0.5°C (room temperature)		start permeate flux 36 L/(m²·h), stable long-term permeate flux 12 L/(m²·h); dye rejection 99.9%	coagulation & flocculation	[147]
Textile Industry	artificial dye-containing wastewater (50 ppm Congo red); -	0.25 g/mL P(SSA-co-MA)-Na-1 (polyelectrolyte salt-poly sodium)	18.9 cm²	flat-sheet FO; TFC (HTI)	ALFS	circulation; -; - (300 mL/min)	25±1°C (room temperature)	2 h	3 L/(m²·h)	NF	[148]
Textile Industry	artificial dye-containing wastewater (50 ppm Acid Orange 8); 500 mL	0.24/0.36/0.48/ 0.60 g/mL PAA-Na (poly acrylic acid sodium salt); 300 mL	-	hollow fiber FO; CTA, self-manufactured	ALDS	circulation; concurrent; - (FS 100 mL/min, DS 500 mL/min)	50±0.5°C, 60±0.5°C, 70±0.5°C, 80±0.5°C	2 h	permeate flux decreased from 25 to 15.5 L/(m²·h)	MD	[149]
Textile Industry; Coal gasification	artificial dye-containing wastewater (80 ppm methylene blue); 50 mL	brown coal powder; 1 g placed on membrane support layer	1.33 cm²	flat-sheet FO; CTA (HTI)	ALFS	no circulation!	room temperature	8-11 h	0.979 and 0.900 L/(m²·h) (first hour; two different brown coals)	**direct FO application**	[50]
Textile Industry	artificial dye-containing wastewater (15 g/L NaCl + 25/500/750/ 1000 mg/L of Acid Green 25 dye or Remazol Brilliant Orange or Remazol Blue); -	real seawater	71 cm²	flat-sheet FO; CTA (HTI)	ALFS ALDS	circulation; counter-current; - (1.5 mL/min)	23±1°C	2 h; 6 h	Average fluxes (2 h, ALFS) = 1,62...2,25 L/(m²·h) (250...1000 mg/L dye) Average fluxes (2 h, ALDS) = 2,12...3,47 L/(m²·h) (250...1000 mg/L dye) Average fluxes (6 h, ALFS) = 1,94...2,76 L/(m²·h) (1000 mg/L dye)	**direct FO application**	[146]
Textile Industry; Oil Industry	artificial dye-containing wastewater (0,05 g/L Reactive Brilliant Red K-2BP); 1000 mL	Polyacrylamide; 500 mL	20 cm²; 7.7x2.6x0.3 cm	flat-sheet FO; TFC	ALFS ALDS	circulation; concurrent; 10 cm/s	25±0.5°C	5 h	ALFS 3.21-2.65 L/(m²·h); ALDS 5.14-4.19 L/(m²·h)	**direct FO application**	[150]

Branche of Industry	FS (type + volume)	DS (type + volume)	Membrane Area; Flow channel	Membrane type	Membrane Orientation	Flow Features	Temp.	Duration	Permeate Flux/Concentration factor/Yield	Hybrid technology	Lit.
3.8 Pulp and Paper Production											
Pulp production; desert restoration	DI water; saline feed (100/2000/ 30'000 mg/L NaCl)	sodium ligning sulfonate (NaLS; 600 g/kg)	50 cm²; 50x100x 2.8 mm	flat sheet FO; 2 CTA (HTI)	ALFS ALDS	circulation; concurrent; FS 29 cm/s; DS 10 cm/s	23°C (constant)	-	FS=DI+ALDS: permeate flux 15 and 10 L/(m²·h); FS=30'000 mg/L NaCl+ALFS: permeate flux 5 and 2 L/(m²·h)	**direct FO application**	[151]
3.9 Electronic Industry											
Electronic Industry (TFT-LCD plant)	KI wastewater from polarizer process (0.6% iodide); 1 L	KOH wastewater; 2 L	41.4 cm²; 45x92x2 mm; Sterlitech	flat sheet FO; CTA & TFC (HTI)	ALFS ALDS	circulation; counter-current; 9.26 cm/s (500 mL/min)	25±0.5°C (constant)	92 h 120 h	average permeate (92 h) flux ALFS 4.9 L/(m²·h) and ALDS 5.7 L/(m²·h); iodide concentration in FS increased to 6.9% (120 h)	**direct FO application**	[154]
Electronic Industry (PCB plant)	Pd catalyst waste solution	electroless nickel plating solution	-	-	ALFS ALDS	circulation; concurrent	-	-	FS concentration yield > 90%; ALDS: Jw = 39,4 L/(m²·h); Js,Ni = 0,43 g/(m²·h) ALFS: ca. Jw = 19 L/(m²·h); Js,Ni = 0,4 g/(m²·h)	**direct FO application**	[153]
3.10 Car Manufacturing Wastewater											
Car Manufacturing	I) rinsing water from cathodic dip painting; II) wastewater from cathodic dip painting; III) wastewater from paint shop pre-treatment; IV) DI water; 1 L	V) cooling tower water; VI) wastewater from cathodic dip painting; VII) 1 M NaCl; 1 L	48 cm²; 1200x40x 0.86 mm	flat-sheet; CTA (HTI)	ALFS	circulation; counter-current; 20 cm/s	room temperature	3x5 h	average permeate flux = 12.1 L/(m²·h) (I)+(VII) = 1.1 L/(m²·h) (IV)+(V) = 7.5 L/(m²·h) (III)+(VII) = 0.3 L/(m²·h) (VI)+(VI) = 19.4 L/(m²·h) (II)+(VII) = 0.1 L/(m²·h) (III)+(V)	-	[115]
3.11 General Industrial Application											
Heavy Metal Elimination	2 g/L CuSO$_4$/Pb(NO$_3$)$_2$/CdCl$_2$	2 M NaCl	9 cm²	flat-sheet FO; TFC, self-manufactured	ALFS	probably no circulation; batch	-	-	Jw = 45-50 L/(m²·h); heavy metal rejection > 99.4%	-	[155]
Heavy Metal Elimination	1/2/5 g/L Cu^{2+}, Ni^{2+}, Pb^{2+}, Zn^{2+}, Cd^{2+}	0.5/1.0/1.5/2.0 M MgCl$_2$	9 cm²	flat-sheet FO; self-manufactured	ALFS ALDS	no circulation; batch	25/45/ 65°C	6 h	AL-DS: rejection > 95.93 %; 23,5 L/(m²·h); AL-FS: rejection > 99.32 %; 14 L/(m²·h) (DS = 1 M MgCl$_2$; FS = 2 g/L metal solution)	-	[49]

Branche of Industry	FS (type + volume)	DS (type + volume)	Membrane Area; Flow channel	Membrane type	Membrane Orientation	Flow Features	Temp.	Duration	Permeate Flux/Concentration factor/Yield	Hybrid technology	Lit.
Heavy Metal Elimination	0.05-1 g/L Cd^{2+}, Pb^{2+}, Cu^{2+}, Zn^{2+} (pH 4.5±0.5)	0.5-2 M NaCl;	-	flat-sheet FO; self-manufactured	-	circulation; concurrent; - (260 mL/min)	25°C (constant)	-	J_W = 27.3-69 L/(m²·h) (DS = 0.5-12.0 M); heavy metal rejection = 94-85% (0.2-1 g/L FS)	-	[157]
Heavy Metal Elimination	0.02-1 mg/L $HgCl_2$; 1 L	0.5-2 M NaCl; 0.5-2 M $MgCl_2$; 1 L	42 cm²; Sterlitech CF042-FO; 9.2x4.6x0.2cm	flat-sheet FO; TFC (HTI)	ALFS	circulation; counter-current	-	-	J_W = 4-9.5 L/(m²·h); mercury rejection = 98%	-	[159]
Heavy Metal Elimination	0.1 g/L $NiCl_2$ + 0/50/100 mg/L NaCl (+ detergent); 1 L	117/155/194.5 mg/L NaCl; 1 L	20 cm²; 7.7x2.6x0.3cm	flat-sheet FO; CTA & TFC (HTI)	ALFS ALDS	circulation; concurrent; 10 cm/s	25°C (constant)	5 h	J_W = 5-34 L/(m²·h);	-	[158]
Heavy Metal Elimination	1/2/5 g/L $Cr_2O_7^{2+}$, $HAsO_4^{2-}$, Pb^{2+}, Cd^{2+}, Cu^{2+}, Hg^{2+}; 0.4 L	bulky hydroacidcomplex $Na_4[Co(C_6H_4O_7)_2] \cdot 2H_2O$ (Na–Co–CA) (1,0/1,5 M); 0.1 L	4 cm²	flat-sheet FO; TFC, self-manufactured	ALFS	circulation; concurrent	23/40/50/60°C	0.5 h	J_W = 10-17 L/(m²·h); heavy metal rejection > 99.7%	-	[156]
Heavy Metal Elimination; Food Industry	Copper solution; chromium solution; wastewater from fish and shell fish processig plant	synthetic seawater; concentrated sugar solution	13 cm²; 58 cm²	flat-sheet RO; 10 commercial membranes	ALFS ALDS	no circulation; concurrent	room temperature	< 6 h	J_W < 4.5 L/(m²·h)		[42,43]
Cooling Water	rainwater	cooling water from a steam plant	20 cm²	flat-sheet FO; CTA (HTI)	ALFS	circulation; counter-current; 45/100 mL/min	3-50 °C	1.5 h	average J_W (23°C) = 1.75 L/(m²·h);		[160]
Cooling Water	I) wastewater from automobile paint shop pre-treatment; II) DI water; 1 L	III) cooling tower water; 1 L	48 cm²; 1200x40x 0.86 mm	flat-sheet; CTA (HTI)	ALFS	circulation; counter-current; 20 cm/s	room temperature	3x5 h	average permeate flux = 1.1 L/(m²·h) (II)+(III) = 0.1 L/(m²·h) (I)+(III)	-	[115]

Annex 2: Supplementary Material to Chapter 4

Table S1. Analytical results of FS1 (RO concentrate UPW) before FO and after FO (S1: 1 mol/L NaCl as DS; S2: Cu filtrate as DS)

	FS_1 RO Concentrate	S1-E1	S1-E2	S1-E3	S2-E1	S2-E2	S2-E3
Conductivity, µS/cm	1.21	1580	1480	1390	238	237	215
pH	5.55	6.63	6.66	6.7	6.78	6.75	6.73
Turbidity, FNU	0.14	0.24	0.14	0.17	0.15	0.16	0.17
H_2O_2, mg/L	<0,5	n.a.	n.a.	n.a.	n.a.	n.a.	n.a.
Zinc, mg/L	<0,02 (0,01)	n.a.	n.a.	n.a.	<0,02	<0,02	<0,02
Ammonium, mg/L	n.a.	n.a.	n.a.	n.a.	0.96	1.13	1.02
Lead, mg/L	<0,02 (0,00)	n.a.	n.a.	n.a.	<0,02	<0,02	<0,02
Cadmium, mg/L	<0,02 (0,00)	n.a.	n.a.	n.a.	<0,02	<0,02	<0,02
Calcium, mg/L	<2 (0,09)	n.a.	n.a.	n.a.	4.50	4.19	3.32
Fluoride, mg/L	<0,01	<0,1	<0,1	<0,1	0.12	0.12	0.12
Chloride, mg/L	<0,02	480	446	403	67.8	67	60
COD, mg/L	n.a.	n.a.	n.a.	n.a.	<5	n.a.	n.a.
Iron, mg/L	<0,02 (0,00)	n.a.	n.a.	n.a.	<0,02	<0,02	<0,02
Potassium, mg/L	<0,02 (0,01)	n.a.	n.a.	n.a.	1.42	1.37	1.32
Copper, mg/L	<0,02 (0,00)	n.a.	n.a.	n.a.	<0,02	<0,02	<0,02
Magnesium, mg/L	<0,02 (0,00)	n.a.	n.a.	n.a.	0.08	0.06	0.05
Sodium, mg/L	<0,02 (0,00)	315	301	282	37.9	34.5	31.3
Nickel, mg/L	<0,02 (0,00)	n.a.	n.a.	n.a.	<0,02	<0,02	<0,02
Nitrate, mg/L	<0,02	<0,2	<0,2	<0,2	0.82	0.79	0.77
Nitrite, mg/L	<0,02	<0,2	<0,2	<0,2	<0,02	<0,02	<0,02
Phosphate, mg/L	<0,2	<2	<2	<2	<0,2	<0,2	<0,2
Sulfate, mg/L	<0,01	<0,1	<0,1	<0,1	1.78	1.72	1.73
Osmolality, mOsmol/kg	2	28	27	25	5	5	4
π (ρ=1000g/L), bar	0.05	0.68	0.66	0.61	0.12	0.12	0.10
π (ρ measured), bar	0.05	0.68	0.66	0.61	0.12	0.12	0.10
Density ρ, g/L	996.8	997.3	997.3	997.2	996.8	996.8	996.9

Table S2. Analytical results of DS1 (Cu filtrate) before FO and after FO (S2: RO concentrate as FS; S3: deionized water as FS)

	DS$_1$ Cu filtrate	S2-E1	S2-E2	S2-E3	S3-E1	S3-E2	S3-E3
Conductivity, µS/cm	12610	10230	10300	10380	10230	10340	10360
pH	8.82	8.15	7.92	7.88	8.51	8.38	8.36
Turbidity, FNU	0.51	0.34	0.32	0.53	0.19	0.15	0.17
H_2O_2, mg/L	<0,5	n.a.	n.a.	n.a.	n.a.	n.a.	n.a.
Zinc, mg/L	<0,02	0.19	0.19	0.17	0.18	0.17	0.17
Ammonium, mg/L	35.6	25.2	27.6	26.5	25.9	23.4	25.2
Lead, mg/L	<0,02	<0,02	<0,02	<0,02	<0,02	<0,02	<0,02
Cadmium, mg/L	<0,02	<0,02	<0,02	<0,02	<0,02	<0,02	<0,02
Calcium, mg/L	1476	1429	1416	1448	1426	1408	1428
Fluoride, mg/L	7.3	6.7	6.8	6.7	7.0	6.9	6.8
Chloride, mg/L	4532	3541	3540	3600	3520	3582	3592
COD, mg/L	<25	n.a.	n.a.	n.a.	n.a.	n.a.	n.a.
Iron, mg/L	0.13	0.08	0.09	0.09	0.07	0.08	0.08
Potassium, mg/L	33.8	20.4	22.1	21.2	20.7	21.0	20.6
Copper, mg/L	0.88	2.49	1.64	1.92	1.88	6.78	2.92
Magnesium, mg/L	39.7	33.6	33.4	33.9	32.6	33.4	34.0
Sodium, mg/L	907	703	717	721	700	712	733
Nickel, mg/L	0.03	0.04	0.05	0.04	0.05	0.07	0.06
Nitrate, mg/L	30.68	28.78	27.82	29.18	29.08	29.63	29.82
Nitrite, mg/L	<1	<1	<1	<1	<1	<1	<1
Phosphate, mg/L	<10	<10	<10	<10	<10	<10	<10
Sulfate, mg/L	250	215	210	215	214	217	215
Osmolality, mOsmol/kg	190	151.5	151	154	148	150	152
π (ρ=1000g/L), bar	4.63	3.69	3.68	3.75	3.61	3.65	3.70
π (ρ measured), bar	4.61	3.68	3.67	3.75	3.60	3.65	3.70
Density ρ, g/L	1004.7	1001.7	1001.6	1001.6	1001.5	1001.6	1001.6

Table S3. Analytical results of FS2 (Neutralization effluent) before FO and after FO (S4: 1 mol/L NaCl as DS; S5: Cu concentrate as DS)

	FS$_2$ Neutralization effluent	S4-E1	S4-E2	S4-E3	S5-E1	S5-E2	S5-E3
Conductivity, µS/cm	8.35	16.08	16.25	16.33	16.02	15.55	15.6
pH	7.8	8.19	8.2	8.21	1.86	1.85	1.88
Turbidity, FNU	1.29	0.72	1.51	0.72	0.36	0.42	0.44
H$_2$O$_2$, mg/L	<0,5	n.a.	n.a.	n.a.	n.a.	n.a.	n.a.
Zinc, mg/L	0.02	0.02	0.02	0.02	0.34	0.15	0.12
Ammonium, mg/L	45.7	29.4	30.9	31.1	38.5	41.6	40.1
Lead, mg/L	<0,02	<0,02	<0,02	<0,02	<0,02	<0,02	<0,02
Cadmium, mg/L	<0,02	<0,02	<0,02	<0,02	<0,02	<0,02	<0,02
Calcium, mg/L	343	573	577	599	444	436	445
Fluoride, mg/L	6.3	7.8	7.8	7.6	6.4	6.4	6.3
Chloride, mg/L	2245	4891	5013	5184	3104	3278	3237
COD, mg/L	n.a.	<25	n.a.	n.a.	n.a.	n.a.	n.a.
Iron, mg/L	0.05	0.09	0.09	0.09	1.86	1.11	0.96
Potassium, mg/L	29	18.3	18.3	16.1	23.7	24.7	25.8
Copper, mg/L	<0,02	<0,02	<0,02	<0,02	5.05	4.11	4.13
Magnesium, mg/L	63.7	78.8	79.8	77.7	57.2	55	56.1
Sodium, mg/L	1327	3016	2988	2992	1708	1703	1711
Nickel, mg/L	<0,02	<0,02	<0,02	<0,02	0.05	0.02	0.02
Nitrate, mg/L	34	< 50	42	42	41	40	40
Nitrite, mg/L	<1	<2	<1	<1	<2	<1	<1
Phosphate, mg/L	<10	<20	<10	<10	<20	<10	<10
Sulfate, mg/L	778	1627	1457	1498	1800	1707	1712
Osmolality, mOsmol/kg	133	277	279	279	241	237	239
π (ρ=1000g/L), bar	3.24	6.75	6.80	6.80	5.87	5.77	5.82
π (ρ measured), bar	3.24	6.71	6.76	6.76	5.85	5.76	5.80
Density ρ, g/L	1001.0	1005.1	1005.1	1005.1	1002.9	1003.1	1003.0

Table S4. Analytical results of DS2 (Cu concentrate) before FO and after FO (S5: Neutralization effluent as FS; S6: deionized water as FS)

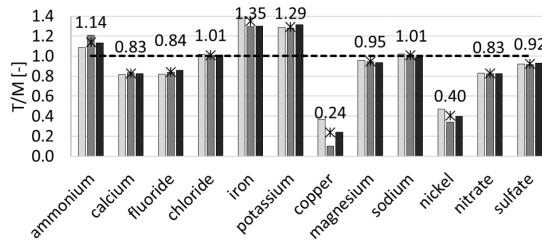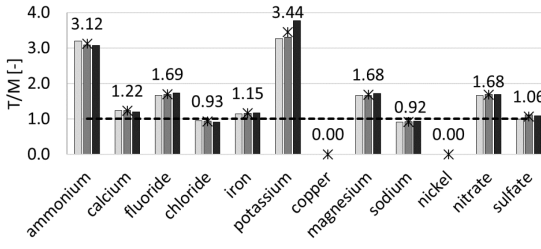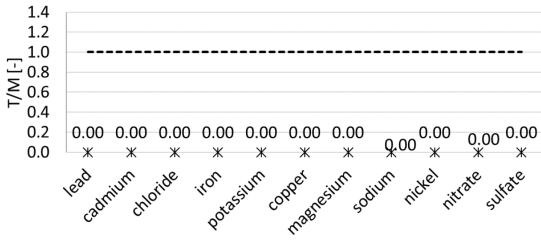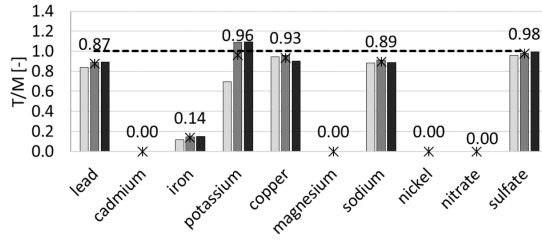|	DS$_2$ Cu concentrate	S5-E1	S5-E2	S5-E3	S6-E1	S6-E2	S6-E3
Conductivity, µS/cm	135.4	101.9	104.2	103.5	95.8	100.6	95.0
pH	0.55	0.72	0.67	0.68	0.74	0.73	0.74
Turbidity, FNU	0.00	0.00	0.00	0.00	0.00	0.00	0.00
H$_2$O$_2$, mg/L	n.a.	n.a.	n.a.	n.a.	n.a.	n.a.	n.a.
Zinc, mg/L	0.13	0.52	0.39	0.35	0.30	0.29	0.26
Ammonium, mg/L	n.a.	n.a.	n.a.	n.a.	n.a.	n.a.	n.a.
Lead, mg/L	5.23	4.49	4.39	4.08	4.23	4.03	4.03
Cadmium, mg/L	<0,02	0.05	0.04	0.04	0.03	0.03	0.03
Calcium, mg/L	<2 (1,8)	2.09	<2 (1,5)	<2 (1,4)	<2	<2	<2
Fluoride, mg/L	<0,5	<0,5	<10	<10	<0,5	<10	<10
Chloride, mg/L	< 350	<350	< 350	< 350	< 350	< 350	< 350
COD, mg/L	n.a.	n.a.	n.a.	n.a.	n.a.	n.a.	n.a.
Iron, mg/L	0.22	3.62	1.66	1.33	1.31	1.03	1.03
Potassium, mg/L	0.35	3.35	2.72	2.55	0.34	0.22	0.22
Copper, mg/L	11'600	9'740	9'780	9'770	8'330	8'290	8'840
Magnesium, mg/L	<0,02	0.70	0.54	0.52	0.02	<0,02	<0,02
Sodium, mg/L	37.8	137	114	108	29.1	28.4	29.4
Nickel, mg/L	<0,02	1.56	1.03	0.85	0.90	0.75	0.73
Nitrate, mg/L	26	<1	<20	<20	<1	<20	<20
Nitrite, mg/L	<1	<1	<20	<20	<1	<20	<20
Phosphate, mg/L	<200 (1:1000)	<10 (1:50)	<200	<200	<10	<200	<200
Sulfate, mg/L	47977	38097	37857	37082	33958	33630	33326
Osmolality, mOsmol/kg	1092	772	788	789	696	709	715
π (ρ=1000g/L), bar	26.60	18.81	19.20	19.22	16.96	17.27	17.42
π (ρ measured), bar	25.39	18.13	18.49	18.53	16.42	16.72	16.87
Density ρ, g/L	1047.6	1037.4	1038.0	1037.6	1032.8	1032.9	1032.8
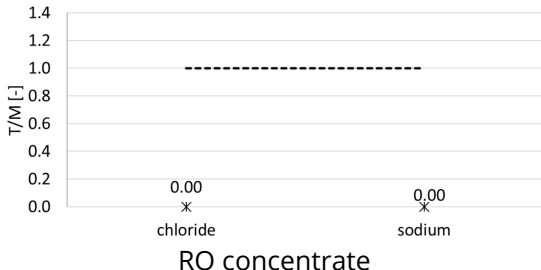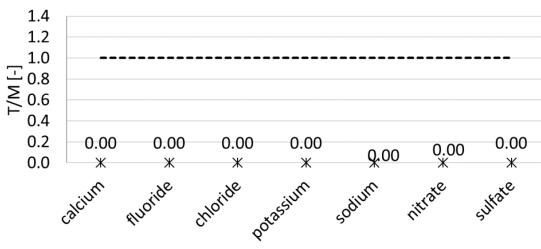
Table S5. Analytical results of deionized water used as FS before FO and after FO (S3: Cu filtrate as DS; S6: Cu concentrate as DS)

	Deionized water	S3-E1	S3-E2	S3-E3	S6-E1	S6-E2	S6-E3
Conductivity, µS/cm	4.0	198	179.7	168.7	3280	3750	3600
pH	7.0	6.72	6.96	7.1	2.1	2.08	2.08
Turbidity, FNU	n.a.	0.16	0.13	0.19	0.21	0.20	0.38
H_2O_2, mg/L	n.a.	n.a.	n.a.	n.a.	n.a.	n.a.	n.a.
Zinc, mg/L	n.a.	<0,02	<0,02	<0,02	0.18	0.16	0.15
Ammonium, mg/L	n.a.	<0,15	<0,15	<0,15	<0,15	<0,15	<0,15
Lead, mg/L	n.a.	<0,02	<0,02	<0,02	0.27	0.26	<0,02
Cadmium, mg/L	n.a.	<0,02	<0,02	<0,02	<0,02	<0,02	<0,02
Calcium, mg/L	n.a.	2	1.4	1.1	<2	<2	<2
Fluoride, mg/L	n.a.	0.12	<0,01	<0,01	<0,01	<0,01	<0,01
Chloride, mg/L	n.a.	51.1	45.5	42.3	8.0	7.6	7.6
COD, mg/L	n.a.	<5	n.a.	n.a.	253	319	248
Iron, mg/L	n.a.	<0,02	<0,02	<0,02	0.53	0.53	0.71
Potassium, mg/L	n.a.	1.26	1.18	1.16	0.02	0.02	0.02
Copper, mg/L	n.a.	<0,02	<0,02	<0,02	1.67	2.08	1.86
Magnesium, mg/L	n.a.	<0,02	<0,02	<0,02	<0,02	<0,02	<0,02
Sodium, mg/L	n.a.	31.5	29.8	28.8	2.17	2.3	2.25
Nickel, mg/L	n.a.	<0,02	<0,02	<0,02	0.16	0.16	0.14
Nitrate, mg/L	n.a.	1.2	1.2	1.2	1.0	1.0	1.0
Nitrite, mg/L	n.a.	<0,02	<0,02	<0,02	<0,02	<0,02	<0,02
Phosphate, mg/L	n.a.	<0,2	<0,2	<0,2	<0,2	<0,2	<0,2
Sulfate, mg/L	n.a.	2.8	2.8	2.7	428	477	487
Osmolality, mOsmol/kg	2	4	3	3	39	49	43
π (ρ=1000g/L), bar	0.05	0.10	0.07	0.07	0.95	1.19	1.05
π (ρ measured), bar	0.05	0.10	0.07	0.07	0.95	1.20	1.05
Density ρ, g/L	996.9	997.0	996.9	996.8	997.2	997.3	997.3

Table S6. Mass data for all test series

	$m_{FS,start}$	$m_{FS,end}$	concentration factor $m_{FS,start}/m_{FS,end}$	$m_{DS,start}$	$m_{DS,end}$	concentration factor $m_{DS,start}/m_{DS,end}$
S1-E1	1008.1	196.1	5.1	1026.00	1841.2	0.6
S1-E2	1031.0	207.5	5.0	1014.3	1812	0.6
S1-E3	1012.4	220.7	4.6	1015.3	1800.1	0.6
S2-E1	1014.8	753.8	1.3	1014.7	1272.7	0.8
S2-E2	1008.7	743.2	1.4	1021.9	1273.3	0.8
S2-E3	1014.3	756.8	1.3	1015.4	1258.7	0.8
S3-E1	1009.5	731.2	1.4	1009.5	1281.1	0.8
S3-E2	1004.9	738.8	1.4	1010.5	1270.4	0.8
S3-E3	1010.5	749.2	1.3	1011.4	1263.9	0.8
S4-E1	1006.7	489.4	2.1	1005.3	1520.00	0.7
S4-E2	1000.4	480.3	2.1	1008.6	1521.8	0.7
S4-E3	1006.0	481.5	2.1	1014.4	1524.8	0.7
S5-E1	1014.3	710.0	1.4	1007.5	1308.9	0.8
S5-E2	1007.8	708.3	1.4	1015.3	1295.8	0.8
S5-E3	1009.4	712.1	1.4	1008.2	1296.8	0.8
S6-E1	1018.0	524.3	1.9	1006.6	1485.5	0.7
S6-E2	1005.2	531.0	1.9	1007.6	1470.6	0.7
S6-E3	1006.2	536.6	1.9	1008.8	1465.4	0.7

Table S7. T/M-values of test series

	Feed Solution	Draw Solution

S1 — RO concentrate / No analysis performed of 1 mol/L NaCl.

S2 — See Figure 8 left in the main text. / See Figure 8 right in the main text.

S3 — Deionized water / Cu filtrate

S4 — Neutralization Effluent / No analysis performed of 1 mol/L NaCl.

S5 — See Figure 11 left in the main text. / See Figure 11 right in the main text.

S6 — Deionized water / Cu concentrate

Legend: E1 E2 E3 × Average --- T/M=1